Fakultät für Medizin

Institut/Klinik/Lehrstuhl für Innere Medizin, Schwerpunkt, Gastroenterologie

The pancreas specific role of Fibronectin (FN) in Pancreatic Diseases

Ezgi Kaya Aksoy

Vollständiger Abdruck der von der Fakultät für Medizin der Technischen Universität München zur Erlangung des akademischen Grades eines

Doctor of Philosophy (Ph.D.)

genehmigten Dissertation.

Vorsitzender: Prof. Dr. Stefan Engelhardt

Betreuer: Prof. Dr. Hana Algül

Prüfer der Dissertation:

1. Priv.-Doz. Dr. Guido von Figura

2. Prof. Dr. Philipp J. Jost

Die Dissertation wurde am 22.06.2020 bei der Fakultät für Medizin der Technischen Universität München eingereicht und durch die Fakultät für Medizin am 09.09.2020 angenommen.

1 ABSTRACT

Fibronectin (FN) is a major extracellular matrix (ECM) component which supports the cell-ECM interaction. This interaction has inevitable role in pancreatic ductal adenocarcinoma (PDAC) surrounded by highly desmoplastic stromal reaction as one of the key hallmarks of PDAC. As other ECM components, the exact role of FN during tumor development and progression has been highly controversial. Especially in PDAC, FN is primarily expressed in the stroma, therefore the field has mainly focused on the role of FN in tumor stroma. Yet, the primary function of FN in cancer structures remains unknown. By taking the advantage of this unanswered question about FN, we have shown that it is also expressed in pancreatic cancer cells and that research into its role is warranted in this context. To investigate the specific role of fibronectin in the pancreas, we have generated mice harboring an oncogenic Kras mutation as well as homozygous deletion of FN (*Kras; FN∆panc*) and compared them with mice expressing only the oncogenic Kras (*Kras*) in exocrine pancreatic cells. Mice were analyzed at specific time points and at signs of sickness. Pancreata were collected and evaluated by histological analysis and immunohistochemistry. Isolated primary tumor cells from *Kras* and *Kras; FN∆panc* mice were characterized and analyzed regarding their response upon treatment with conventional chemotherapies, ER stress inducers, and cell death inducers. In addition, isolated cell lines were used to perform transcriptome analysis with or without treatment of tunicamycin.

In early time points, acinar cell loss and decreased pancreas to body weight ratio were observed in *Kras; FN∆panc* mice. Even though FN deletion did not alter Kras activity or PanIN formation, a higher number of acinar to ductal metaplasia (ADM) structures was found in *Kras; FN∆panc* pancreata in 9-week-old mice, indicating that FN deletion increased the early onset of tumorigenesis. However, this effect was lost in 18-week-old mice and no difference in tumorigenesis between *Kras* and *Kras; FN∆panc* mice could be observed. Also, immune infiltration was elevated in *Kras; FN∆panc* compared to *Kras* pancreata in 9-week and 18-week time points. Additionally, the induction of inflammation-induced carcinogenesis by cerulein treatment resulted in acinar cell loss, immune infiltration, and micro carcinoma formation in *Kras; FN∆panc* pancreata. *Kras; FN∆panc* survival mice, opened upon obvious signs of sickness, presented pancreatic atrophy, lipogenesis, and micro carcinoma formation, but the stromal reaction, which

was observed in early time points was unequivocally reduced. Kaplan-Maier analysis demonstrated that the median survival of *Kras; FN∆panc* mice was significantly reduced compared to *Kras* mice. While the tumor incidence was higher in *Kras; FN∆panc* mice, the metastatic incidence was lower compared to *Kras* controls. Considering the pancreatic atrophy phenotype, response of the cells to cell death inducers were analyzed, indicating that *Kras; FN∆panc* cell lines were more susceptible to necroptosis and ER stress inducers compared to *Kras* cell lines. In line with that, transcriptomics showed that Hypoxia signaling was the most enriched pathway in *Kras; FN∆panc* compared to *Kras* cell lines.

In summary, pancreas specific deletion of fibronectin had a double-edged effect in pancreatic cancer. During tumorigenesis, the role of FN should be considered as compartmental specific and clinical decision-making in pancreatic cancer should consider FN regulated therapeutic liabilities.

2 ZUSAMMENFASSUNG

Fibronektin (FN) ist ein wichtiger Bestandteil der extrazellulären Matrix (EZM), der die Wechselwirkung zwischen Zellen und der EZM unterstützt. Diese Wechselwirkung spielt eine wichtige Rolle bei der pankreatischen Karzinogenese. Eines der Hauptmerkmale des duktalen Adenokarzinoms des pankreas (PDAC) ist eine starke desmoplastische Reaktion. Welche Rolle FN bei der Tumorentwicklung und -progression spielt, wird sehr kontrovers diskutiert. Im Pankreaskarzinom wird Fibronektin hauptsächlich im Stroma exprimiert, weshalb sich auch die meisten Studien hauptsächlich auf die Rolle von FN im Tumorstroma konzentrieren. Wir haben jedoch gezeigt, dass FN auch in Pankreaskrebszellen exprimiert wird und dass die Erforschung seiner Rolle in diesem Zusammenhang sinnvoll ist.

Um die Pankreas-spezifische Rolle von Fibronektin zu untersuchen haben wir Mäuse generiert, die eine onkogene Kras-Mutation sowie eine homozygote Deletion von FN (Kras; FNΔpanc) aufweisen und sie mit Mäusen verglichen, die nur die onkogene Kras-Muatation (Kras) in ihren exokrinen Pankreaszellen aufweisen. Die Mäuse wurden zu bestimmten Zeitpunkten oder bei Anzeichen von Krankheit analysiert. Pankreata wurden gesammelt und mittels histopathologischer Analyse bewertet. Isolierte primäre Tumorzellen aus Kras und Kras; FNΔpanc Mäusen wurden charakterisiert und hinsichtlich ihres Ansprechens auf Behandlung mit herkömmlicher Chemotherapie, ER-Stress-Induktoren und Zelltodinduktoren analysiert. Zusätzlich wurden isolierte Zelllinien verwendet, um eine Transkriptomanalyse mit oder ohne Behandlung mittels Tunicamycin durchzuführen.

Zu frühen Zeitpunkten wurden bei Kras; FNΔpanc Mäusen der Verlust von Azinuszellen und ein reduziertes relatives Pankreasgewicht beobachtet. Obwohl die Deletion von FN weder die Kras-Aktivität noch die Progression intraepithelialer Neoplasien des Pankreas (PanIN) veränderte, wurde in den Pankreata von 9 Wochen alten Kras; FNΔpanc Mäusen eine höhere Anzahl von metaplastichen Strukturen (Acinär-duktale Metaplasie) gefunden, was darauf hinweist, dass die FN-Deletion die initiale Phase der Tumorentstehung antreibt. Dieser Effekt ging jedoch bei 18 Wochen alten Mäusen verloren und zwischen Kras und Kras; FNΔpanc Mäuse konnten keine Unterschiede in der Tumorentstehung beobachtet werden. Auch die Infiltration mit

Immunzellen war in 9 und 18-Wochen alten Kras; FNΔpanc Mäusen im Vergleich zu Kras Mäusen erhöht.

Zusätzlich führte die Induktion einer entzündungs-induzierten Karzinogenese durch die Injektion von Cerulein zu einem Verlust der Azinuszellen, vermehrter Infiltration mit Immunzellen und erhöhter Mikrokarzinombildung im Pankreas von Kras; FNΔpanc im Vergleich zu Kras Mäusen. Zwar zeigten Kras; FNΔpanc Überlebensmäuse, die bei offensichtlichen Anzeichen von Krankheit analysiert wurden, Anzeichen von Pankreasatrophie, Lipogenese und Mikrokarzinombildung, jedoch war die zu frühen Zeitpunkten beobachtete Stromareaktion eindeutig reduziert. Die Kaplan-Maier-Analyse zeigte, dass das mediane Überleben von Kras; FNΔpanc Mäusen im Vergleich zu Kras Mäusen signifikant reduziert war. Während die Tumorinzidenz bei Kras; FNΔpanc Mäusen höher war, war die Metastaseninzidenz im Vergleich zu Kras Kontrollen niedriger.

Unter Berücksichtigung des Phänotyps der Pankreasatrophie wurde die Reaktion der Zelle auf Zelltodinduktoren analysiert und Hinweise darauf gefunden, dass die aus Kras; FNΔpanc Tumoren isolierten Zelllinien im Vergleich zu Kras Zelllinien anfälliger für Nekroptose- und ER-Stressinduktoren sind. Dementsprechend zeigte die Transkriptomanalyse, dass von allen Signalwegen die Hypoxie Signalkaskade in Kras; FNΔpanc Zelllinien am stärksten angereichert war, im Vergleich zu Kras Zellen.

Zusammenfassend hat die pankreas-spezifische Deletion von FN eine doppelte Wirkung. Während der pankreatischen Karzinogenese sollte die Rolle von FN als kompartiment-spezifisch betrachtet und dies auch mit Hinblick auf therapeutische Strategien berücksichtigt werden.

3 TABLE OF CONTENT

Table of Contents

4 INTRODUCTION

4.1 Pancreas

4.1.1 Pancreatic Morphology and Physiology

The pancreas is a retroperitoneal organ located in the upper abdomen behind the stomach, surrounded by several organs and blood vessels. It is separated into three different parts known as head, body, and tail. The head is located near the duodenum and the tail extends to the hilum of the spleen. Slight functional differences between the regions exist and some diseases even have predilections for specific parts. Physiologically, the pancreas is a combined endocrine and exocrine gland closely associated with the upper duodenum. As such, it takes part in digestion by secreting proteases, lipases, and amylases into the intestine and it controls energy metabolism and storage throughout the body by producing hormones. The exocrine tissue consists of digestive enzyme secreting acinar cells, bicarbonate-secreting ductal-cells, and centro-acinar cells, which lie at the junction between acinar cells and terminal ductal epithelium; the endocrine tissue contains hormone-secreting islets. Interspersed between are inactive stellate cells (Grendell, 2014).

Embryonic development initiates from a multipotent cell population in the foregut endoderm. The endocrine and exocrine epithelium develops from common progenitor cells expressing Pdx1, Sox9, and Ptf1a. In the presence of factors such as Ngn3, NeuroD, Hnf6 and Pax4F, these cells contribute to endocrine proliferation and differentiation. Replacement of pro-endocrine factors with Mist1 and Ptf1a on the other hand shapes the exocrine compartment. Overall, Notch, Wnt and Hedgehog pathways are crucial for pancreatic development (Pandiri, 2014).

4.1.2 Pancreatic Pathologies

Acute pancreatitis (AP) is an inflammatory disease of the pancreas, usually caused by gallstones and alcohol misuse. Smoking can also be a risk factor for AP. Pathogenesis of AP involves improper conversion of trypsinogen to trypsin. Pancreatic duct blockage hinders the exocytosis of zymogenes from acinar cells. Consequently, zymogene granules merge with intracellular lysosomes containing lysosomal enzymes.

Lysosomal enzymes, especially Cathepsin B, can activate trypsinogens and turn them into trypsin, which accumulates in vacuoles and activates downstream digestive enzymes. These enzymes lead to autodigestive injury in acinar cells and the release of cytokines and vasoactive mediators, which induce edema and apoptosis. Subsequently, immune cells infiltrate, particularly macrophages and neutrophils, and produce tumor necrosis factor alpha (TGFα) and interleukin-1, 6, 8 (IL-1, IL-6, IL-8). These cytokines can then trigger an inflammatory cascade, causing systemic inflammatory response syndrome (SIRS) (Lankish, Lancet 2015).

Chronic pancreatitis (CP) is another pathological syndrome resulting in progressive inflammation and chronic fibrosis of the exocrine pancreas with permanent structural damage. CP has been demonstrated to have 25 % mortality rate (Hammad, Ditillo and Castanon, 2018). Moreover, studies reported that 12 % of patients with AP can ultimately progress to CP (Lew, Afghani and Pandol, no date). The most common cause of CP is chronic alcohol consumption. The exact mechanism is still not well known. Alcohol metabolites seem to exert a toxic effect on acinar cells by blocking endoplasmic reticulum activity ultimately leading to oxidative stress. Another risk factor is Tobacco smoking, which can increase CP-risk in a dose-dependent manner. 20 %-50 % of CP-cases in Western countries are non-alcoholic and non-tobacco associated and may arise due to metabolic diseases, genetic predispositions, and auto-immune diseases (Kleeff *et al.*, 2017). Additionally, CP is described as an important risk factor for pancreatic cancer (PC) (Lew, Afghani and Pandol, 2017).

Adenocarcinomas of ductal origin are the major subtypes of malignant pancreatic neoplasms; rare malignancies include neuroendocrine tumors, acinar carcinomas, colloid carcinomas, pancreatoblastomas, and solid-pseudopapillary neoplasms. Ductal adenocarcinoma currently is the fourth leading cause of cancer associated-mortality and expected to become second in line within the next decade (Kleeff *et al.*, 2016). Main risk factors are alcohol abuse, smoking, obesity, diabetes mellitus, family history, and genetic factors. Most patients are diagnosed late with locally advanced or metastatic tumor due to insufficient imaging and lack of symptoms in the early stage. Moreover, as a result of fast progression, high recurrence rate, undetected micro-metastasis, drug resistance and thus, lack of proper therapy, pancreatic cancer is related to very poor prognosis (Zeng *et al.*, 2019). Up to date, surgery with adjuvant chemotherapy is the only possible option for PC but only less than 20 % patients are

suitable for resection (Lafaro and Melstrom, 2019). In the last decade, gemcitabine has been used as a first-line treatment for advanced PC. However, in recent years, two combination therapies, namely Fluorouracil (5-FU)/Leucovorin with Irinotecan and Oxaliplatin (FOLFIRINOX) as well as Gemcitabine with nab-paclitaxel, have become a golden standard for metastatic PC treatment. A recent study demonstrated that FOLFORINOX as adjuvant therapy results in longer survival than gemcitabine in resected PC patients (Zeng *et al.*, 2019). Despite the recent improvements in treatments, the overall 5-year survival is still only 8 % (Lafaro and Melstrom, 2019).

PC possesses a complex mutational landscape. Activating mutation in the Kras oncogene is the most abundant genetic abnormality, occurring in 90 % of tumors (Makohon-Moore and Iacobuzio-Donahue, 2016). Inactivating mutations of TP53, CDKN2A, BRCA1/2, and, SMAD4 exist in over 50 % of pancreatic tumors analyzed with infrequently mutated genes having less than 5 % prevalence (Biankin and Maitra, 2015). However, targeting the genetic or epigenetic alterations has not been successful yet as a therapeutic agent against PDAC. Despite the heterogeneous mutational profile, mutated genes usually accumulate into molecular pathways involving TGFβ signaling, DNA repair, cell cycle regulation, chromatin regulation, and axon guidance. As a consequence of the mutations and pathways involved, pancreatic adenocarcinoma has been classified into four subtypes including squamous, pancreatic progenitor, immunogenic, and aberrantly differentiated endocrine exocrine (ADEX) (Bailey *et al.*, 2016). Ultimately, this classification may help to develop new therapeutic approaches and a conclusive, conventionally used solution resulting in better outcomes for PC patients.

4.1.3 Pancreatic Stromal Reaction and Tumor microenvironment

Biochemical and physical features of the tumor microenvironment (TME) significantly contribute to tumor progression and metastasis. TME is often described as a “wound that cannot heal” due to the resemblance of wound healing to desmoplastic stromal reaction. Presence of desmoplastic stromal reaction is one of the most outstanding features of pancreatic ductal adenocarcinoma (PDAC) (Chu *et al.*, 2007) and leads to exocrine and endocrine insufficiencies. The desmoplastic reaction consists of non-cellular and cellular stromal components such as extracellular matrix (ECM), activated fibroblasts and myofibroblasts, inflammatory cells, blood and lymphatic vessels.

Interaction between neoplastic and non-neoplastic cells in the TME leads to stimulation of an extensive desmoplastic reaction by activating multiple cancer-derived signaling pathways including transforming growth factor β (TGFβ), hepatocyte growth factor (HGF/Met), fibroblast growth factors (FGFs), insulin-like growth factor 1 (IGF-1), and epidermal growth factor (EGF) through autocrine and paracrine mechanisms (Ide *et al.*, 2006). Stimulation of the above pathways results in production of ECM-components such as proteoglycans, collagens, and fibronectin as well as catalytically active enzymes such as proteinases (Mahadevan and Von Hoff, 2007). Pancreatic stellate cells (PSCs) are the most prominent element of the desmoplastic reaction and the most predominant cell type of the pancreatic tumor stroma. In the normal pancreatic parenchyma, PSCs are inactivated carrying abundant Vitamin A and lipid droplets. Physiologically, PSCs play a role in phagocytosis, stimulation of amylase secretion, and immune reaction. During tumorigenesis, PDAC cells activate PSCs. Consequently, PSCs transform losing their lipid droplets and Vitamin A while elevating the production of alpha smooth muscle actin (a-SMA) and secreting ECM molecules, cytokines, and growth factors which in turn influence tumor progression and metastasis by altering pancreatic tissue architecture (Bynigeri *et al.*, 2017). These dramatic changes in the TME result in vascular dysfunction and hypovascularity rearranging the molecular signatures of cancer cells. Studies demonstrated that the stroma induced hypoxia causes modifications in gene expression of cancer cells and supports adaptation to the continuous alterations of the TME (Chan and Giaccia, 2007). Another study described upregulation of the multidrug-resistance gene by hypoxia-inducible-factor-1a (HIF-1a), revealing a mechanism by which the TME might influence chemotherapy (Comerford *et al.*, 2002).

The ECM is a 3D-like complex of proteoglycans and fibrous matrix proteins composed of collagen, fibronectin, laminins, which are mainly secreted by activated PSCs, and soluble factors such as cytokines, chemokines and growth factors. These components support tissue architecture by providing a physical and structural scaffold. In addition, ECM proteins produce plenty of biochemical signals that dynamically control cellular behavior and function. ECM remodeling is regulated by various enzymes such as matrix metalloproteinases (MMPs), lysly oxidase (LOX), tissue inhibitors of metalloproteinases (TIMPs), and cathepsins (Neesse *et al.*, 2011). In recent years, ECM proteins have become attractive biomarkers predicting clinical outcomes. One

study reported that expression of desmoplastic reaction markers, such as collagen and HA, negatively correlate with PDAC patient survival. A significant difference of collagen or HA expression between primary tumor and metastatic lesions could not be found (Whatcott *et al.*, 2015). On the other hand, Erkan et al proposed an independent prognostic marker for PDAC by quantifying the number of activated PSCs and collagen deposition in resected pancreas samples of PDAC patients, labeled activated stroma index (ASI). They showed that whereas high collagen deposition and low stromal activity associated with a better prognosis, low collagen deposition and high stromal activity correlated with worse patient outcome, emphasizing once more the clinical relevance and importance of TME in tumor progression (Erkan *et al.*, 2008). Overall, the results are still contradicting, highlighting that we have not yet fully comprehended the role of ECM components in PC.

Resistance to chemotherapy is a major problem in cancer treatment leading to more aggressive and metastatic cancer cells. Underlying mechanisms of chemoresistance comprise epithelial to mesenchymal transition (EMT), apoptosis evasion, intratumor heterogeneity, increased drug efflux, enhanced DNA repair, and TME characteristics (Uzunparmak and Sahin, 2019). Chemoresistance in cancer cells is usually connected to heterogeneity within tumor cells resulting from genetic and epigenetic alterations affecting drug responsiveness. In addition, differences in the TME in terms of stromal cell composition, oxygenation, and acidity play an important role. Moreover, ECM components can generate a barrier around the cancer preventing effective drug delivery (Senthebane *et al.*, 2017). In the light of these properties, research has focused on tumor-stroma relationship and development of stroma targeted therapies. In 2009, Olive et al demonstrated that the Hedgehog pathway inhibitor, IPI-926, enhanced Gemcitabine perfusion by increasing the density of blood vessels and ultimately the overall survival of mice (Olive *et al.*, 2009). HA is an extracellular component elevated in pancreatic cancer and can lead to poor vascularity and inhibition of drug delivery. Along these lines a study showed that pegylated human recombinant PH20 Hyaluronidase (PEGPH20) increased the efficacy of Gemcitabine delivery and again improved overall survival (Provenzano *et al.*, 2012). Due to the promising preclinical results, stroma depleting agents and sonic hedgehog inhibitors are now used in clinical trials. Recently, combination therapy of PEGPH20 with nab-paclitaxel and gemcitabine has been analyzed in Phase II studies, showing enhanced

progression free survival (Hingorani *et al.*, 2018). However, Ramanathan et.al reported early terminations of treatment with the combination of PEGPH20 and FOLFIRINOX because of high toxicity (Ramanathan *et al.*, 2018). Another phase II trial of sonic hedgehog inhibitor IPI-926 (Saridegib) in combination with Gemcitabine reported reduced overall survival compared to placebo control (*Infinity Reports Update from Phase 2 Study of Saridegib Plus Gemcitabine in Patients with Metastatic Pancreatic Cancer | Business Wire*, no date) Moreover, the Phase III trial of PEGPH20 in combination with Nab-paclitaxel and Gemcitabine was terminated due to the lack of benefit over standard care. Considering all the controversial results obtained from the above clinical studies, a “back to the bench” approach has been adopted. Researchers showed that stroma depletion after inhibition of a-SMA, genetically accelerated pancreatic cancer and was characterized by decreased survival and no benefits in Gemcitabine treatment (Özdemir *et al.*, 2014). Consistently, another study demonstrated that impeding sonic hedgehog signaling chemically and genetically results in more aggressive tumors and does not any affect Gemcitabine therapy (Rhim *et al.*, 2014). Thus, tumor stroma seems to consist of elements, which can either increase or confine tumor progression. Accordingly, a recent study focused on the different roles of stroma derived and tumor cell derived ECM proteins through mass spectrometry based proteomics. They showed that whereas ECM components secreted by tumor cells coincided with poor patient survival, those produced by stroma correlated with both improved and poor patient survival (Tian *et al.*, 2019). Therefore, non-selective stroma depletion can result in worsened patient outcome suggesting that more detailed understanding of stromal elements is necessary to detect plausible biomarkers for patient stratification and precise targets for treatment.

4.2 Fibronectin

Fibronectin (FN) was firstly discovered as a high-molecular weight fibroblast cell surface antigen in 1970s (Hynes, 1973) (Ruoslahti *et al.*, 1973). FN is abundantly found in the ECM and body fluid (Kaspar, Zardi and Neri, 2006) regulating cellular and developmental processes including cell adhesion, migration, growth, proliferation, and wound healing. Moreover, it maintains direct tissue organization and ECM composition by guiding ECM protein assembly, including collagen I and II, fibrilin-1, fibulin-1, latent TGFβ binding protein-1, fibrinogen, thrombosphondin-1, and tenascin-C. Importantly,

FN is required for the initiation and stabilization of ECM assembly (Kumra and Reinhardt, 2016). Regarding its localization, as Yamada reported at 1978, FN appears extracellularly as fibrillary structures under and between cells as well as intracellularly in form of diffused granular particles. Intracellular localization of FN occurs after synthesis and before secretion from the cell surface in Endoplasmic reticulum (Yamada, 1978). Subsequently, FN is secreted as a dimer composed of two 250 kDA subunits covalently linked by a pair of disulfide bonds near the C-termini. Each monomer consists of an array of multiple repeated protein domains termed FNI, FNII and FNIII, characterized by binding affinities to varying ECM proteins and cell surface integrin receptors. While Type I FN has affinity to fibrin, collagen, and heparin, Type II FN only exists in the collagen-binding domain whereas Type III FN is part of the cellular binding region (Lenselink, 2015). In total, FN contains 12 FNI, 2 FNII, and 15-17 FNIII domains (Schwarzbauer and DeSimone, 2011).

Even though FN is encoded by a single gene, alternative splicing of the precursor mRNA and post-translational modifications allow formation of multiple isoforms. Splicing occurs in three regions namely in two exons corresponding to FNIII domains, known as EDA (extra-domain A) or EIIIA and EDB (extra-domain B) or EIIIB, and near the C-terminal end, known as variable (V) or IIICS (type-III connecting segment). Hence, cellular FN consists of a heterogeneous isoform group with up to 20 variants in human. The alternative splicing events result in two main FN types, soluble plasma FN and insoluble cellular FN (To *et al.*, 2011). Soluble plasma FN (pFN) is synthesized by hepatocytes and secreted into the blood plasma and other body fluids. pFN, contains only the V domain and is a major component of fibrin clots. It can non-covalently interact with fibrin molecules via FNI1-5 and FNI10-12 domains (Han and Lu, 2017a). Initiation of the coagulation cascade leads to covalent crosslinks between FN and fibrin via N-terminal glutamine residues. FN incorporation into the fibrin matrix is crucial for differentiating platelet function, including adhesion, migration, and aggregation (To *et al.*, 2011) (Kumra and Reinhardt, 2016). On the other hand, cellular FN is produced by various cell types such as endothelial cells, fibroblasts, chondrocytes, synovial cells and myocytes. It is a product of fibrilogenesis (polymerization of FNs), which creates a multidimensional platform that can interact with other ECM molecules and cell surface receptors (Han and Lu, 2017b). Cellular FN consists of different FN isoforms formed by alternative splicing of EDA, EDB, and

V domains. The EDA domain regulates various processes including cell adhesion, myofibroblast differentiation, wound healing, cell cycle progression, and mitogenic signal transduction. The role of the EDB domain is not well known. However, some studies describe that EDB deficiency results in delays of cell growth and matrix assembly (Kaspar, Zardi and Neri, 2006).

4.2.1 Role of Fibronectin in Cancer

FN participates in tissue homeostasis affecting cell growth, migration, differentiation, wound healing, and blood coagulation. In tumors FN expression is elevated enhancing growth, invasion, migration, and chemoresistance (Stenman and Vaheri, 1981)(Wang and Hielscher, 2017).

As aforementioned above, FN has a pivotal role in the interaction between cells and ECM. FN signaling is mediated by integrin receptors, the most well-defined receptors for FN. Integrin receptors consist of α and β subunits that facilitate interaction between cells and ECM. Even though FN can interact with different β1 and β3 integrins, $\alpha5\beta1$ integrin is the major receptor for FN (Kim *et al.*, 2000). Through integrin binding FN orchestrates important cellular process such as cell proliferation, adhesion differentiation, and migration in various cell types (Harburger and Calderwood, 2009). Accordingly, multiple researches have focused on FN-stimulated integrin signaling. A study reported that FN induces phosphorylation of PI3K in bronchial epithelial cells subsequently activating the downstream PI3K/AKT pathway thereby resulting in Cyclin D1 upregulation and p21/p53 downregulation (Han and Roman, 2006). In cancer, the pro-survival mode of FN is regulated through FAK dependent PI3K/AKT/mTOR pathway. Activation of this cascade diminishes apoptosis by upregulating Bcl2 expression thus blocking cytochrome-c release from mitochondria (Han, Khuri and Roman, 2006) (Czabotar *et al.*, 2014). In addition, FN-stimulated FAK activation promotes cell proliferation by activating Ras pathway through the recruitment of SH2-binding proteins like Grb2 and Src (T, 1994). Similarly, the role of FN in PI3K/AKT activation through $\alpha5\beta1$ integrin receptor has been identified in non-small lung carcinoma and in breast cancer (Ritzenthaler, Han and Roman, 2008) (Korah, Boots and Wieder, 2004) (Han, Khuri and Roman, 2006). So far a lot of evidence exists showing the contribution of full length FN to tumorigenesis. Isoforms of FN, such as EDA and EDB variants, are also implicated in tumor growth regulation. EDA and EDB

variants are even referred to as oncofetal variants, since they are expressed at the time of development and thereafter re-expressed during tumorigenesis (Kumra and Reinhardt, 2016). For example, EDA-FN is highly expressed in the vasculature of liver metastasis from F9 teratocarcinoma cells compared to the healthy organs in a murine model (Rybak *et al.*, 2007). Another study reported that high EDA-FN expression induces tumor growth and elevates pro-angiogenic cytokine vascular endothelial growth factor-C (VEGF-C) levels via PI3K/AKT pathway in colorectal cancer cells (Xiang *et al.*, 2012). All the above studies suggest a key role for the FN- integrin receptor interaction in facilitating tumor cell proliferation and survival.

Immunohistochemical analysis of FN has been performed in many cancer types including lung, esophageal, breast, and thyroid cancer. Bea et al showed that cancer and stromal cell derived FN is associated with aggressiveness of breast cancer. Patients with FN expression in cancer cells exhibit deteriorated clinical outcome with poor overall and disease free survival (Bae *et al.*, 2013). Similarly, another study showed that colorectal cancer patients with low FN survive longer compared to those with high FN expression. In addition, knock down of FN impedes proliferation, migration, and invasion of colorectal cancer cells and results in cell cycle arrest with subsequent apoptosis induction (Yi *et al.*, 2016).

Most of cancer-related deaths are associated with metastasis. Metastatic lesions arise from disseminated cells, which are often in a dormant state. Functional characterization of cells in the dormant state is thus of utmost importance to impede disease progression (Aguirre-Ghiso, 2007). Strikingly, a recent study demonstrated that TGFβ-dependent FN assembly in breast cancer cell lines coincides with the commencement of a serum-deprivation-derived dormancy state through αvβ1 and α5β1 integrin mediated adhesion and ROCK-generated cell tension. After the dormant state, cells recover by degrading the deposited FN through activation of MMP2. Therefore, targeting the mechanism of dynamic FN assembly and disassembly could be essential to eliminate dormant cells and prevent their reactivation (Barney *et al.*, 2020).

Besides the importance of FN in tumor progression, contribution of FN to EMT, which converts polarized epithelial cells into a mesenchymal phenotype, has been well described. TGFβ, which is major inducer of EMT, stimulates expression and secretion

of FN into the ECM resulting in enhanced cell motility (Ignotz and Massague, 1986). This is reversed by the inhibition of Snail and Smad, the major transcription factors of TGFβ (Olmeda *et al.*, 2007). Accordingly, plenty of researches have demonstrated a contribution of FN to invasion and metastasis. For instance, Balanis et al reported that addition of FN to 3D-cultivated breast cancer cells promotes cellular outgrowth and increases metastatic capacity (Balanis *et al.*, 2013). Another study found that FN stimulated FAK phosphorylation activates downstream proteins ERK1/2 and PI3K/AKT inducing invasion and migration of lung cancer cells in trans-well chambers (Meng *et al.*, 2009). Moreover, human glioblastoma cells expressing FN enhance angiogenic tumor growth, invasion, and resistance to ionizing irradiation (Serres *et al.*, 2014).

Studies also showed that FN is implicated in chemoresistance. Co-incubation of human and mouse breast cancer cells with FN enables cancer cells to resist tamoxifen via B1-integrin mediated PI3K/AKT and MAPK/ERK1/2 pathways (Pontiggia *et al.*, 2012). Similarly, another study reported that FN and B1-integrin expression is considerably elevated in tamoxifen insensitive compared to tamoxifen sensitive breast cancer cells (J. Yuan *et al.*, 2015). Moreover, researchers also analyzed the interaction of cells with fibronectin regarding cytotoxicity of EGF receptor inhibitor cetuximab. For example, human non-small lung carcinoma cell lines cultured on top of a FN-coated surface were characterized by reduced cytotoxicity to cetuximab and radiation. Along the same lines, cetuximab increased the expression of FN via p38-MAPK-ATF2 signaling pathway and accordingly knockdown of FN enhanced Cetuximab cytotoxicity (Eke *et al.*, 2013).

Altogether, these results highlight the importance of FN as a guardian of cell survival and chemoresistance.

4.2.2 Role of Fibronectin in Pancreatic Cancer

One hallmark of pancreas cancer is the desmoplastic stromal reaction that can constitute 90% of the tumor mass (Lafaro and Melstrom, 2019). As described above, FN is an integrin binding protein that is upregulated in many solid tumors, especially in PDAC, and it is one of the essential stromal components transmitting multiple signaling pathways in PDAC.

One earlier study showed that the human PDAC cell line Mia Paca-2 plated onto FN-coated dishes displayed integrin dependent elevation in Interleukin-8 (IL-8), an essential chemokine for PDAC progression and metastasis (Shi *et al.*, 1999). In addition, seeding human PDAC cell lines Panc-1 and Capan-1 on FN-coated plates augmented resistance to chemotherapeutic agents such as doxorubicin, gemcitabine, and cisplatin (Miyamoto *et al.*, 2004). Indeed, PSC secreted FN implements resistance of human PDAC cell lines to Gemcitabine by increasing ERK1/2 activity and protecting cells from gemcitabine induced cytotoxicity. FN or MEK/ERK inhibition counteracts Gemcitabine insensitivity suggesting that the combination therapy of gemcitabine with a FN or MEK/ERK inhibitor could overcome resistance (Hu *et al.*, 2019).

Survival of pancreatic cancer cells is also increased by FN induced ROS production. Modest increase in ROS molecules can promote proliferation and survival through Ras-Raf-MEK-ERK and NFkB signaling pathways respectively (Reuter *et al.*, 2010). One study found that Capan-1, Panc-1, and Mia Paca-2 cell lines cultivated on FN coated plates, activated NADPH-oxidase and 5-lipoxygenase-dependent ROS production. Subsequently, survival of the cells was increased and accordingly antioxidants could reverse the effect (Edderkaoui *et al.*, 2005).

FN stimulates cell motility and metastasis, a fact well established in multiple cancer types including PDAC. One study described Pak1, which is highly expressed in pancreatic cancer, as a novel FN regulator. Induction of FN by Pak1 is mediated by the NFkB-p65 pathway subsequently enhancing invasion of human pancreatic cancer cells (Jagadeeshan *et al.*, 2014). Strikingly, another study found that the Wnt2 gene is enriched in circulating tumor cells (CTCs) isolated form a mouse pancreatic cancer model, where Wnt2 inhibits anoikis and augments anchorage-independent sphere formation. Overexpression of Wnt2 leads to upregulation of FN whereas FN knockdown impedes the effect of Wnt2 on anchorage dependent growth (Yu *et al.*, 2012). Recently, another study proved a prominent role for FN in liver metastasis of murine pancreatic cancer. Costa-silva et al found that PDAC derived exosomes shape the pre-metastatic niche by inducing TGFβ secretion from Kupffer cells, which subsequently induce production of FN only. Other ECM components are not produced. Bone-marrow derived macrophages and granulocytes then interact with FN-expressing hepatic stellate cells ultimately forming the pre-metastatic niche (Costa-Silva *et al.*, 2015).

“Matricellular proteins” are extracellular components without structural function in the matrix regulating ECM-receptor interactions. One is Fibulin-5, which competes with FN in the FN-integrin interaction (Lomas *et al.*, 2007). Topalovski et al reported that Fibulin-5 expression is elevated in pancreatic stroma compared to normal pancreas. In addition, it enhances PDAC progression by interfering with integrin binding and hence, blocking FN-mediated, Integrin-induced ROS production (Topalovski *et al.*, 2016). Another matricellular protein found in the pancreatic stroma is Tenascin-C. It interacts with different ECM components and integrin receptors. It co-localizes with FN and acts as endogenous inhibitor of FN signaling by blocking the interaction of FN with integrin (Chiquet-Ehrismann *et al.*, 1988)(Paron *et al.*, 2011). Another study described that cytokine endothelial monocyte activating polypeptide II (EMAP II) represses proliferation and angiogenesis of PDAC through impeding the FN-Integrin interaction (Schwarz *et al.*, 2010). In short, understanding of matricellular proteins could be necessary to consider novel ways targeting FN-Integrin signaling.

As aforementioned above, tumor heterogeneity is one of the major obstacles in chemotherapy. Strikingly, a recent study demonstrated contribution of cancer associated fibroblasts (CAFs) to pancreatic tumor heterogeneity through combining single cell RNA sequencing (scRNAseq) and protein analytics. Co-culturing PDAC cells with medium or low CAF content resulted in distinct phenotypes characterized by either invasive epithelial-mesenchymal transition (EMT) or proliferation (PRO). Ki67 and FN were used as markers for the PRO and EMT phenotypes respectively. Surprisingly, in the highest CAF content condition, a subpopulation of cells with PRO and EMT phenotypes simultaneously was identified, named double-positive (DP). In DP cells, MAPK and STAT3 pathways were activated increasing the MEK and STAT3 inhibitor combination treatment sensitivity. The existence of these phenotypes was also validated in human PDAC samples, which were classified depending on their DP, EMT, PRO, and double negative cellular composition. Consequently 8 different tumor glands were described. Importantly, tumor glands including DP or EMT cells significantly correlated with poor patient survival, whereas glands having only PRO cells associated with improved survival (Ligorio *et al.*, 2019). Taken together, these data highlighted a significant contribution of the stroma to pancreatic tumor heterogeneity with profound impacts on tumor biology, chemotherapy response, and patient outcomes. Also, quantifying distinct

protein expressions among pancreatic cancer cells, like in the case of FN, could be beneficial for patient stratification and determination of therapeutic efficacy.

4.3 ER stress in pancreatic cancer

The proliferation capacity of tumor cells goes hand in hand with their ability to evade apoptosis. Because of that, apoptosis induction has been focused on as a target for cancer therapy (Reed, 1999). Two main mechanisms control apoptosis: the extrinsic and the intrinsic pathway. The intrinsic apoptotic pathway, also known as the mitochondrial mediated apoptotic pathway, encompasses permeabilization of the mitochondrial outer membrane (MOMP), an event resulting in the release of cytochrome C and subsequent caspase-9 and caspase-3 cleavage. The extrinsic apoptotic pathway is mediated by death receptors, which activate the FAS-associated death domain (FADD) consequently forming the death inducing signaling complex (DISC), which in turn stimulates the downstream caspases 8,7,6, and 3 (Fulda and Debatin, 2006). Interestingly, studies have demonstrated a role for the Endoplasmic Reticulum (ER) in determining cell fate, as the cellular stress response triggered by misfolded proteins can ultimately lead to apoptosis (Kim, Xu and Reed, 2008).

The ER is a specialized organelle exerting essential functions such as maintenance of intracellular Ca^{+} homeostasis and synthesis, assembly, folding, transportation, and degradation of proteins destined for the plasma membrane or the extracellular space. All steps in the ER-mediated cascades are tightly controlled. Unfolded or misfolded protein accumulation rapidly induces ER stress and the unfolded protein response (UPR). The UPR is an intricate signaling event with the purpose to diminish protein synthesis while elevating the ER-folding capacity. Upon success of the UPR, protein synthesis proceeds and cellular homeostasis is reestablished. On the other hand, if ER stress continues, the UPR will induce oxidative stress and cell death (Wang and Kaufman, 2016).

ER stress is regulated by three receptors which are located in the ER membrane; Protein Kinase-R like ER Kinase (PERK), inositol-requiring protein 1α (IRE1α), and cyclic AMP-dependent transcription factor 6α (ATF6α) (Wu, Ng and Thibault, 2014). In non-stress conditions, the ER chaperone binding protein (BiP), also called 78 kD glucose related protein (GRP78), binds to PERK and IRE1α, keeping them inactive.

Increasing amounts of misfolded proteins attach to Bip, which in turn releases PERK and IRE1α initiating their dimerization, auto-phosphorylation, and thus activation (Carrara *et al.*, 2015). Active PERK subsequently phosphorylates the eukaryotic translation initiation factor 2 α (eif2α) to cease protein translation. Phosphorylation of IRE1α stimulates its own RNAase subunit, which splices 26 nucleotides from XBP1 mRNA resulting in the active form of XBP1, a multifunctional transcriptional factor. ATF6α is a transcription factor, which initiates gene transcription upon dissociation from Bip. All three pathways of the UPR orchestrate ER stress with the ultimate goal to restore homeostasis (Hetz and Papa, 2018).

ER stress and UPR activation have been connected to pathologic conditions such as cardiovascular diseases, neurodegenerative diseases, and cancer. UPR-associated proteins, like GRP78 and XBP1, are upregulated in ischemic regions of tumors *in vivo* and are overexpressed *in vitro* in cells under hypoxic conditions. Importantly, ER stress and the subsequent protective action of UPR occur in rapidly proliferating cells, overwriting the suppressive signals of low oxygen and nutrient stress. Therefore, blocking the vital components of the UPR could be a significant therapeutic option preventing adaptation of cells to an inhospitable environment (Jeffrey *et al.*, 2008)(Shuda *et al.*, 2003).

The exocrine pancreas is essential in enabling food digestion and maintaining energy homeostasis. Particularly, exocrine pancreatic acinar cells produce digestive proenzymes including proelastase, trypsinogen, and chymotrypsinogen in addition to a bicarbonate rich fluid for effective dietary intake. To comply with the high enzymatic demand, acinar cells exhibit one of the fastest protein synthesis rates among all organs of the body. Thus, the necessity of ER homeostasis and ER stress relief is unequivocal (Kubisch and Logsdon, 2008). GRP78 has been shown to be upregulated in PDAC cancer cells compared to healthy cells and associated with poor prognosis and chemoresistance (Niu *et al.*, 2015). In addition, overexpression of GRP78 enhances the invasive capacity of PDAC cells by activating FAK and JNK proteins (X. P. Yuan *et al.*, 2015). Furthermore, GRP78 significantly affects chemoresistance. Downregulation of GRP78 sensitizes PDAC to multiple chemotherapeutic agents through decreasing ABC transporter activity (Dauer *et al.*, 2018). Along the same lines, ATF4, a transcription factor activated by PERK, is connected to tumor cell survival and overexpressed in pancreatic neuroendocrine tumors (Klieser *et al.*, 2015).

Interestingly, Gemcitabine treatment upregulates ATF4 expression in PDAC cells. Therefore, ATF4 downregulation could be a promising treatment option in combination with Gemcitabine ultimately stimulating apoptosis (Palam *et al.*, 2015). IRE1α activates the transcription factor XBP1, which in turn regulates other ER stress response genes. Overexpression of XBP1 in PDAC cells has been reported highlighting the importance of IRE1α/XBP1 inhibition as a target for anticancer therapies (Koong, Chauhan and Romero-Ramirez, 2006). ATF6α is another important player in the ER stress response. ATF6α activation occurs in the Golgi apparatus triggering its translocation to the nucleus where it regulates expression of survival genes to neutralize ER stress and block apoptosis. One study reported that downregulation of ATF6α stimulates apoptosis in pancreatic neuroendocrine tumors through p38 activation (Teodoro *et al.*, 2012). Furthermore, high expression of ATF6α and low expression of activated p38 has been associated with poor patient outcome (Martinez-Useros *et al.*, 2015).

Interestingly, a recent study showed that latent metastasis after primary tumor resection with the ability to form bigger lesions, requires quiescent cancer cells lacking CK19 and MHCI. Single cell RNAseq of disseminated cancer cells showed that while PERK pathway is activated, IRE1α pathway is not active, suggesting unresolved ER stress. When ER stress is pharmacologically relieved, cells start to express MHCI and CK19 and are able to fully grow out of the single seeds. Together, unresolved ER stress permits disseminated cancer cells to evade immunity and assemble hidden metastatic colonies (Pommier *et al.*, 2018).

ER stress response has recently attracted considerable attention as a therapeutic approach targeting proliferating or dormant cancer cells which originate from many cancer types. However, few reliable studies exist concerning PDAC related ER stress. Nevertheless, inducting chronic ER stress or limited ER stress could represent beneficial options to promote chemosensitivity, apoptosis, or cell cycle arrest in cancer cells.

4.4 Aim

The primary purpose of this study was to uncover the pancreas specific role of *FN* in pancreatic carcinogenesis by using an *in vivo* mouse model of pancreatic cancer. *FN* was homozygously deleted in the pancreas of *Kras* G12D expressing mice (*Kras; FNΔpanc*) and compared to only *Kras* G12D expressing controls (*Kras*). Pancreata from mice with aforementioned genotypes were subsequently analyzed by histology and immunohistochemistry at different time points (4, 9, 18 weeks, and endpoint determined by state of sickness). Tumor cells were isolated and characterized by immunoblotting and proliferation assay. Sensitivity of the isolated cells to different cell death/ ER stress pathways was examined via treatment with cell death and ER stress inducers. Transcriptomics analysis was then performed to understand the prominent differences between isolated cell lines with or without ER stress induction (Tunicamycin). In order to reach clinical relevance, the role of pancreas specific *FN* deletion was also analyzed in *p53* deleted and *Kras* G12D expressing mice (*Kras; p53Δ; FNΔpanc).* Pancreata were described by histology and isolated cells were characterized in more detail. In addition, the effect of pancreas specific *FN* deletion was also investigated in the context of experimental (cerulein-induced) pancreatitis. Histology and immunohistochemistry were applied to assess changes in pancreatic morphology.

5 MATERIALS AND METHODS

5.1 Mice

5.1.1 Mouse models

- *FN1*$^{flox/flox}$(Sakai *et al.*, 2001): Exon 1 of *FN1* gene is flanked by two loxP sites.
- *Ptf1a-cre*^{ex1} (Nakhai *et al.*, 2007): Exon 1 part of the *Ptf1a* locus is replaced with the *Cre* recombinase.
- *LSL-Kras*^{G12D} knock-in mouse (Jackson *et al.*, 2001): *Kras*$^{LSL-G12D}$ strain contain a *Kras* point mutation (G12D) whose expression is inhibited by the *loxP*-sided stop codon. Due to the Cre-mediated recombination, the stop codon is removed and allow the expression of oncogenic *Kras* protein.
- *Trp53*^{tm1Brm} *(P53*$^{flox/flox}$*)* (Marino *et al.*, 2000)*:* Exons 2-10 are flanked by loxP sites.

Mouse strain combinations included:
FN$^{flox/flox}$*, Ptf1a-cre*^{exon1}*, LSL-Kras*^{G12D} mouse strains were interbred to generate compound mutant *FN*$^{lox/flox}$; *Ptf1a-cre*^{exon1}*; LSL-Kras*^{G12D} (termed as Kras; FNΔpanc),) *and Ptf1a-cre*^{exon1}*; LSL-Kras*^{G12D} (termed as Kras). *FN*$^{flox/flox}$*, Ptf1a-cre*^{exon1}*, LSL-Kras*^{G12D} *and Trp53*^{tm1Brm} mouse strains were interbred to generate compound mutant *FN*$^{lox/flox}$; *Ptf1a-cre*^{exon1}*; P53*$^{flox/flox}$*; LSL-Kras*^{G12D} (termed as Kras; p53Δ; FNΔpanc),) *and Ptf1a-cre*^{exon1}*; P53*$^{flox/flox}$*; LSL-Kras*^{G12D} (termed as Kras; p53Δ;panc) Littermate mice without *Ptf1a-cre*^{exon1} expression were used for orthotopic transplantation.

In this study, mice were bred and held in a specific pathogen-free (SPF) animal housing facility with free access to food and water for all the experiments. All mouse-related procedures were evaluated and reviewed by the Zentrum für Präklinische Forschung of the Technische Universität München, which follows the federal German guidelines for ethical animal treatment (Regierung von Oberbayern).

5.1.2 Orthotopic Transplantation

8-week-old *Kras; FNΔpanc* without *Ptf1a-cre*^{ex1} mice were transplanted orthotopically with either *Kras; p53Δ;panc* or *Kras; p53Δ; FNΔpanc* murine tumor cells. Cells were resuspended in DMEM without additions (Thermo Fisher, Dulbecco's Modified Eagle Medium, no glucose, no glutamine, no phenol red), each mouse was injected with 1x 10^6 cells using a 26G needle. Transplanted mice were sacrificed 4 weeks after transplantation or earlier in case of morbidity. Pancreatic tissues and other tissues like liver, lung, duodenum, kidney, spleen, and lymph nodes were collected if required, and embedded in paraffin blocks. Tissues were cut by microtome and stained with hematoxylin and eosin (H&E).

5.1.3 Acute Pancreatitis Model

For cerulein induced pancreatitis, 8-12-week-old *FNflox* and *FNΔpanc* mice were injected intraperitoneally with 0.1 g/ g body weight of cerulein (American peptide Cerulein 46-1-50) in saline 8 times over the course of 8 hours. After 24h, mice were sacrificed, and pancreas histology was analyzed. To detect the pancreatic regeneration, mice received intraperitoneal injections of cerulein two days in a row and mice were sacrificed after 3 days.

5.1.4 Chronic Pancreatitis Model

Chronic cerulein injections into *Kras* and *Kras; FNΔpanc* mice has been performed to induce inflammation driven carcinogenesis of PDAC. The cholecystokinin analog cerulein, which leads to pancreatic inflammation and damage by activating pancreatic enzymes, is used to stimulate chronic pancreatitis. 8-week-old mice were injected intraperitoneally for 5 days, once a day with 100 µl of 0.2 µg/ µl stock (American peptide Cerulein 46-1-50) per mouse and sacrificed one month after the last injection.

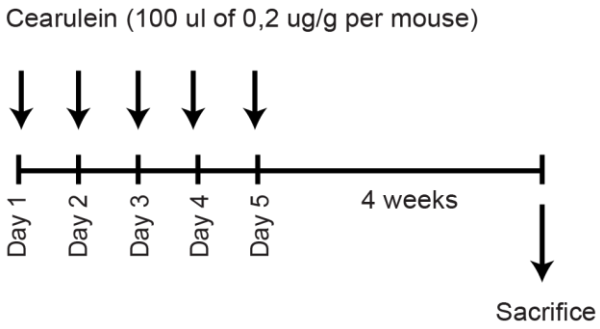

Schema 1: Schedule of Chronic Pancreatitis Induction

5.2 DNA/RNA studies

5.2.1 Mouse genotyping

Mouse Genotyping was performed on DNA extracted from the tail tip of mice. Tail tips were obtained from 4-week-old mice and were lysed in Tail Lysis Buffer (#102-T Viagen Biotech Inc) for overnight at 55°C. After incubation with lysis Buffer, samples were thoroughly mixed and incubated for 1 hour at 85°C to inactivate Proteinase K. Genotyping PCR was performed with 2 µl of DNA using the GreenTaq Ready Mix (KAPA2G Fast Hotstart Genotyping mix). A standard PCR protocol is indicated below (Table 1). All primers (Table 2) were used at a final concentration of 10 pmol. After sacrifice, post-genotyping is also performed to verify the genotype.

Step	Temperature	Time	Cycle number
Pre-incubation	95°C	5 min	1x
Amplification	95°C 60°C 72°C	30 secs 30sec 60 secs	35x
Cooling	4°C	∞	1x

Table 1: Genotyping PCR standard protocol

Name	Primer forward (5´-3´)	Primer reverse (5´-3´)	Product (bp)
FN1$^{F/F}$	GTACTGTCCCATATA AGCCTCTG	CTGAGCATCTTGAGTG GATGGGA	Wildtype: 250 Floxed: 300
FN1 recombi-nation	GTACTGTCCCATATA AGCCTCTG	CAGAAGAATTGCTCCC AAGT	Cre recombin-ation: 288 No recombin-ation: 1100
Kras	GTCTTTCCCCAGCA CAGTGC	AGCTAGCCACCATGGC TTGAGTAAGTCTGCA	Wildtype: 622 Mutated: 500
	CTCTTGCCTACGCCACCAGCTC		
Cre	ACCAGCCAGCTATC AACTCG	TTACATTGGTCCAGCC ACC	Wildtype: 350 Mutated: 200
	CTAGGCCACAGAAT TGAAAGATCT	GTAGGTGGAAATTCTA GCATCATCC	

Table 2: Genotyping primer sequences and product sizes.

5.2.2 Agarose gel electrophoresis

For agarose gel preparation, agarose (Biozym, Hess. Oldendorf) was dissolved in 1xTAE-Buffer (0.4 M Tris, 0.2 M acetic glacial acid, 0.01 M EDTA x NA_2 x $2H_2O$) by heating in microwave. Optimal percentage of gel was chosen based on the PCR product size. After agarose solution was cooled down to approximately 50°C, 5 µl of RotiGel Stain (Carl Roth Gmbh) for each 100 ml agarose solution was added. The agarose solution was poured into an electrophoresis chamber and cooled down to polymerize. PCR-products diluted in loading buffer (peqGOLD DNA Ladder Mix VWR) along with a DNA-ladder (peqGOLD DNA Ladder Mix VWR, 10 kb) were run horizontally at 100 V. Gel was visualized under UV-light (EX/EM 312/516-518 nm, GelDoc^{TM}XR system)

5.2.3 RNA extraction

After mice were sacrificed, small parts of pancreas were removed from three different regions and immediately homogenized in RLT lysis buffer (1015762 Qiagen, Hilden,

Germany) supplemented with 1% β-mercaptoethanol (M6250 Sigma) and then snap frozen in liquid nitrogen. RNeasy Mini Kit (74104 Qiagen) was used to extract RNA from lysed pancreas samples of *Kras* and *Kras; FNΔpanc* and tumor isolated cell lines. NanoDrop 2000 spectrophotometer (Peqlab, Erlangen, Germany) was used to measure RNA concentration and RNA purity through the absorbance ratios at 260 nm/280 nm and 260 nm/230 nm.

5.2.4 cDNA synthesis

Complementary DNA (cDNA) was synthesized by SuperScript II Reverse Transcriptase (#18064-014 Invitrogen, Darmstadt Germany) along with 1-5 µg RNA at 55 °C. The reaction mix consist of dNTPs, oligo(dt) primers, First Strand reaction buffer (#Y02321 Invitrogen) and DTT (#Y00147 Invitrogen). Concentration equivalency of cDNAs obtained from the reaction were verified

5.2.5 Quantitative real time PCR analysis

Quantitative RT-PCR was performed using the LightCycler 480 Sybr Green Master Mix 1 (#04887352001 Roche) along with 1 µl of cDNA as a template and 10 µM of target gene primer on a LightCycler 480 (Roche). Reaction conditions are indicated below in Table 3. Target mRNA expression was normalized to housekeeping genes which are endogenous *Cyclophilin* for pancreatic tissue and endogenous *GAPDH* for tumor cells and quantified by the delta-delta CT method ($2^{\text{DeltaCT (Housekeeping gene) – DeltaCT (target gene)}}$). Melting curves were also analyzed to verify primer specificity. Primers are listed in table 4.

Step	Temperature	Time	Cycle number
Pre-incubation	95°C	10 min	1x
Amplification	95°C	10 sec	45x
	60°C	20 sec	
	72°C	10 sec	

Melting	95°C 55°C 98°C	1 min 1 sec Continuous 0.11°C/sec	5 acquisitions/sec
Cooling	37°C	5 min	1x

Table 3: qRT-PCR program

Name	Primer forward (5´-3´)	Primer reverse (5´-3´)
FN	TGTACCATTGCAAATCGCTGC	CCATTCCCCTTTTCCATTTCC
XBP1	CCATGCGAAGATGTTCTGGG	ACACGCTTGGGAATGGACAC
CHOP	CTGGAAGCCTGGTATGAGGAT	CAGGGTCAAGAGTAGTGAAGG
ATF3	CGAAGACTGGAGCAAAATGAT	CAGGTTAGCAAAATCCTCAAATAC
ATF4	CTCTTGACCACGTTGGATGAC	CAACTTCACTGCCTAGCTCTAAA
BIP	ACTTGGGGACCACCTATTCCT	ATCGCCAATCAGACGCTCC
GAPDH	ATGTTCCAGTATGACTCCACTCACG	GAAGACACCAGTAGACTCCACGACA
Xbp1	ACACGCTTGGGAATGGACAC	CCATGGGAAGATGTTCTGGG
CyclophilinA	ATGGTCAACCCCACCGTGT	TTCTGCTGTCTTTGGAACTTTGTC

Table 4: qRT-PCR primer sequences.

5.3 Histology

5.3.1 Tissue sections

After mice were sacrificed, organs were fixed in 4% PFA (Merck, Darmstadt, Germany) in PBS for 48 h, dehydrated and embedded in paraffin blocks. Paraffin blocks were cut into 2.0-10.0 µm thick sections using a microtome (HM 355 S, MICROM, Walldorf, Germany). Tissue sections were placed on adhesive-coated slides (SuperFrost® Plus, Menzel, Braunschweig, Germany) and air-dried at approximately 25°C for 12-18 h. Sections were stored at 25°C for further experiments.

5.3.2 Hematoxylin and eosin (H&E) staining

Firstly, paraffin-embedded tissue sections were deparaffinized in Xylol (Merck) for 2 x 3 minutes followed by rehydration in ethanol (100%, 96%, 70%) and water (2 x 5 minutes). Rehydrated tissue slides were incubated in hematoxylin solution (Merck Millipore, Billerica, MA) for 5 minutes. Stained slides were rinsed with running tap water for 10 minutes and incubated in Eosin solution (Merck) for 3.5 minutes. Tissues were dehydrated with 96% Ethanol followed by Isopropanol for 25 sec. each and then incubation with Xylol (2 x 3 minutes). Tissue slides were mounted (Pertex, Medite GmbH) and covered with coverslips (Merck). Axiostar Plus microscope (Carl Zeiss, Gottingen, Germany) was used for histological analysis.

5.3.3 Immunohistochemistry

As described above in section 4.3.2, slides were deparaffinized and rehydrated. After this step, heat induced antigen retrieval was performed by boiling the slides in 0.01 M citrate buffer (pH 6.0) for 10 minutes in microwave. Slides were cooled down at room temperature for 20 minutes in citrate buffer and then two times washed with water. Slides were incubated in 3% hydrogen peroxide for 15 min at RT in the dark to block the endogenous peroxidase activity. Slides were washed two times for 5 minutes with wash buffer (TBS, TBS-T, PBS, or PBS-T (Table 5) depending on the primary antibody). To prevent unspecific bindings, slides were blocked with 5% serum blocking solution (5% rabbit or 5% goat serum, depending on the secondary antibody, in wash buffer) for 1 hour at RT. Then, slides were incubated with the primary antibody diluted

in blocking solution for O/N at 4°C. Primary antibodies that were used include: anti-BrdU (1:250) (MCA2060 AbD Serotec), anti-Ki67 (1:200) (Abcam), anti-FN (1:250) (Abcam), anti-hFN (1:200) (R&D), anti CD45 (1:20) anti-F4/80 (1:100) (MF-48000 Invitrogen), anti-CK19 (1:200) (TROMA III Developmental Studies Hybridoma Bank), Secondary antibodies including biotinylated anti-rabbit in goat (BA 1000 Vector), anti-mouse in goat (BA 9200 Vector), and anti-rat in rabbit (BA 4000 Vector) were implemented for 1h at RT and avidin-biotin peroxidase complex for biotinylated secondary antibodies was then applied by following to manufacturer protocol (Vector Laboratories, CA). DAB reagent (Vector Laboratories, CA) was used to develop the staining. Counterstaining was performed by Hematoxylin and in final step slides were dehydrated and mounted as indicated above (4.3.2).

Name	Components	pH
TBS	20 mM Tris, 137 mM NaCl	7.6
TBS-T	TBS-buffer, 0.1% (v/v) Tween-20	7.6
PBS	137 mM NaCl, 2.7 mM KCl, 10 mM Na_2HPO_4, 10 mM KH_2PO_4	7.4
PBS-T	PBS-buffer, 0.1% (v/v) Tween-20	7.4

Table 5: Buffers used for washing steps of immunohistochemistry.

5.3.4 Co-immunofluorescence

Paraffin-sections of *Kras* and *Kras; FNΔpanc* pancreas were processed as described (4.3.1-3). Heat induced antigen retrieval was performed by boiling the slides in 0.01 M citrate buffer (pH 6.0) for 10 minutes in microwave. Slides were cooled down at room temperatures for 20 minutes in citrate buffer and then two times washed with water. Then, slides were incubated in %0,1 Triton-X for 15 min at RT and washed two times for 5 min. with water. Unspecific binding was blocked with 5% serum blocking solution (5% goat or 5% rabbit serum, depending on the secondary antibody, in wash buffer (table 7)) for 1h at RT and subsequently incubated O/N at 4°C with the primary antibody. Primary antibody anti-CK19 (1/200; TROMA III Developmental Studies Hybridoma was diluted in blocking solution and anti-FN (1:200, ab199056 Abcam). Next day, slides were washed 3 times for 5 minutes with wash buffer and secondary

anti-rat in goat Alexa Fluor 488 nM (1:300, A11006 Invitrogen) for CK19, anti-rabbit in goat Alexa 568 (1:300, A11036 Invitrogen) for FN staining, containing 1:10000 DAPI were implemented for 1h at RT at dark. In final step, the slides were washed and covered mounting medium (H-1200 Vector Laboratories) and analyzed by fluorescence microscopy (Axiostar Plus FL, Carl Zeiss).

5.3.5 ADM and PanIN Quantifications

Paraffin-embedded tissue sections from 9-week old and 18-week old *Kras* and *Kras; FN∆panc mice* were stained by H&E and photographed at 100x magnification. The number of ADMs, reactive ductal structures and PanIN structures were counted in each picture using Zeiss Axiovision software. Measurements from multiple photographs per tissue slide were summed up and expressed as ADM per High Power Field (HPF). Results from each photograph were averaged per genotype.

5.3.6 Quantification of Immune Cell Infiltration (CD45-Positive)

To quantify the CD45 positive cells in pancreas tissues from *Kras* and *Kras; FN∆panc* mice, paraffin embedded tissue sections were stained for CD45 via immunohistochemistry, as described above and photographed at 200x magnification. Number of CD45 positive cells were quantified in Aperio Images scope software and the % of positive nuclei/all nuclei were determined.

5.3.7 Quantification of Collagen Staining with Masson Trichrome

Pancreas tissues from *Kras* and *Kras; FN∆panc* mice were deparaffinzed and rehydrated as described above. Slides were fixed in 40mL Boulin's Solution at RT overnight. Next day, slides were washed in running tap water to remove the yellow solution from the slides. Tissue sections were stained with Weigert's Iron Hematoxylin Solution for 5 minutes. Slides were washed in running tap water for 2 minutes and subsequent wash step with distilled water performed. Then tissues were stained in Biebrich Scarlet-Acid Fucshin solution for 5 minutes and subsequently slides were washed again in distilled water. After that, slides were put in Phosphotungstic/ Phosphomolybdic Acid solution for 5 minutes and placed in Aniline Blue Solution for another 5 minutes. At the end, slides were placed in Acetic Acid 1% for 30 secs to

discard the solution. Slides were rinsed and dehydrate as usual consequently incubated in xylene and slides mounted.

5.3.8 Quantification of BrdU and Ki67 positive PanINs and acinar cells

BrdU-positive and Ki67-positive acinar cell and PanINs were also quantified in the original tumors of *Kras* and *Kras; FNΔpanc* mice. Paraffin embedded tissue slides were stained with the respective antibodies and the % of positive nuclei/ all nuclei were determined with Zeiss Axiovision software.

5.3.9 Quantification of Intact Acinar Area

9-week old and 18-week old *Kras* and *Kras; FNΔpanc* paraffin-embedded tissue sections were stained by H&E and photographed at 100x magnification. The intact acinar area is quantified with Zeiss Axiovision software.

5.3.10 Quantification of Relative Pancreatic Weight, Tumor Incidence, Metastasis Incidence, Tumor and Metastasis Burden

4, 9, and 18 weeks old *Kras* and *Kras; FNΔpanc* mice were chosen to analyze the tumorigenesis as time point and the time point of sickness were used to analyze survival rate. Relative pancreatic weight was calculated by using the pancreas and body weight obtained during sacrifice (pancreas weight/ body weight). Based on histological analysis, tumor incidence and metastasis incidence (% of tumor or metastasis-positive mice relative to all mice sacrificed) were determined. Metastasis-positive mice are from population of pancreatic tumor positive mice having metastasis in liver, lung, or diaphragm. Ascites, lymph node, spleen, or kidney infiltration was also considered.

5.4 *In Vitro* Experiments and Protein biochemistry

5.4.1 Measurement of Serum Amylase and Lipase

Serum was collected from mice having acute pancreatitis induction after sacrifice at 8-12-week-old and diluted 1/10 with 0.9% NaCl. Amylase activity (AMYL2 Cobas, Roche)

was evaluated by a colorimetric assay in line with the IFCC method. Lipase activity (LIPC Cobas, Roche) was evaluated via DGGR substrate-based assay.

5.4.2 Tumor Cell Isolation and Cultivation

Primary pancreatic tumor cell lines were established from murine pancreatic tumors. To isolate cancer cells, small pieces of pancreatic tumors from Kras, Kras; FNΔpanc, Kras; p53Δ;panc, and Kras; p53Δ; FNΔpanc mice were chopped into small pieces and placed in cell culture dish in full culture medium and cancer cells were growth out of the tissue. Tumor cell lines were cultured under standard conditions (5% CO_2, 37°C) in culture media (Dulbecco's modified Eagle medium (DMEM) supplemented with 10%FBS (#10082147; Gibco), 1% PenStrep (#1500-063; Gibco), 1% Non-Essential-Amino-Acids (NEAA #11140050; Gibco)).

5.4.3 Acinar cell isolation and Ras activity assay

To isolate acinar cells, whole pancreas was removed and placed into a Petri Dish containing PBS on ice. Pancreas was transferred to a Petri Dish containing 5 ml Solution II and the pancreas was injected with Solution II repeatedly. Then, pancreas was chopped into small pieces with sterile scissors and incubated at 37°C for 10 min. The suspension was transferred into a 50-ml falcon tube. Plate was rinsed with 10 ml Solution I and all tissues were collected. Suspension was centrifuged at 0,3 rcf at 18°C for 5 min. After the supernatant was removed, tissues were incubated again in 5 ml Solution II at 37°C for 10 min. As previous step, again the suspension was transferred into a 50-ml falcon tube. Plate was rinsed with 10 ml Solution I and all tissues were collected. Suspension was centrifuged at 0,3 rcf at 18°C for 5 min. The supernatant was removed, resuspended in 5 ml Solution I and filtered through a sieve with 100-μm mesh. Dish was rinsed again to with 5 ml Solution I to collect all tissues on the sieve. Filtered suspension was centrifuged at 0,3 rcf at 18°C for 5 min twice and cell pellet was resuspended in culture medium and left in incubator for 4 hour at most to discard the immune cells before collect.

Solution I	McCoy's Medium 0,1% BSA (49,5 ml Medium + 500 μl 10% BSA)
Solution II	McCoy's Medium 0,1 BSA 1,2 mg/ml Collagenase Type VIII (#C2131, Sigma) (10ml Solution I + 12mg Collagenase)

Table 6: Solutions of acinar cell isolation protocol for one pancreas

To examine the Ras activity of acinar cells, 4-week-old mice were taken and removed the pancreas and isolated acinar cells by following the protocol explained above. Then, tissue lysis buffer was prepared which includes 1x MLB buffer, 1:50 phosphatase inhibitor and 1:50 proteinase inhibitor. 300 μl of Tissue lysis buffer was added to each sample and homogenized. Samples were incubated for 20 minutes on ice. After that samples were centrifuged for 30 minutes at highest speed. Concentration of samples were adjusted to 1 μg/ml in 500 ml.

10 μl of Ras-Assay Beads was added to each sample and left it on rotating shaker for 45-60 min at cold room. Samples were spun down at highest speed for 15 sec. Supernatant was removed and washed with 1 ml 1x MLB buffer 3 times. Supernatant was removed again and left 20 μl of beads-MLB buffer mixture and 20 μl of 2x Laemmli buffer added to these samples. Samples were boiled at 95°C and run entire volume of samples at 12% Gel at 70V for 3 hour for western blotting.

5.4.4 Protein isolation and Quantification

For protein isolation from cells, collected cell pellets were lysed in ice-cold protein lysis buffer (NaCl (1M), NP40 /1%), Sodium deoxycholate (0,5%), SDS (0,5 %) Tris (50mM, pH 7.4) and ddH_2O) freshly supplemented with a cocktail of protease (2% (v/v))/phosphatase (1% (v/v)) inhibitors (SERVA, Heidelberg, Germany). Lysates were incubated on ice for 30 min, after centrifuged at 13,000 rpm for 30 min, 4°C supernatants were collected. Protein concentration was measured by the Bio Rad Protein Assay Kit (Bio Rad, München, Germany). 200 μl Bio Rad Protein Assay

Solution (diluted 1/5 in H_2O) was mixed with 1 µl of isolated protein in a 96-well plate. BSA (1 mg/ml; Sigma) was used as a standard and RIPA-buffer was used as blank Absorbance of each sample was measured at 595 nm and their protein concentration were calculated by the standard curve. Concentration of samples were consequently fixed to 3 µg/µl with 5 x Laemmli buffer (300 mM Tris-HCl, pH 6.8, 10% (w/v) SDS, 50% (v/v) Glycerol, 0.05% (w/v) Bromophenol blue, 5% (v/v) β-mercaptoethanol). Samples were denatured for 5 min at 95°C, cooled down on ice shortly and stored at -80°C for further experiments.

5.4.5 SDS-Polyacrylamide gel electrophoresis

Protein separation was performed in a Mini-Protean® 3 Cell System (Bio Rad). 60-80 µg of denatured protein per sample in Laemmli-buffer (depending on the protein of interest) were loaded on the gel. A protein standard (Bio Rad) was used to estimate the molecular weight of the proteins. Polyacrylamide based SDS-page gel contains two different gel. Upper Stacking gel contains 10% polyacrylamide concentration and a lower Separating gel could contain 7.5-15% polyacrylamide concentration contingent upon protein size. Samples were run in Running buffer at 90 V for 20 min followed by 90-120 V depending on polyacrylamide concentration until protein separation. Buffer contents for SDS-PAGE are demonstrated in Table 7. Gel preparation protocols for different acrylamide concentrations are showed in Table 8 and 9.

Name	Components	pH
Stacking Gel Buffer	0.5 mM Tris	6.8
Separating Gel Buffer	1.5 mM Tris	8.8
Running Buffer	25 mM Tris-HCL, 192 mM Glycine, 0.1% (w/v) SDS	-

Table 7: Detailed components of buffers used for SDS-PAGE.

dH_2O	4,5 ml
Stacking Gel Buffer	2 ml
30%/0.8% Acrylamide solution (Roth, Karlsruhe, Germany)	1,1 µl
10% SDS	75 µl
10% APS (Sigma)	38 µl
TEMED (Fluka, Buchs, Schweiz)	15 µl

Table 8: Ingredients of Stacking gel

Concentrations	7.5%	10%	12%	15%
dH_2O	7,4 ml	6,2 ml	5,1 ml	3,8 ml
Separating Gel Buffer	3,9 ml	3,9 ml	3,9 ml	3,9 ml
30%/0.8% Acrylamide/Bis solution	3,8 ml	5 ml	6 ml	7,5 ml
10% SDS	150 µl	150 µl	150 µl	150 µl
10% APS	75 µl	75 µl	75 µl	75 µl
TEMED	23 µl	23 µl	23 µl	23 µl

Table 9: Ingredients of Separating gels depending on varying polyacrylamide concentration (for 1.5mm plates).

5.4.6 Western blotting

After proteins were run on SDS-PAGE, protein transfer onto a nitrocellulose or PVDF membrane was performed in the Mini Trans-Blot Cell™ System (Bio Rad). The PVDF membranes, but not the nitrocellulose membranes, were hydrophilized in 100% methanol for 1 min. Both membrane types were washed in transfer buffer (Table 10) before protein transfer was performed in ice-cold transfer buffer on ice at 100 V for 1-2 h depending on the protein size. After protein transferring membranes were blocked for 1 h in 5% Milk solution or 5% BSA solution (Table 10), depending on which antibody was used, to prevent unspecific bindings. Subsequently, membranes were incubated in antibody solution (Table 10) overnight at 4°C on a shaker. The primary antibodies are; Anti-FN (1/1000) (Abcam #199056), ERK1/2 (1:1000) (Santa Cruz #93, #154), p-ERK1/2 (1:1000) (Cell Signaling #9106S), cMET (Abcam #51067), AKT(1:1000) (Cell

Signaling #9272),p-AKT (1:500) (Cell Signaling #9271),p38 (Cell Signaling #9212),p-p38 (1:1000) (Cell Signaling #4631), PTEN (1:1000)(Cell Signaling #13866), PCNA (1:1000) (Santa Cruz #56), Hsp90 (1:1000) (Santa Cruz #7947), Arginase (1:1000) (BD Bioscience #610708), c-Caspase 3 (1:1000) (Cell Signaling #9661), CK19 (Troma III-S), p-Stat3 (1:300)(Cell Signaling #9134), p-Src (1:1000) (Cell Signaling #2101), Src (1:1000)(Cell Signaling #2109), anti-p62 (1/1000) (GP62-C Progen), anti-LC3 (1:1000) (PD014 MBL International),p-AMPK (1:1000) (Cell Signaling #2535), p-eif2a (1:1000) (Cell Signaling #3597), Atg101 (1:1000) (Cell Signaling #E1Z4W), Beclin-1 (1:1000) (Cell Signaling #3738), MTOR (1:1000) (Cell Signaling #2972), p-MTOR (1:1000) (Cell Signaling #2971), ULK1(1:1000) (Cell Signaling #D8H5)), p-ULK1 (1:1000) (Cell Signaling # D1H4), CCPG1(1:1000) (Origine), anti-p53 (1:500) (NCL-p53-CM5p Novocastra), anti-BiP (1:1000) (AB21685 Abcam), Anti-β-Actin (1: 2000) (A5441, Sigma). The following day, membranes were washed 3 times for 5 min with TBS-T or PBS-T and the membranes were incubated in antibody solution (Table 12) for 1h at RT on a shaker. Used secondary antibodies are horseradish peroxidase-conjugated anti-mouse (1/2000; NA931V GE Healthcare), anti-rabbit (1/2000; NA934V GE Healthcare), or anti-guinea pig (1/2000; A7289, Sigma)). Membranes were washed again 3 times for 5 min with TBS-T or PBS-T. Amersham ECL™ Western blot detection reagent (GE Healthcare, Buckinghamshire, UK) and the Amersham Hyperfilm™ ECL (GE Healthcare) were used for membrane development.

Name	Components
Transfer buffer	25 mM Tris-HCl, 192 mM Glycine, 20% (v/v) Methanol
Blocking solution	5% BSA or 5-10% milk in TBS-T or PBS-T (depending on antibody)
Antibody solution	2% BSA or 2% milk in TBS-T or PBS-T (depending on antibody)

Table 10: Components of solutions used for western blot

5.4.7 Colony Formation Assay

$1x10^3$ *Kras* and *Kras; FNΔpanc* cells were seeded as triplicates in 6-well plates and allowed them to grow for 5 days in culture media. Colonies were stained by 2% crystal violet (C3886; Sigma) for 25 min. at RT. After washing with water, plates were left to dry. ImageJ used for the area quantification. Treatments which were applied during the colony formation assays indicated below; 10% FCS-containing medium, Tunicamycin (5ug/ul), Thapsigargin (1 uM).

5.5 RNA sequencing

For RNA sequencing, *Kras* and *Kras; FNΔpanc* cell lines were seeded as 300.000 per well into 6-well plate in 2 ml medium and growth for 2 days until they reach 80% confluency. Then, they were treated with Tunicamycin (5 ug/ml) for 24 h then collected and RNA was isolated by using Maxwell 16LEV simplyRNA purification kit and instrument from untreated and treated cells as triplicate. To test the quality of RNAs, samples were run in 2% agarose gel and rRNA bands were checked. RNA concentrations were adjusted to 25 ng/μl. After that, 96-well plate with diluted RNAs (25 ng/μl) was prepared and run for sequencing.

5.6 Statistics

Data are demonstrated as averages ± standard deviations (SD) and were analyzed by using the statistical software Prism 5 (GraphPad Software, Inc.). For group comparison two-tailed Student t-test was used and statistical significance was set at $*P<0.05$, $**P<0.01$, $***P<0.001$. Kaplan-Meier curves were analyzed by using long-rank test in GraphPad Software.

6 RESULTS

6.1 Role of Fibronectin (FN) in Acute Pancreatitis (AP)

6.1.1 Pancreas specific deletion of FN aggravates AP

To interpret the role of FN in acute pancreatitis, we have induced mice with *FNflox* and *FN∆panc* genotype by hourly 8 repetitive i.p injection of cerulein (0,1 ug/g) which is Cholecystokinin analog and sacrificed them at 4h, 8h, 12h, 24h, and 32h time points. Histological analyses of pancreas from 8h and 24h cerulein-induced mice with both genotypes showed that necrosis is higher in *FN∆panc* pancreas compared to *FNflox* control (Figure 1A). Pancreatic tissue damage and pancreatitis response have been determined by the measurements of serum amylase and lipase levels that demonstrated significant increase in *FN∆panc* mice at 8h time point of cerulein induction compared to the *FNflox* control mice (Figure 1B). As histologically shown that, cerulein induction elevated the lung inflammation in *FN∆panc* mice at 8h time point (Figure 1C). Even though, FN expression was too low in the normal pancreas, it was upregulated with cerulein induction in both *FN∆panc* and *FNflox* pancreas where necrosis occurred (Figure 1D). Besides, gradual increase of FN expression also has been reported in the lysates from 0h, 4h, 8h and 24h time point of cerulein induced *FN∆panc* and *FNflox* pancreas tissues (Figure 1E).

A

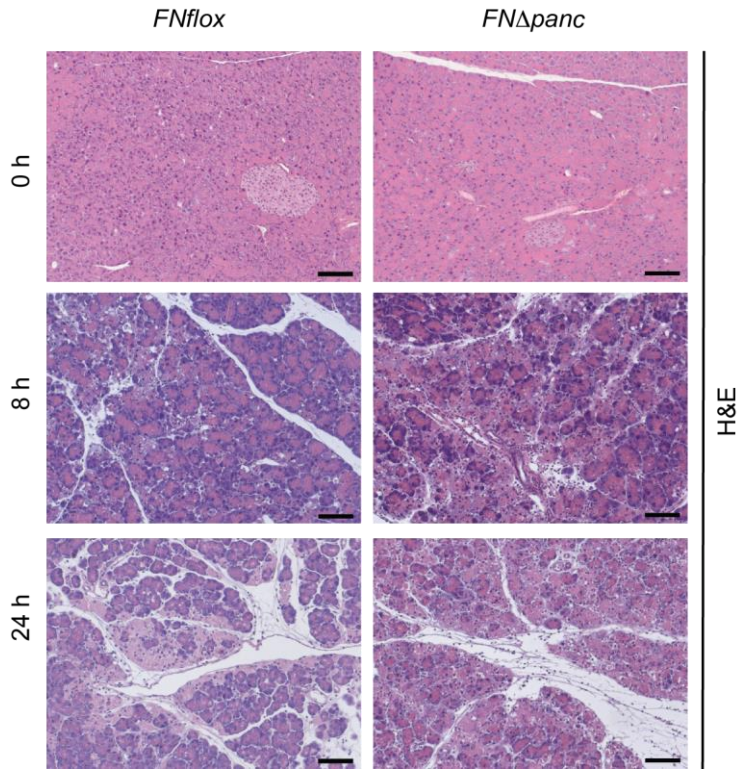
FNflox
FNΔpanc
0 h
8 h
24 h
H&E

B

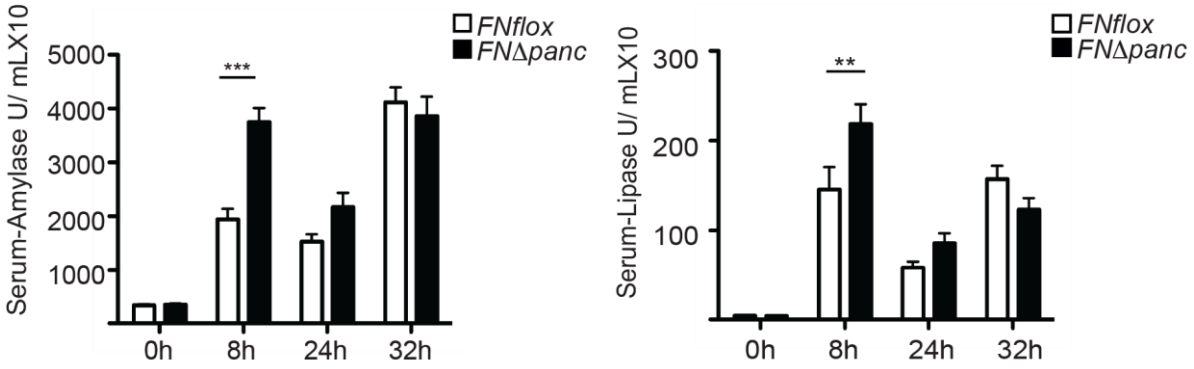
Serum-Amylase U/ mLX10
5000
4000
3000
2000
1000
***
FNflox
FNΔpanc
0h
8h
24h
32h
Serum-Lipase U/ mLX10
300
200
100
**
FNflox
FNΔpanc
0h
8h
24h
32h

C

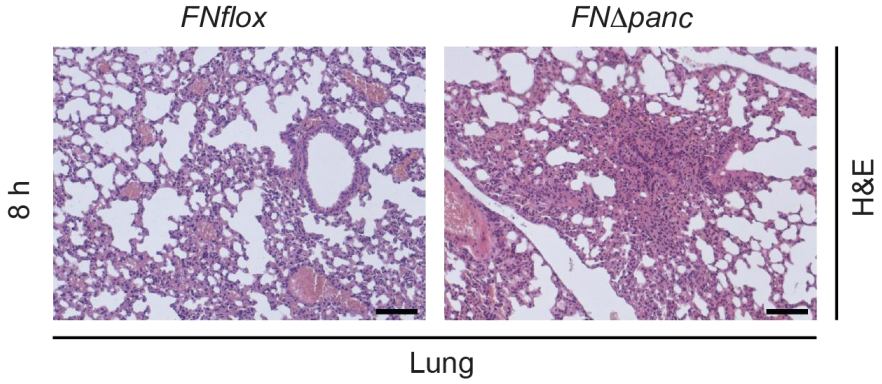
FNflox
FNΔpanc
8 h
H&E
Lung

D

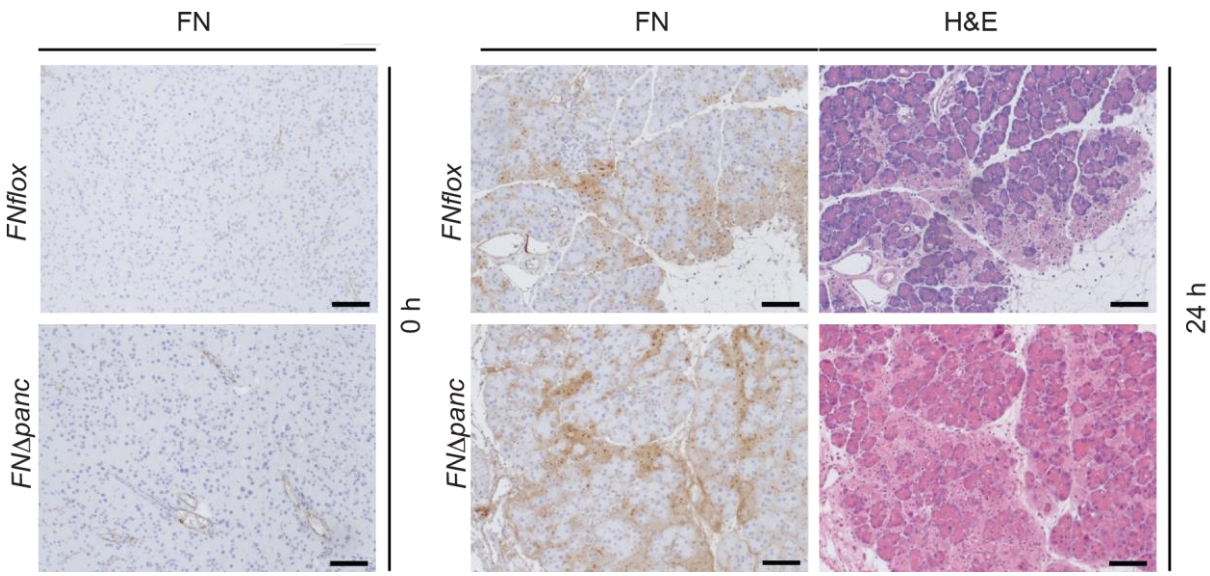

E

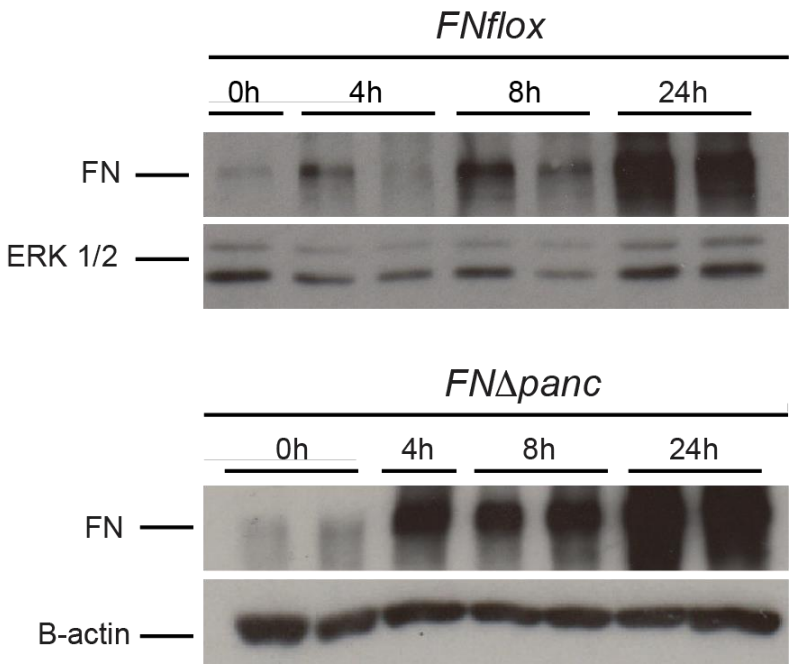

Figure 1: Pancreas specific deletion of FN aggravates AP. *(*A) *FNflox* and *FNΔpanc* mice were treated 8 times hourly by i.p injections of cerulein (0,1 ug/g) and sacrificed at 8, 12, 24 and 32 hours after first injection. Representative H&E staining from cerulein-induced *FNflox* and *FNΔpanc* mice at indicated time points and showed increased necrosis in *FNΔpanc* pancreas. (B) Measurement of amylase and lipase levels in the serum of *FNflox* (n=12) and *FNΔpanc* (n=14) mice at the indicated time points. *** *p< 0,001, **p<0,01* by two-way Anova; n, number of mice (C) Representative H&E staining of lung tissue from 8h cerulein-treated *FNflox* and *FNΔpanc* mice. (D) IHC analysis of FN in pancreas from 0h and 24h cerulein-treated *FNflox* and *FNΔpanc* mice. Scale bars equal 100µm. (E) Immunoblot analysis of FN in pancreas tissue lysates from cerulein-treated *FNflox* and *FNΔpanc* mice at 0h, 4h, 8h and 24h time points.

6.1.2 Pancreas specific deletion of FN accelerates inflammation driven carcinogenesis.

Studies reported that FN is augmented and disorganized in fibrotic tissues in CP (Shimoyama *et al.*, 1995) (Kennedy *et al.*, 1987). To analyze the effect of FN deletion on inflammation driven carcinogenesis, *Kras* and *FNΔpanc*; *Kras* mice have been treated with 5 daily injections of cerulein to mimic chronic pancreatitis induced PDAC generation (Figure 2A). Morphological analysis of pancreata from chronic pancreatitis induced *Kras and FNΔpanc*; *Kras* mice showed that tumor structures were observed in *Kras; FNΔpanc* pancreata while only low grade PanIN structures were found in Kras pancreata (Figure 2A). In addition, the quantification of relative pancreatic weight ratio and intact acinar area revealed the pancreatic atrophy in *Kras; FNΔpanc* pancreata (Figure 2B and Figure 2C) Besides, the BrdU positive cells in PanIN structures decreased in *Kras; FNΔpanc* pancreata compare to *Kras* control indicating the reduction in the proliferation capacity of PanIN cells in *Kras; FNΔpanc* pancreata with the induction of chronic pancreatitis (Figure 2D).

A

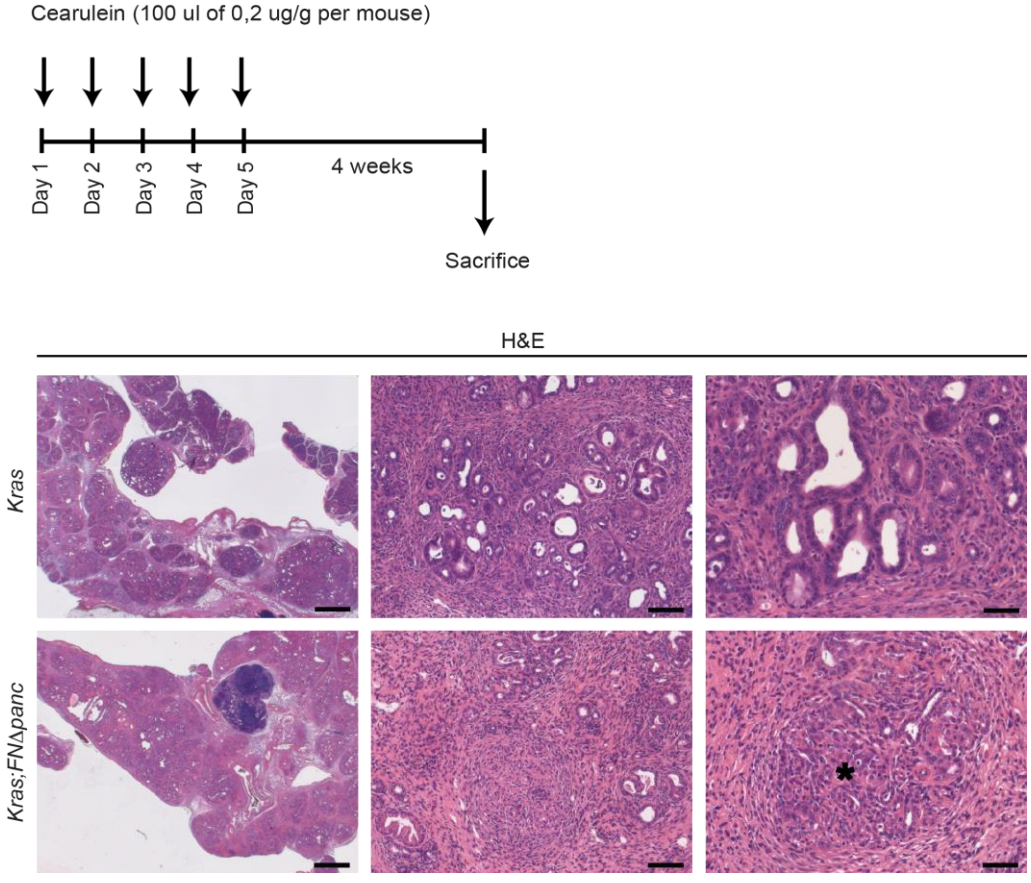

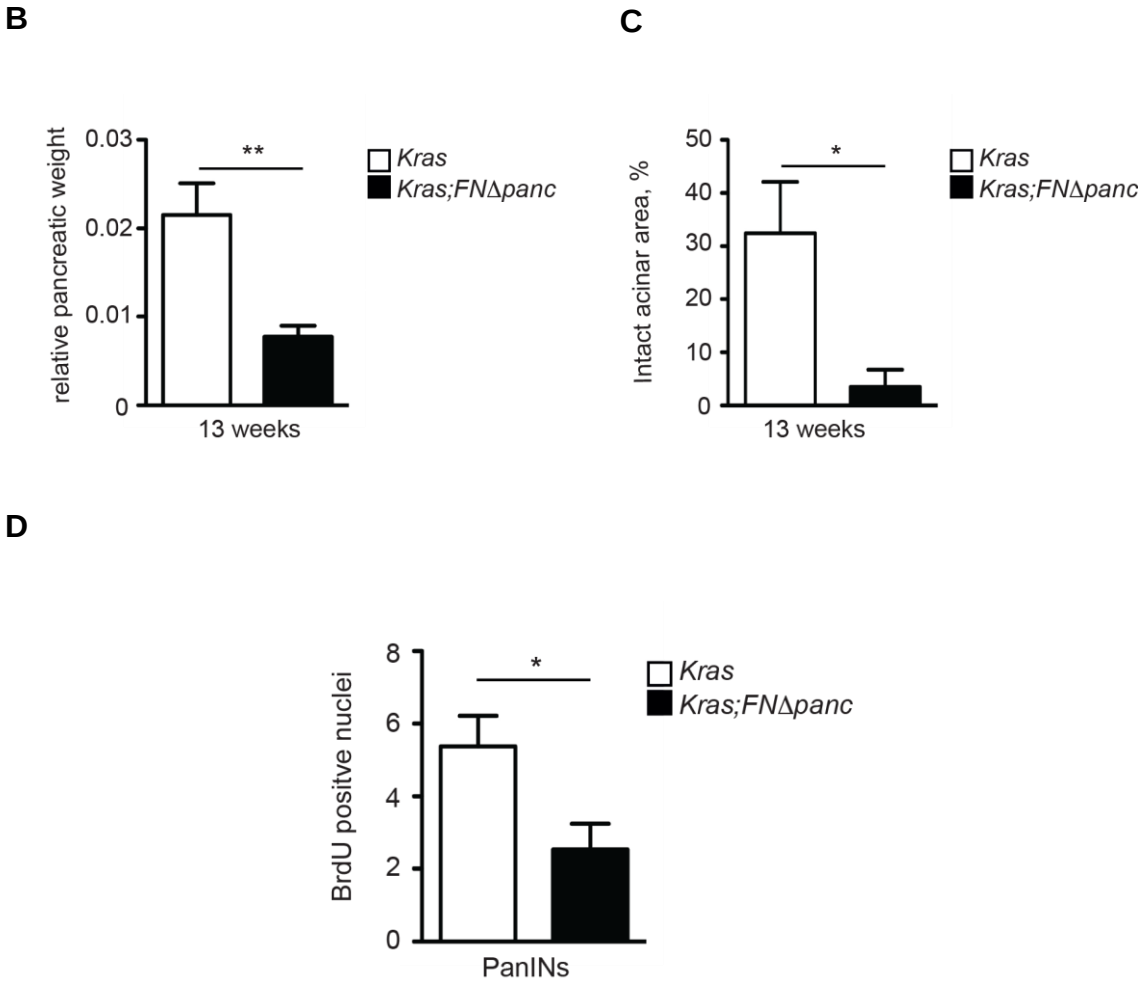

Figure 2: Pancreas specific deletion of FN in the model of inflammation driven carcinogenesis. (A) Morphological analysis of chronic pancreatitis induced *Kras* and *Kras; FNΔpanc* pancreata. Black asterisk indicates the micro-carcinoma structure. Scale bars; 1000um, 100um, 50um. (B) Quantification of intact acinar area in pancreas from inflammation driven carcinogenesis model of *Kras* (n=5) and *Kras; FNΔpanc* (n=5) mice (13- week-old). Mean ± SD; * *p< 0,05* by unpaired t-test; n, number of mice. (C) Pancreas to body weight ratio in 13- week-old chronic pancreatitis-induced *Kras* (n=6) and *Kras; FNΔpanc* (n=5) mice. Mean ± SD; n=5; ** *p=0,0081* by unpaired t-test; n, number of mice. (D) Proliferation index of PanIN cells from mice with indicated genotypes. The number of BrdU positive nuclei counted in all PanIN structures per mouse. Mean ± SD; n=5; * *p< 0,05* by unpaired t-test; n, number of mice.

6.1.3 FN expression is present in pre-malignant and malignant cells during pancreatic tumorigenesis in mouse

FN expression is pivotal protein which has been shown to be upregulated in many cancers at distinct steps of tumorigenesis (Wang and Hielscher, 2017). To demonstrate the expression and the localization of FN during pancreatic tumorigenesis, we have performed immunofluorescence staining of FN in the

pancreatic tissues from different stage of tumorigenesis using *WT, Kras* and *Kras; p53Δpanc* mice. In the *WT* pancreas, FN expression was very low and visible in the extracellular matrix. During pancreatic tumorigenesis, cellular FN expression was detectable in pre-malignant acinar-to-ductal metaplasia structures (ADM), pancreatic intraepithelial neoplasia (PanIN), as well as in fully developed pancreatic tumors and liver metastasis (Figure 3A). The localization of FN was also identified by immunocytochemistry of FN inside the cancer cells isolated from pancreatic tumor and liver metastases from *Kras* and *Kras; p53Δpanc* mice showing cytosolic and membranous localization of FN. FN expression was also observed in the membranes of vesicles which might be endosomes or lysosomes. In cells from liver metastasis, FN was also detectable in the extracellular region (Figure 3B). Immunoblotting of FN in the lysates from *Kras* and *Kras; p53Δpanc* mice was supporting the cellular FN inside the pancreatic cancer cells (Figure 3C).

A

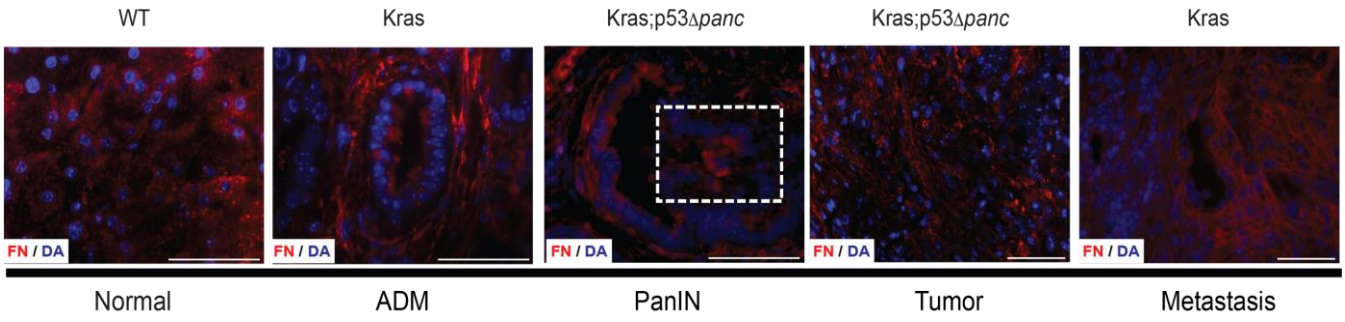

B

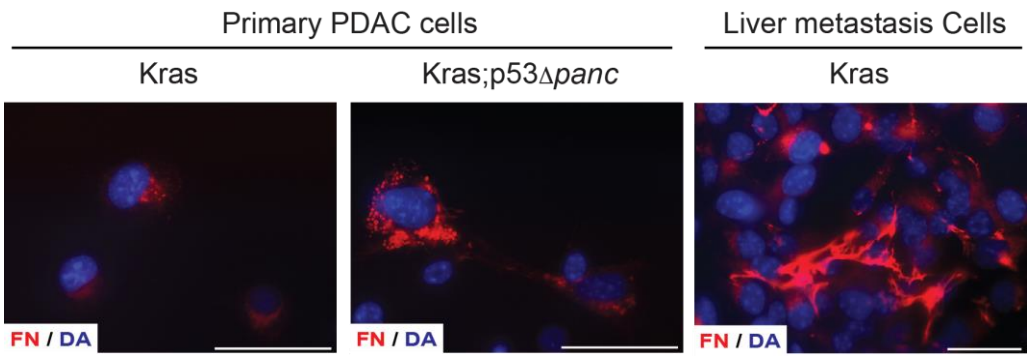

C

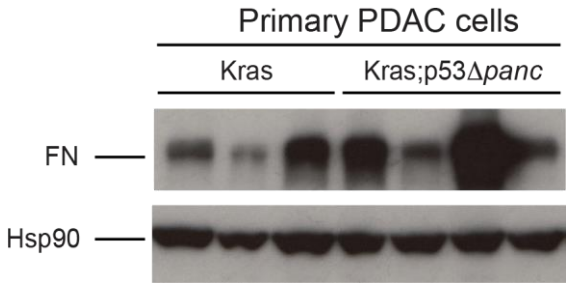

Figure 3: Fibronectin localization in normal pancreas and pancreatic tumorigenesis. (A) Immunofluorescent staining of FN in pancreas from different stage of pancreatic tumorigenesis. Scale bar: 50 um. *White square* indicates FN expressing PanIN cells. (B) Immunofluorescent staining of FN in cancer cells isolated from *Kras*, *Kras; p53Δpanc* tumors and liver metastasis. Scale bar: 50 um (C) Immunoblot analysis of FN in tumor cells isolated from *Kras* and *Kras; p53Δpanc* mice.

6.1.4 FN expression is detected in pre-malignant cells, stromal cells and ECM in human

Differential expression of FN in different human PDAC tissue samples was identified by Immunohistochemical staining of FN. As representative images showed that FN is expressing by cells of pre-malignant PanIN structures, stromal cells and found also in ECM (Figure 4A). Cellular expression of FN was supported by immunoblot analysis in established human PDAC cell lines isolated from primary and metastatic side (Figure 4B). As it is known, secretion of FN was also shown by immunoblotting of FN in supernatant of established human PDAC cell lines (Figure 4C).

A

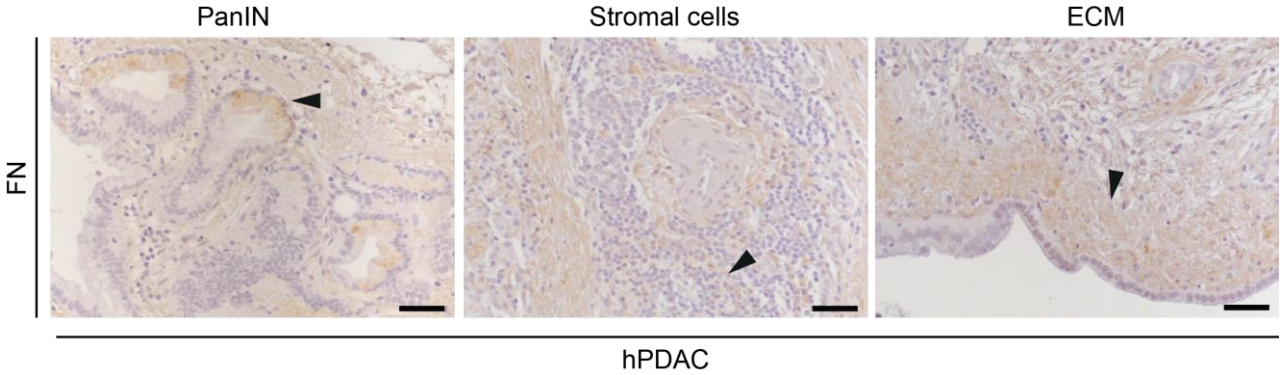

B

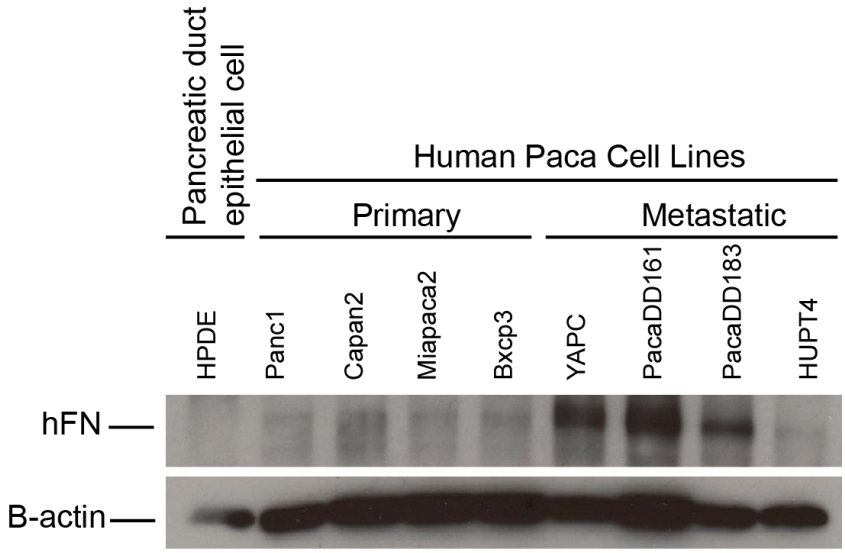

C

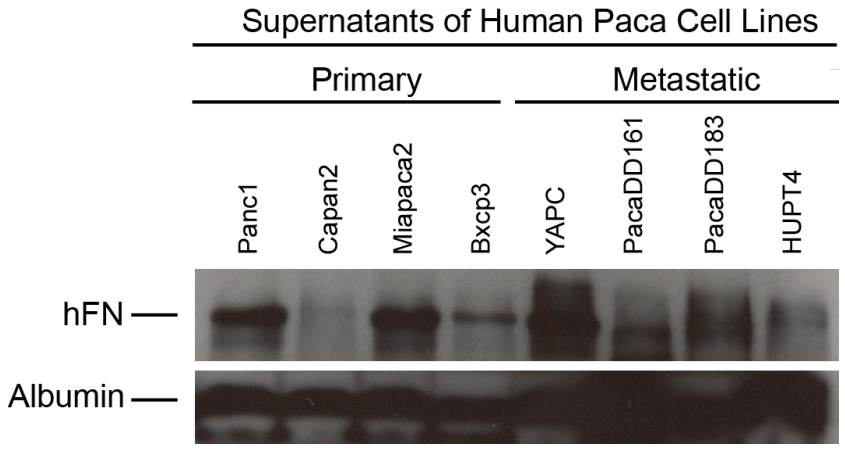

Figure 4: Fibronectin is expressed by cancer cells and tumor microenvironment in human PDAC. (A) IHC analysis of FN in human PDAC tissues. Black arrows point out the PanIN structures, stromal cells and ECM structures, respectively. Scale bar: 100 um (B) Immunoblot analysis of FN in established primary and metastatic human PDAC cell lines and pancreatic duct epithelial cells as control. (C) Immunoblot analysis of FN in supernatant of established primary and metastatic human PDAC cell lines.

6.1.5 Pancreas-specific ablation of Fibronectin leads to loss of exocrine tissue and decrease proliferation of cells in acinar compartment

Research is mainly focused on the role of FN in ECM structures. However, as we also showed that FN is present during pancreatic cancer development and progression. To analyze the cellular role of FN during PDAC formation, we have generated mice with pancreas specific homozygous deletion of *FN* (*Kras; FNΔpanc*), compared them with control mice with only *Kras*-mutation (*Kras*) and analyzed them during tumorigenesis at different time points. Morphological analysis showed that even though there was no difference at 4-week-old mice, loss of intact acinar area was detected at 9-week-old and 18-week-old mice (Figure 5A, B, F, G). Besides, loss of exocrine pancreas was supported by the significant decrease in pancreas to body weight ratio and the reduced proliferation rate of the acinar cells at 18-week-old mice (Figure 5H). Loss of FN accelerated the initiation of tumorigenesis by significantly elevating ADM formation at 9-week-old mice (Figure 5D). Nevertheless, acceleration of carcinogenesis was not observed at 18-week-old time point compared to control mice. Number of the ADM and PanIN structures remained same and the proliferation rate of the cells in PanINs was not significantly different compared to *Kras* control mice (Figure 5D, I)

A

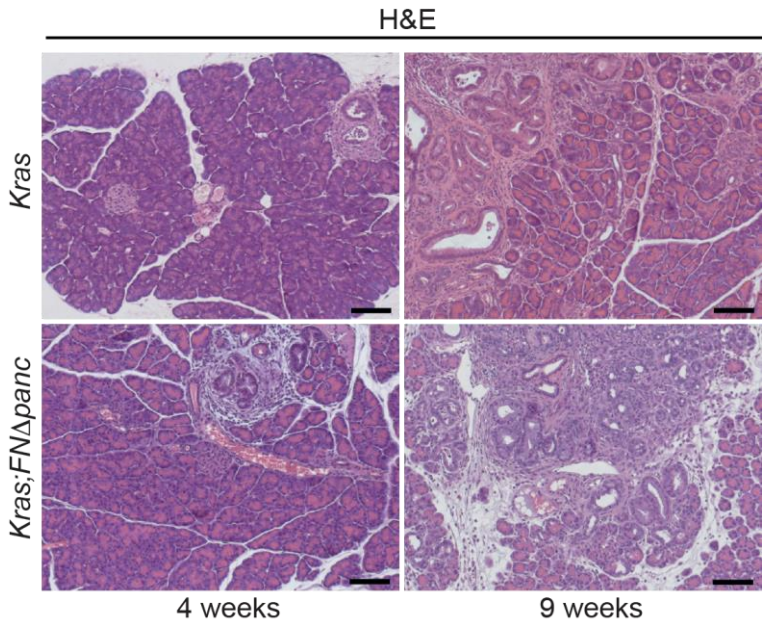

B

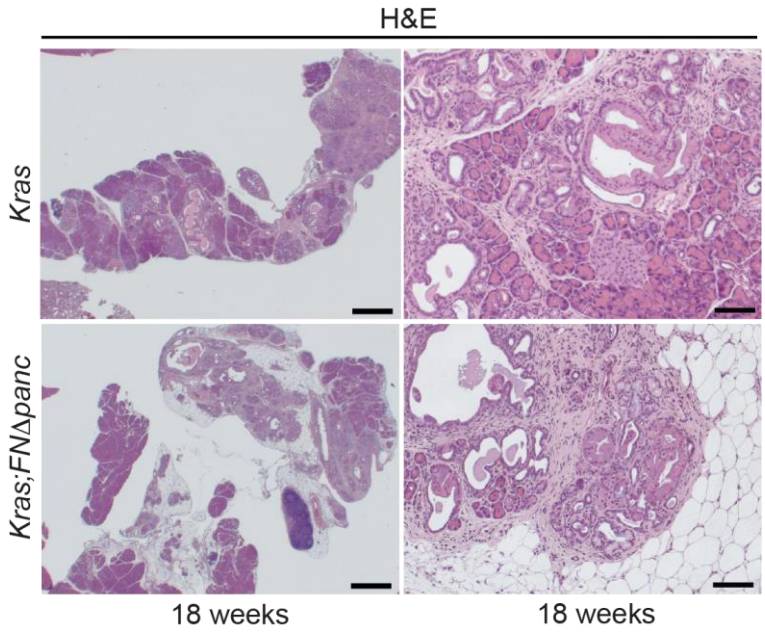
H&E
Kras
Kras;FNΔpanc
18 weeks
18 weeks

C

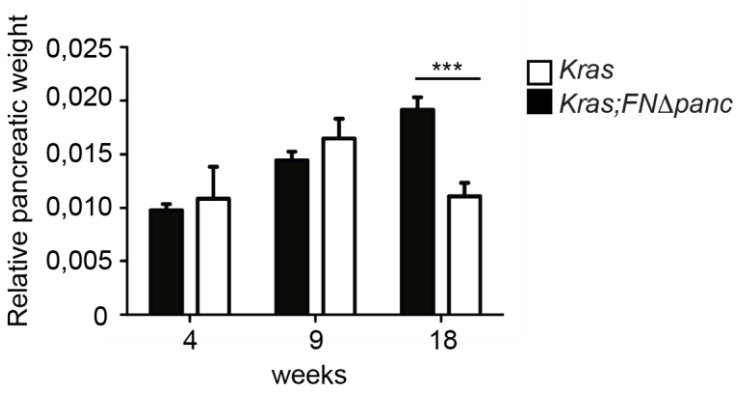
Relative pancreatic weight
0,025
0,020
0,015
0,010
0,005
0
***
4
9
18
weeks
Kras
Kras;FNΔpanc

D

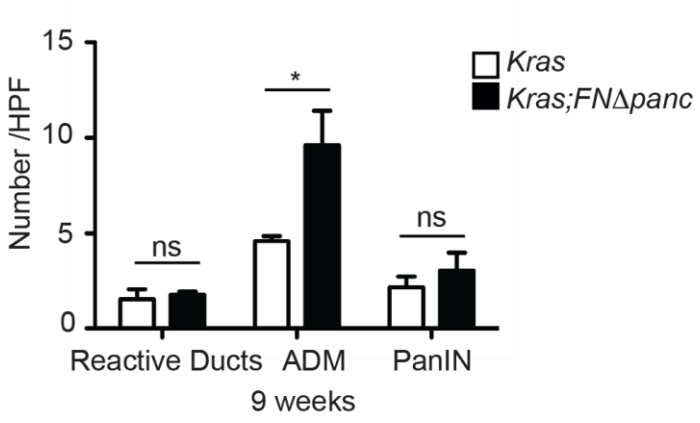
Number /HPF
15
10
5
0
*
ns
ns
Reactive Ducts
ADM
PanIN
9 weeks
Kras
Kras;FNΔpanc

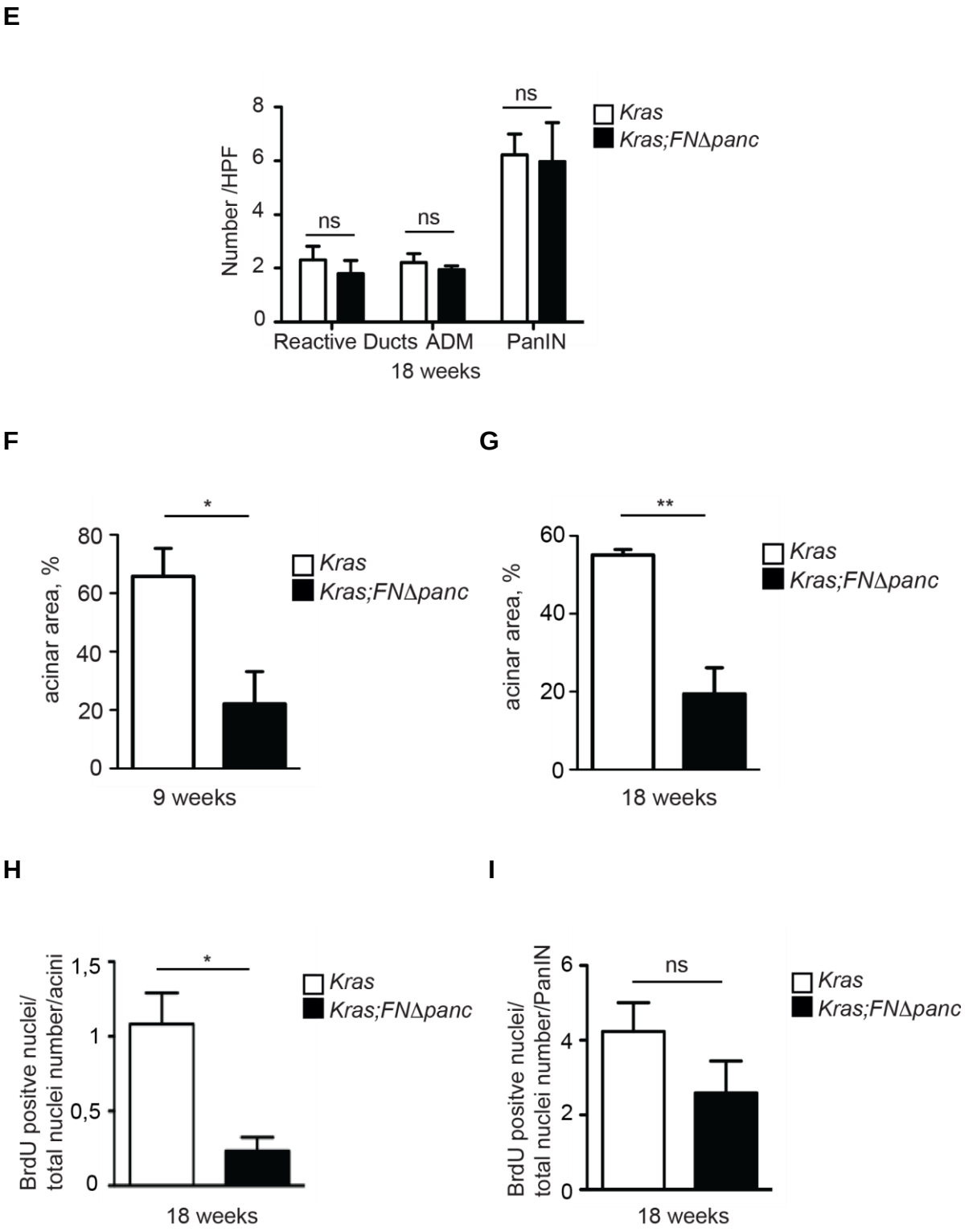

Figure 5: Pancreas-specific ablation of Fibronectin leads to loss of exocrine tissue and decrease proliferation of cells in acinar compartment. (A) Morphological analysis of pancreas from 4-week and 9-week-old *Kras* and *Kras; FNΔpanc* mice. Scale bar: 100 um (B) Morphological analysis of pancreas from 18-week-old *Kras* and *Kras; FNΔpanc* mice. Scale bar: 1000 um, 100 um (C) Number of ADM, reactive ducts and PanIN structures were counted in pancreas from 9-week-old *Kras* and *Kras; FNΔpanc* mice per 200x field. Mean ± SD; * *p< 0,05* by unpaired t-test. (D) Pancreas to body weight ratio in 4 weeks, 9 weeks and 18 weeks old *Kras* and *Kras; FNΔpanc* mice. Mean ± SD; *** *p< 0,001* by unpaired t-test. (E) Number of ADM, reactive ducts and PanIN structures were counted in pancreas from 18-week-old *Kras* and *Kras; FNΔpanc* mice per 200x field. (F-G) Quantification of intact acinar area

in pancreas from 9-week-old and 18-week-old *Kras* and *Kras; FNΔpanc* mice. Mean ± SD; * *p< 0,05*; ***p< 0,01* by unpaired t-test. (H-I) Proliferation index of acinar cells and cells in PanIN structures from 18-week-old mice with indicated genotypes. The number of BrdU positive nuclei counted in PanIN structures per mouse. Mean ± SD; * *p< 0,05* by unpaired t-test.

6.1.6 Loss of FN does not alter the Ras activity

To investigate whether loss of FN alters the Ras activity, RAF-RBD agarose affinity precipitation assay has been performed by using acinar cells isolated from 4-week-old mice with *Kras* and *Kras; FNΔpanc* genotype. Active Ras did not be altered by the homozygous deletion of FN has been shown (Figure 6).

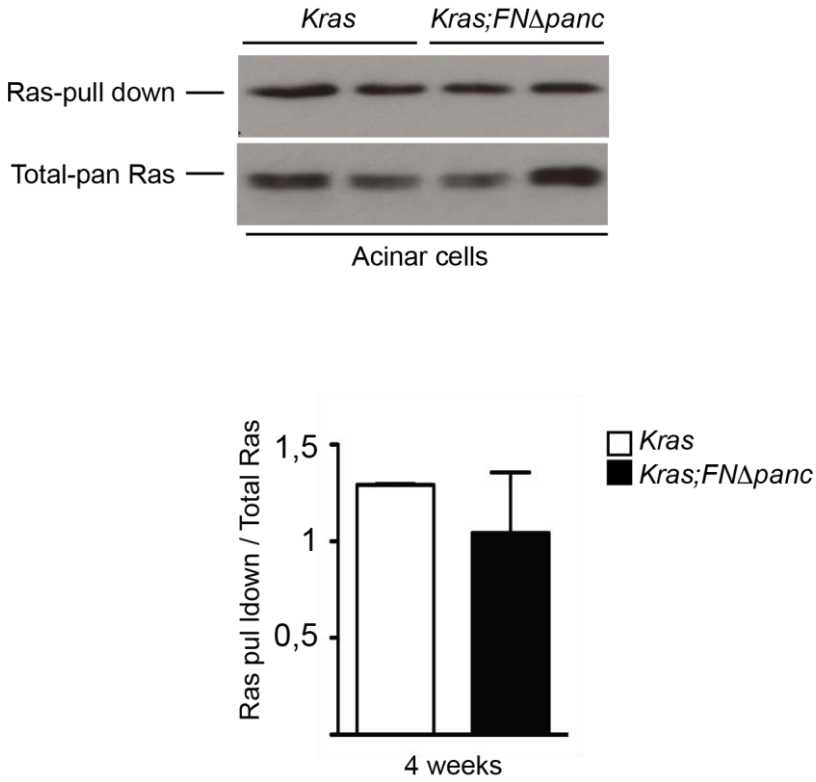

Figure 6: Loss of Fibronectin does not alter the Ras activity. RAF-RBD agarose affinity precipitation assay of representative samples (two biological replicates per genotype) from pancreatic tissue (4-week-old mice) with *Kras* and *Kras; FNΔpanc* genotypes.

6.1.7 Homozygous deletion of FN enhances immune infiltration

PDAC is characterized by the immunosuppressive microenvironment consist of various immunosuppressive immune cells including myeloid-derived suppressor cells (MDSCs), tumor associated macrophages (TAMs), regulatory T cells (Tregs)

(D'Angelo *et al.*, 2019). To examine immune infiltration profile after deleting *FN* in pancreas during pancreatic carcinogenesis, Immunohistochemical staining of common immune cell marker, CD45 has been performed on pancreas tissue from 9-week-old and 18-week-old *Kras* and *Kras; FNΔpanc* mice. CD45 staining interpreted that loss of FN significantly elevated the infiltrated immune cells compared to *Kras* control (Figure 7A, B, C).

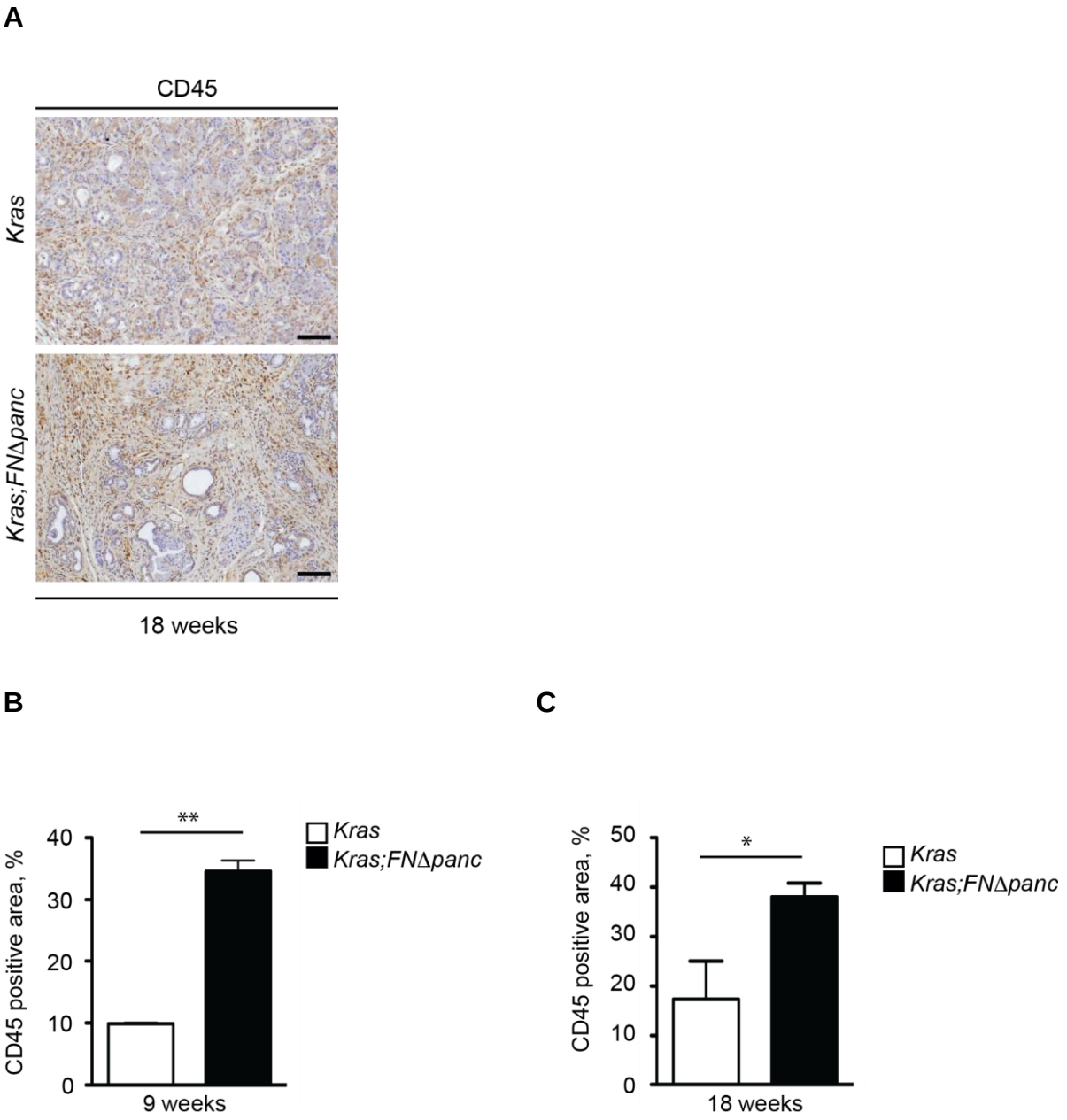

Figure 7: Loss of Fibronectin enhances immune infiltration (A) Representative IHC staining of CD45 in pancreas from mice with indicated genotypes. (B) Quantification of CD45 positive area in pancreas from 9-week-old *Kras* (n=2) and *Kras; FNΔpanc* (n=3) mice. (C) Quantification of CD45 positive area in pancreas from 18-week-old *Kras* (n=3) and *Kras; FNΔpanc* (n=4) mice. Mean ± SD; * *p< 0,05; **p< 0,01* by unpaired t-test; n, number of mice.

6.1.8 Homozygous deletion of Fibronectin increases tumor incidence, decreases stromal reaction, induces pancreatic atrophy and reduces survival of Kras Mice

To analyze the long-term effect of *FN*-deficiency and survival difference between *Kras* and *Kras; FNΔpanc* mice, we have sacrificed the mice at the time of sickness. Histological analysis was clearly demonstrating pancreatic atrophy in *Kras; FNΔpanc* survival mice (28-week-old) (Figure 8A). Besides, general pathological findings also included cyst formation, micro carcinoma structures and lipomatosis (Figure 8B). Observed severe pancreatic degeneration due to pancreatic atrophy can be associated with the significant reduction in survival rate of *FN*-deficient mice (Figure 8 C). Analysis of stromal reaction by Masson Trichrome staining demonstrated that loss of *FN* diminished the collagen production in long term (Figure 8D). Interestingly, even though limited number of fibrotic PDAC tumors (n=3) were observed in *Kras; FNΔpanc* mice, pathological examinations interpreted that micro carcinoma structures were abundant in *Kras; FNΔpanc* mice. With this indication, it is concluded that the tumor incidence was significantly higher in *Kras; FNΔpanc* mice in comparison with *Kras* mice (Figure 8E). On the other hand, loss of *FN* was significantly diminished the metastasis rate (figure 8F).

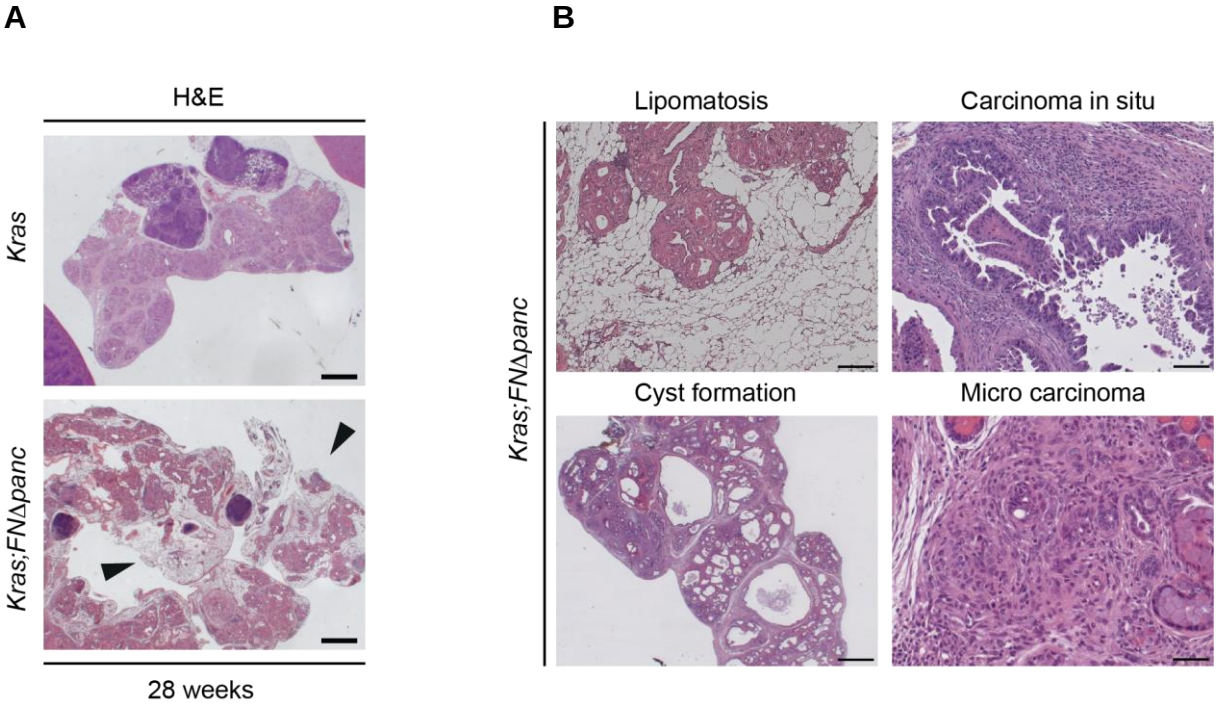

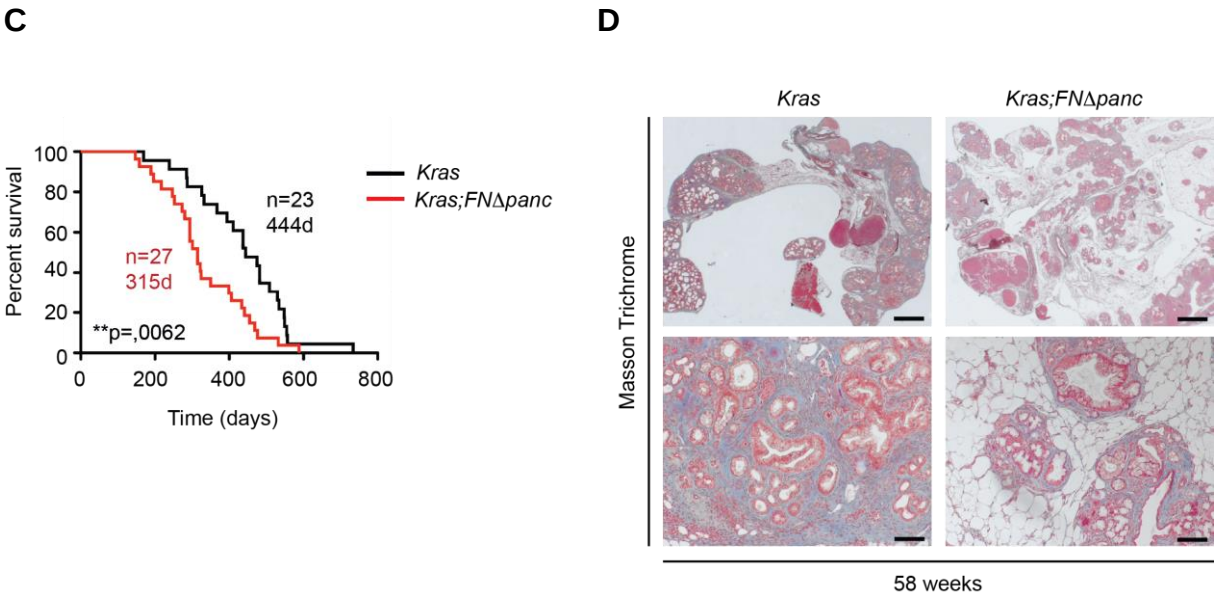

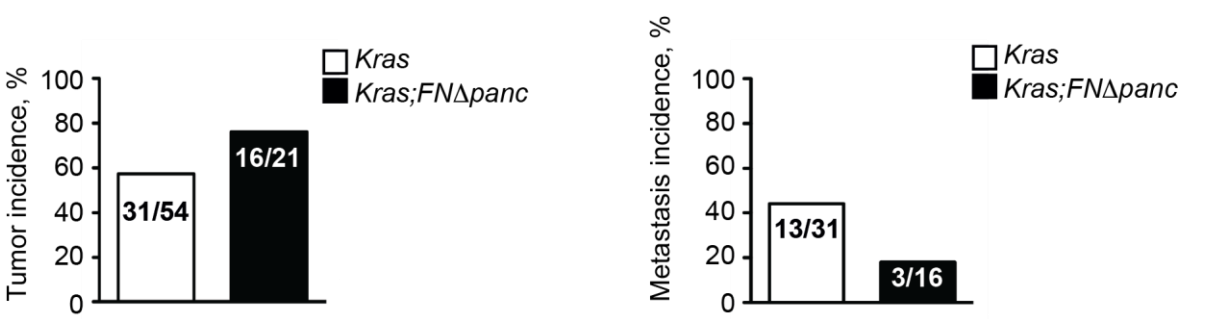

Figure 8: **Homozygous deletion of Fibronectin increases tumor incidence, decreases stromal reaction, induces pancreatic atrophy and reduces survival of KrasG21D Mice**. (A) Morphological analysis of pancreas from *Kras* (28-week-old) and *Kras; FNΔpanc* (28-week-old) survival mice. blackarrows indicates the pancreatic atrophy. (B) General pathological findings in *Kras; FNΔpanc* pancreata were represented. (C) Kaplan-Maier analysis shows a median survival in *Kras; FNΔpanc* mice of 315 days, significantly less than *Kras* mice (444 days). (***p= 0,0061* long-rank test, for pairwise combination) (D) Representative Masson Trichrome staining of pancreas from *Kras* (58-week-old) and *Kras; FNΔpanc* (58-week-old) survival mice. (E) Tumor incidence (%) in *Kras* (n=54) and *Kras; FNΔpanc* (n=21) mice. (F) Metastasis incidence (%) in *Kras* (n=31) and *Kras; FNΔpanc* (n=16) mice.

6.1.9 P53 deletion is enough to switch the phenotype of FN deficient Kras mutated pancreas

As aforementioned, loss of FN in Kras mutated mouse model mostly resulted in soft pancreatic tissue with micro carcinoma structures and stroma around cancer structures were dramatically decreased. In contrast, in p53 deficient Kras mutated mouse model, loss of FN did not diminish the stromal reaction in tumor and all tumors from this genotype were fibrotic as seen in pancreas images in Figure 9A. Histological analysis showed that *Kras; p53Δpanc; FNΔpanc* tumors were mixed subtype including differentiated and undifferentiated structures. One out of three tissues have liver metastasis (Figure 9A). Kaplan-Maier analysis showed that there was no difference in median survival (61 days) between mice with *Kras; p53Δpanc and Kras; p53Δpanc; FNΔpanc* genotypes (Figure 9B). Moreover, relative pancreatic weight to body weight ratio between indicated genotypes were not distinct (Figure 9C). To monitor the tumor growth and metastasis, isolated mouse cell from mice with *Kras; p53Δpanc and Kras; p53Δpanc; FNΔpanc* genotypes implanted into wild type littermate mice as orthotopic model (4 technical replica and 1 cell line from each genotype used). Histological analysis demonstrated that tumor formation and tumor morphology were similar in transplanted mice with *Kras; p53Δpanc and Kras; p53Δpanc; FNΔpanc* cells lines. Nevertheless, lung metastasis and kidney invasion were observed in mice with *Kras; p53Δpanc; FNΔpanc* cells whereas only spleen invasion was observed in both (Figure 9D). Further transplantation experiments with other cell lines isolated from *Kras; p53Δpanc; FNΔpanc* mice is necessary to make a conclusion about the invasiveness and metastatic capacity.

A

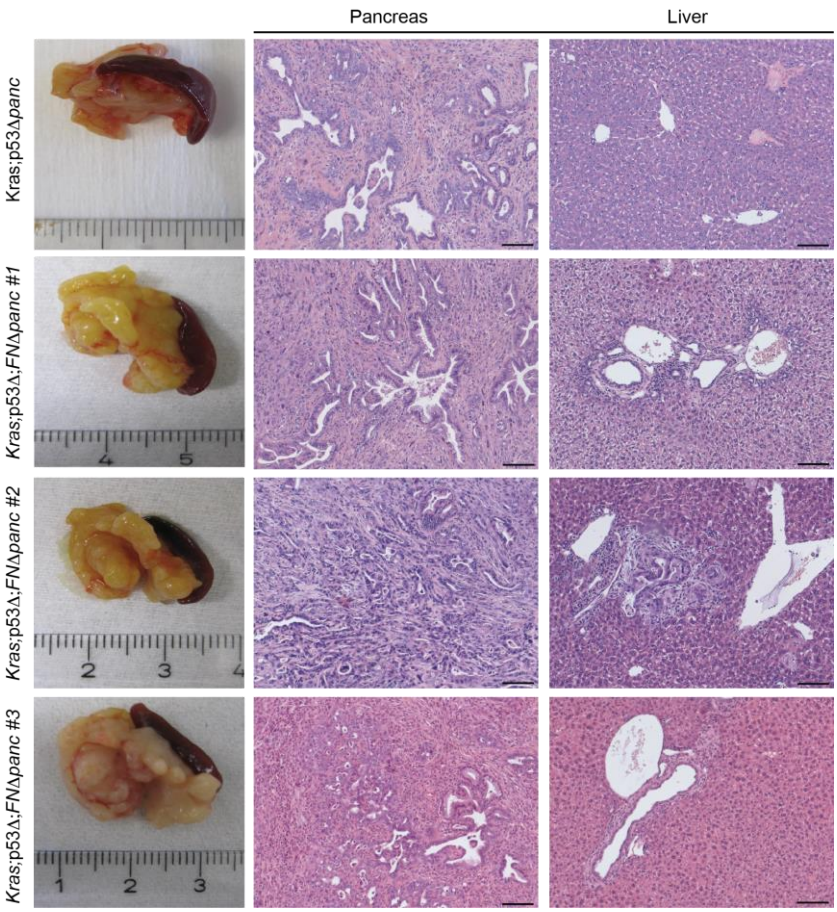
Pancreas
Liver
Kras;p53Δpanc
Kras;p53Δ;FNΔpanc #1
Kras;p53Δ;FNΔpanc #2
Kras;p53Δ;FNΔpanc #3

B

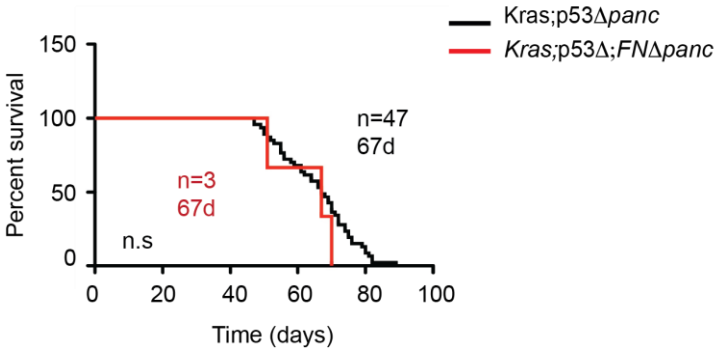
Kras;p53Δpanc
Kras;p53Δ;FNΔpanc
Percent survival
150
100
50
0
n=47
67d
n=3
67d
n.s
0
20
40
60
80
100
Time (days)

C

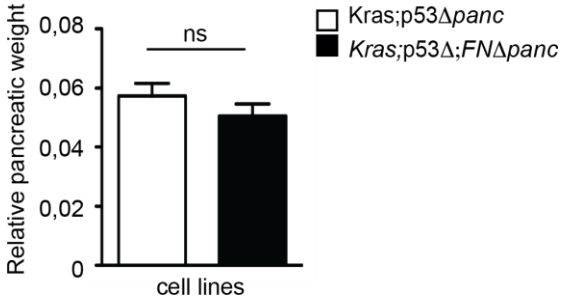
Kras;p53Δpanc
Kras;p53Δ;FNΔpanc
Relative pancreatic weight
0,08
0,06
0,04
0,02
0
ns
cell lines

D

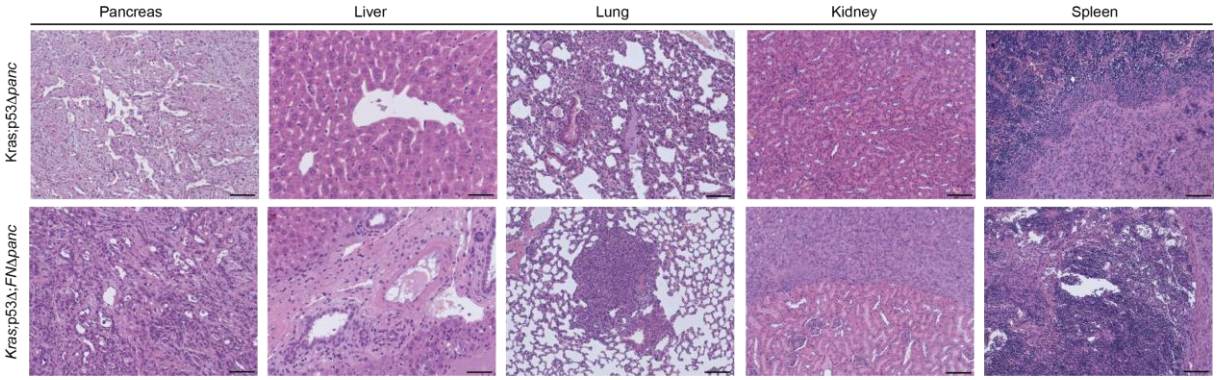

Figure 9: p53 deficiency is enough to switch the phenotype of *FN* deficient *Kras*-mutated pancreas. (A) Representative pancreas images and histology of pancreas and liver from *Kras; p53Δpanc* and *Kras; p53Δpanc; FNΔpanc* mice. (B) Kaplan-Maier analysis shows a median survival in both *Kras; p53Δpanc* and *Kras; p53Δpanc; FNΔpanc* mice of 61 days. (C) Pancreas to body weight ratio in survival mice with *Kras; p53Δpanc* and *Kras; p53Δpanc*; *FNΔpanc* genotypes. (D) Representative histological images from orthotopic transplanted mice with *Kras; p53Δpanc* and *Kras; p53Δpanc; FNΔpanc* cell line (n=4 technical replicates for each genotype)

6.1.10 Characterization of cells isolated from *P53* deletion *FN*-deficient *Kras*-mutated tumors

To analyze the colony formation capacity of cells isolated from *Kras; p53Δpanc and Kras; p53Δpanc; FNΔpanc* tumors, cells were seeded as 200.000 cell per well in 6 well plate. After 72h, cells were stained with Cristal Violent and the colony area was quantified. Results indicated that *Kras; p53Δpanc; FNΔpanc* cells had significantly less colony then *Kras; p53Δpanc* cells (Figure 10A). For characterization of the cell lines, several markers of essential signaling pathways for pancreatic cancer were analyzed. Firstly, *FN* deletion was validated in *Kras; p53Δpanc; FNΔpanc* cell lines. Ductal adenocarcinoma marker, CK19 indicated that all tumor cells are ductal type. Proteins which are essential for PDAC tumorigenesis, such as p-Stat3, p-Src, Src, p-Akt, Akt, c-met, PCNA, ERK and p-ERK were analyzed and no clear differences were detected (Figure 10B).

A

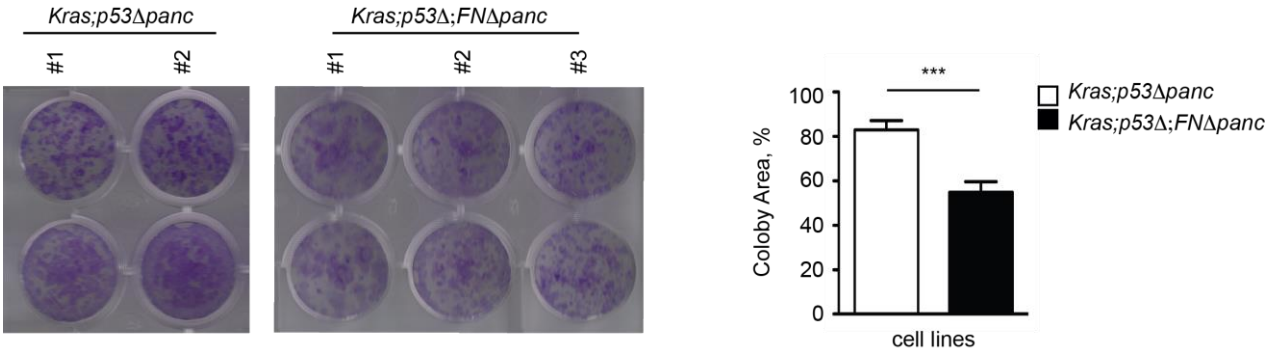

B

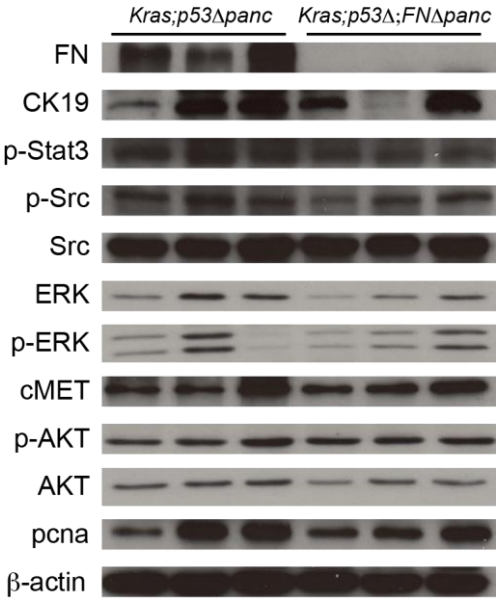

Figure 10: Characterization of *Kras; p53Δpanc* and *Kras; p53Δpanc; FNΔpanc* cell lines. (A) Colony formation assays of *Kras; p53Δpanc* (n=2 biological replicates) and *Kras; p53Δpanc; FNΔpanc* (n=3 biological replicates) cell lines and colony area is quantified at 72h after seeding. Mean ± SD; ****p< 0,001* by two-tailed t-test. (B) Immunoblot analysis of indicated proteins in protein lysates isolated from *Kras; p53Δpanc* and *Kras; p53Δpanc; FNΔpanc* cell lines.

6.1.11 Heterozygous deletion of *p53* decrease the survival of *FN*-deficient *Kras*-mutated mice compared to control

Heterozygous deletion of *p53* resulted in fibrotic, undifferentiated tumors in *FN* deleted *Kras*-mutated mouse model (Figure 11A). Kaplan-Maier analysis showed a median survival in *Kras; p53Δ/+; FNΔpanc* mice of 119 days which is significantly less than *Kras; p53Δpanc* mice (207 days) (Figure 11B).

A

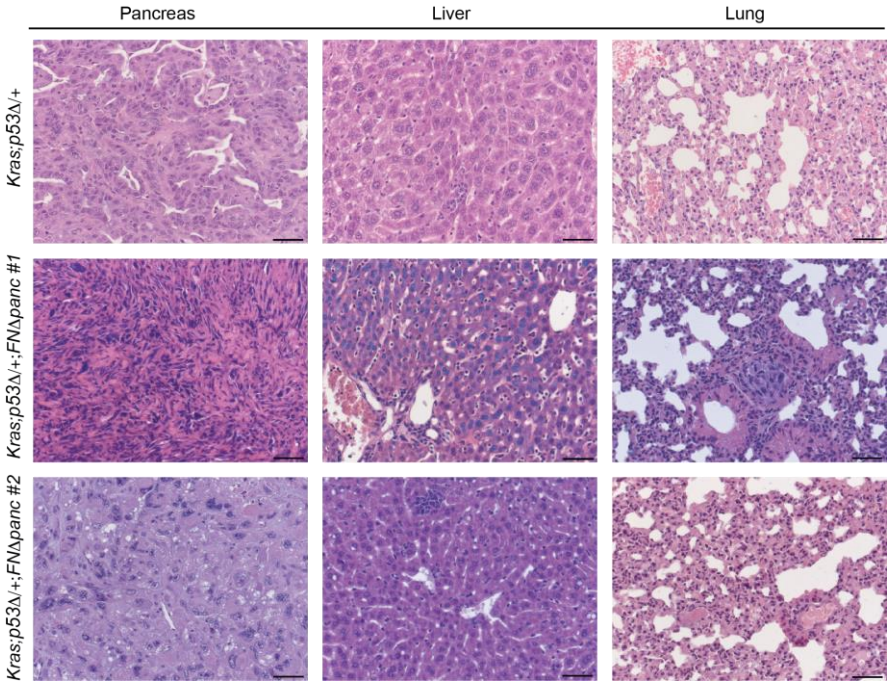

B

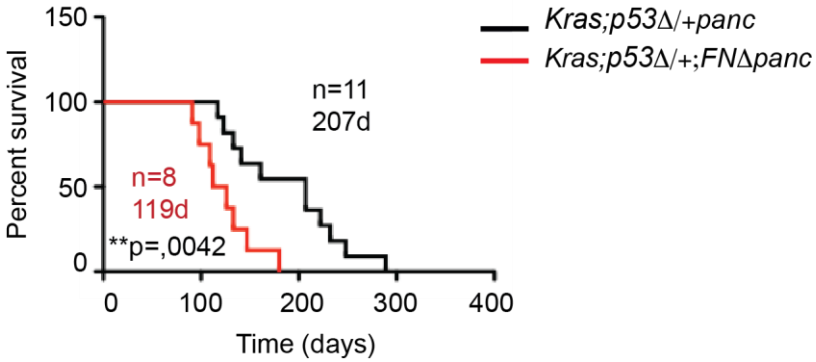

Figure 11: Heterozygous deletion of *p53* reduces survival rate of *Kras; p53Δ/+; FNΔpanc* mice. (A) Morphological analysis of pancreas from *Kras; p53Δpanc* and *Kras; p53Δ/+; FNΔpanc* mice. (B) Kaplan-Maier analysis shows a median survival in *Kras; p53Δ/+; FNΔpanc* mice of 119 days, significantly less than *Kras; p53Δpanc* mice (207 days). (***p= 0,042* long-rank test, for pairwise combination)

6.1.12 Characterization of tumor cell lines isolated from pancreatic tumor with Kras and Kras; FNΔpanc genotype

The role of loss of *FN* was also investigated *in vitro*. In *Kras; FNΔpanc* mouse line, only 3 out of 25 mice had fibrotic tumor. Hereby, 3 different FN-deficient cell lines have been isolated from those tumors as shown in Figure 12A. Immunoblot analysis of FN validated the deletion of *FN* compared to the *Kras* mouse lines. To characterize the cell lines, various proteins from important signaling pathways which are activated in PDAC has been analyzed by immunoblotting (Figure 12B).

A **B**

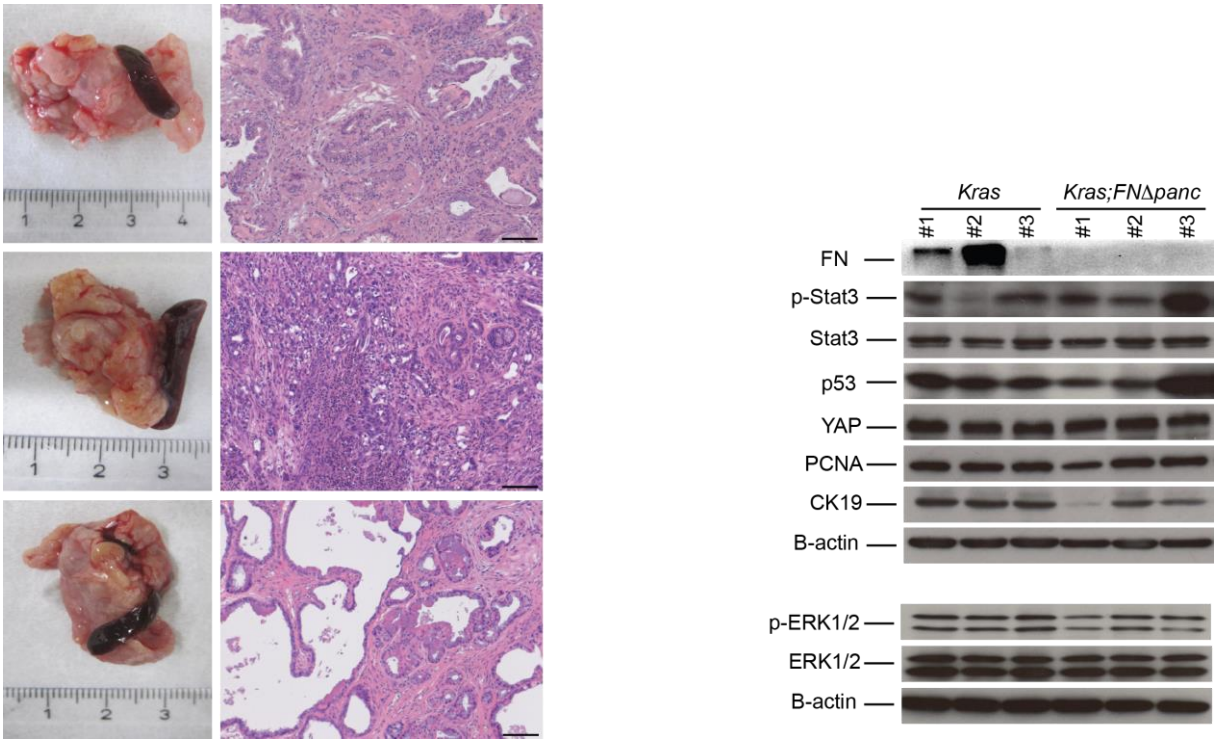

Figure 12: Characterization of tumor cell lines isolated from pancreatic tumor with *Kras* and *Kras; FNΔpanc* genotype. (A) Representative images of pancreatic tumors from *Kras* and *Kras; FNΔpanc* mice. (B) Immunoblot analysis of indicated proteins in cell lines isolated from both genotypes. (C) Proliferation analysis of cell lines isolated from both genotypes.

6.1.13 Loss of FN does not sensitize the susceptibility of cells to conventional chemotherapy, even make slightly resistant

To investigate whether loss of *FN* alters the susceptibility of cell to conventional chemotherapeutics for pancreatic cancer, cell lines isolated from *Kras* and *Kras; FNΔpanc* mice have been treated with Gemcitabine, 5FU, Irinotecan, Oxaliplatin and Paclitaxel for 24h, 48h, 72h, 96h and measured their cell viability by Cell Titer Glo Assay. Results were presented as a fold change of absolute cell number of viable cells in treated *Kras; FNΔpanc* versus *Kras* treated group. It showed that *FN*-deficiency did not sensitize the cells to conventional chemotherapy and even increased the resistance of cells against Gemcitabine, Paclitaxel and Oxaliplatin treatment (Figure 13)

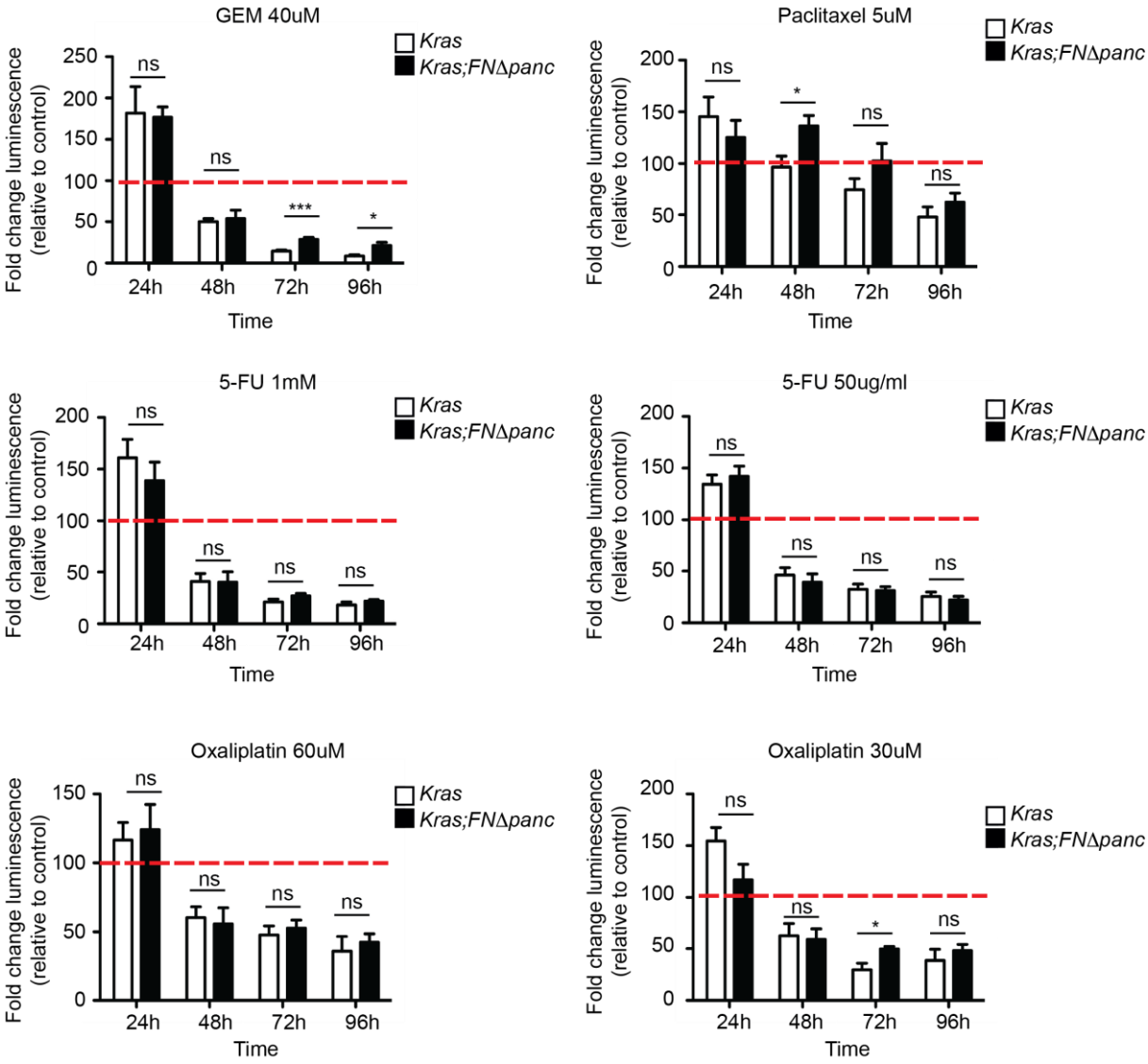

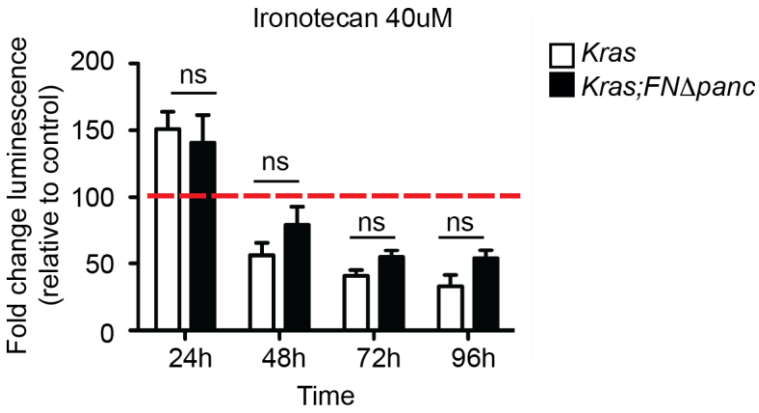

Figure 13: Loss of *FN* does not sensitize the susceptibility of cells to conventional chemotherapy, even make slightly resistant. Cell Titer Glo assay measuring the cellular viability of cells isolated from *Kras* and *Kras; FNΔpanc* pancreatic tumor at indicated time points upon treatment with conventional chemotherapeutics for pancreatic cancer which are Gemcitabine (40uM), 5FU (1mM, 50ug/ml), Irinotecan (40uM), Oxaliplatin (30uM, 60 uM), Paclitaxel (5uM). Mean ± SD; *$p< 0,05$; **$p< 0,01$, ***$p< 0,001$ by two-tailed t-test.

6.1.14 Loss of FN sensitize the cells to ER stress inducers

FN is a secretory protein and it is localized in the ER following production (Yamada, 1978). To investigate whether *FN* loss triggers or relieve stress in the ER, *Kras* and *Kras; FNΔpanc* cell lines were treated with ER stress inducers including Tunicamycin and Thapsigargin. *Kras* and *Kras; FNΔpanc* cell lines were seeded as 1000 per well in 24-well plate. 3 days later, cells treated with increasing dose of Tunicamycin for 12h, 24h, 48h and 72h for colony formation assay. Results indicated that loss of *FN* was significantly sensitize cells to Tunicamycin (Figure 14A) To support this experiment, cell viability of Tunicamycin and Thapsigargin treated *Kras* and *Kras; FNΔpanc* cell lines were measured by Cell Titer Glo assay. Results were presented as a fold change of absolute cell number of viable cells treated versus control treated. It showed that *FN*-deficiency increased the susceptibility of cells to ER stress inducers compared to *Kras* control (Figure 14B, C).

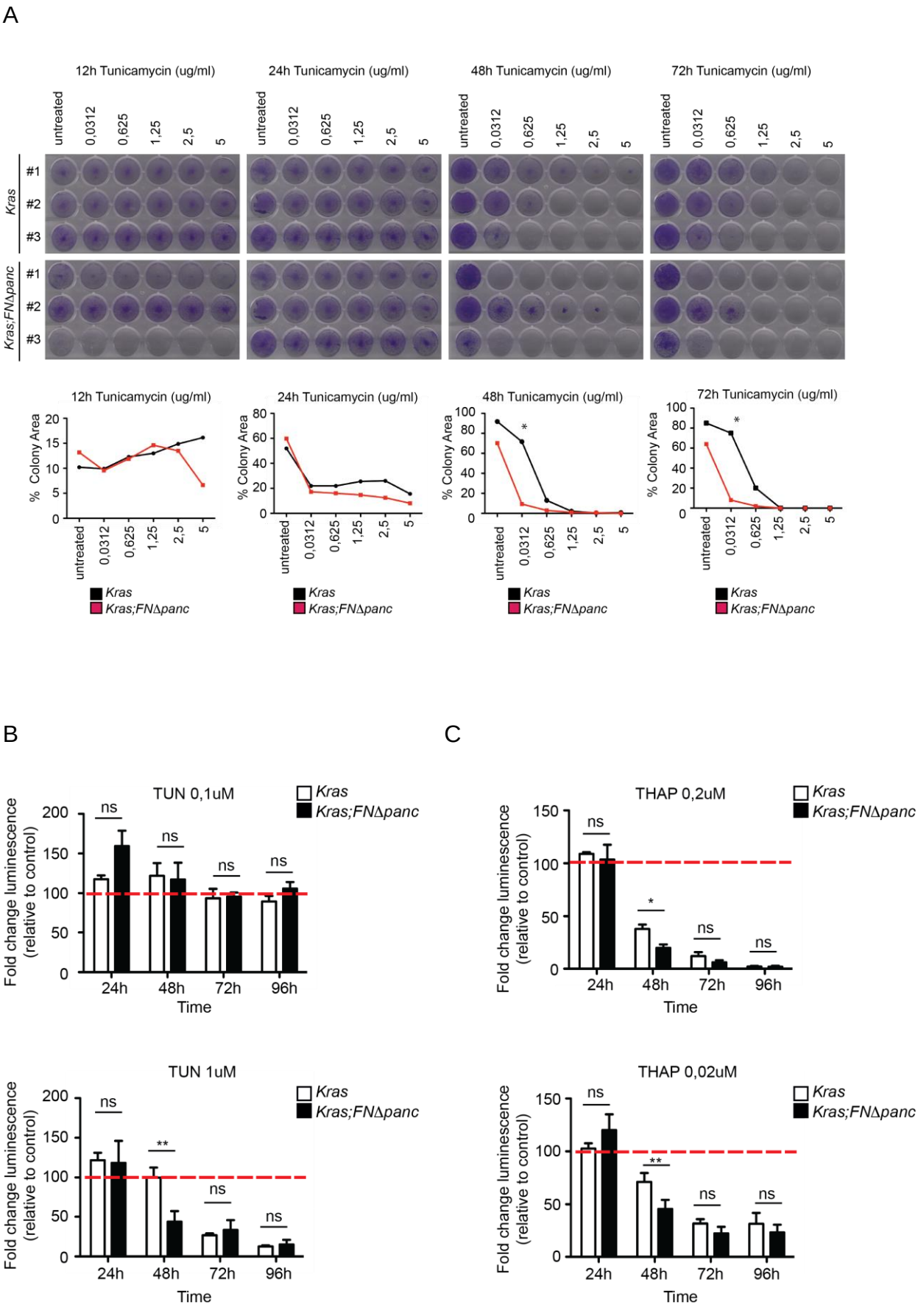

Figure 14: Loss of FN sensitizes the cells to ER stress inducers. (A) Colony formation assays of

Kras and *Kras; FNΔpanc* cell lines at indicated time points (12h, 24h, 48h, 72h) upon dose-dependent Tunicamycin treatment (0,312, 0, 625, 1,25, 2,5, 5 ug/ml). Mean ± SD; *p< 0,05 by two-tailed t-test. (B) Cell Titer-Glo assay measuring the cell viability of *Kras* and *Kras; FNΔpanc* cell lines treated with indicated doses of Tunicamycin 24h, 48h, 72h, 96h time points. (C) Cell Titer-Glo assay measuring the cell viability of *Kras* and *Kras; FNΔpanc* cell lines treated with indicated doses of Thapsigargin 24h, 48h, 72h, 96h time points. Mean ± SD; *p< 0,05; **p< 0,01 by two-tailed t-test.

6.1.15 FN expression is affected by ER stress inducer Tunicamycin

In recent studies, it has been demonstrated that FN expression is downregulated upon Tunicamycin treatment in non-small cell lung cancer cells and colon cancer cells referring to inhibiting effect of Tunicamycin on cell growth and metastasis (Qi *et al.*, 2018) (You, Li and Guan, 2018). Accordingly, FN expression in *Kras* control cell lines were analyzed upon Tunicamycin (5 ug/ml) treatment. As clearly visible in representative bright field images, *Kras; FNΔpanc* cell lines were undergone cell death upon Tunicamycin (5 ug/ml) treatment as also indicated above (Figure 15A). Protein lysates were obtained from 24h treated *Kras* cell lines and immunoblot analysis of FN showed that Tunicamycin treatment dramatically reduced the expression of FN in *Kras* cell lines (Figure 15B). To interpret the time-dependent decrease of FN expression upon Tunicamycin treatment, one *Kras* cell lines was treated with Tunicamycin (5 ug/ml) at 1,5h, 3h, 6h, 12h and 24h time points. Immunoblot analysis of FN showed gradual decrease of FN expression with Tunicamycin treatment (Figure 15C). To validate if Tunicamycin influences the level of secreted FN, supernatant of 24h Tunicamycin (5 ug/ml) treated Kras cell lines were collected. Immunoblot analysis of FN validates secreted FN also reduced upon Tunicamycin treatment (Figure 15D). Furthermore, to check if the FN expression decrease is transcriptionally regulated or not, mRNA levels also analyzed upon Tunicamycin treatment. Quantitative Real-time PCR result showed that FN expression was transcriptionally regulated upon Tunicamycin which induced ER stress markers including CHOP as shown (Figure 15E, 15F).

A

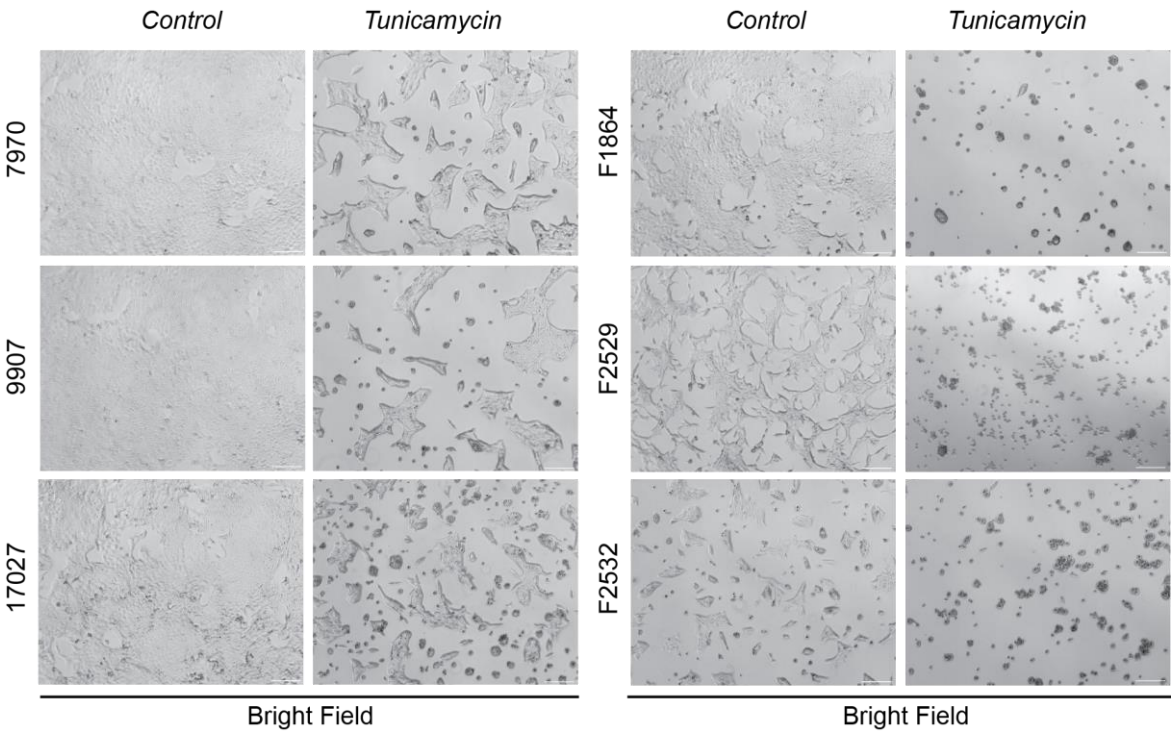
Control
Tunicamycin
Control
Tunicamycin
7970
9907
17027
F1864
F2529
F2532
Bright Field
Bright Field

B

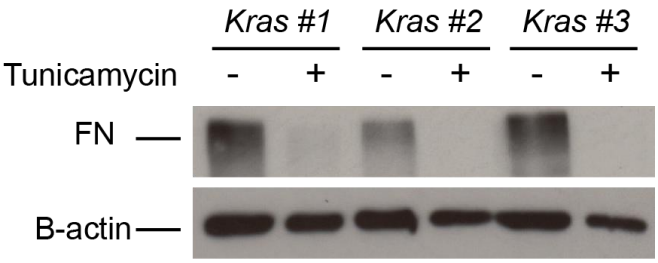
Kras #1
Kras #2
Kras #3
Tunicamycin
- + - + - +
FN
B-actin

C

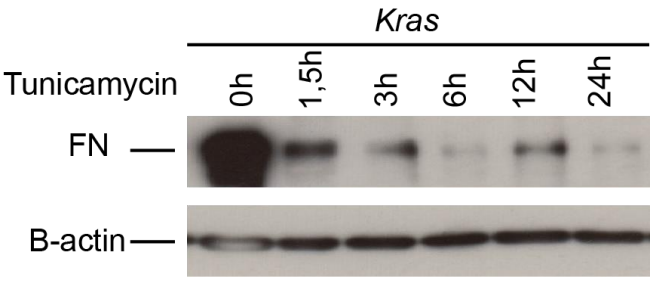
Kras
Tunicamycin
0h
1,5h
3h
6h
12h
24h
FN
B-actin

D

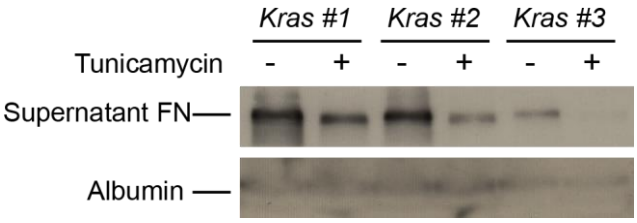

E

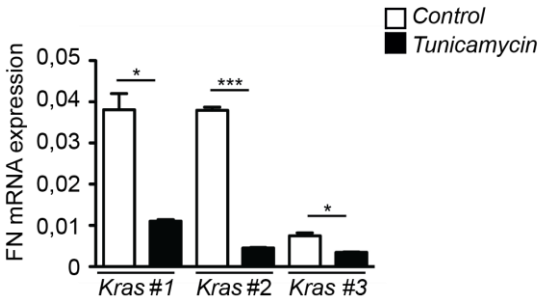

F

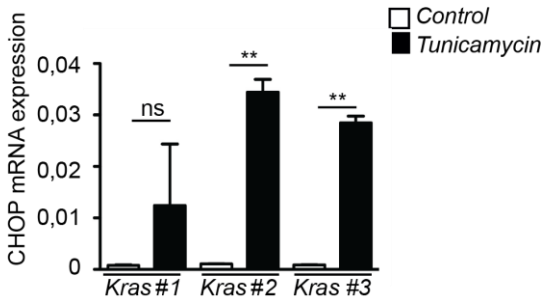

Figure 15: FN expression is affected by ER stress inducer Tunicamycin (A) Representative bright field images of untreated and 24h Tunicamycin (5ug/ml) treated *Kras* and *Kras; FNΔpanc* cell lines. (B) Immunoblot analysis of FN protein in untreated and 24h Tunicamycin (5ug/ml) treated *Kras* and *Kras; FNΔpanc* cell lines. (C) Immunoblot analysis of FN protein in time-dependent Tunicamycin (5ug/ml) treated *Kras* cell lines. (D) Immunoblot analysis of FN in supernatants of untreated and 24h Tunicamycin (5ug/ml) treated *Kras* and *Kras; FNΔpanc* cell lines. (E) Quantitative reverse transcriptase polymerase chain reaction of *FN* normalized to *GAPDH* (n=3). (F) Quantitative reverse transcriptase polymerase chain reaction of *CHOP* normalized to *GAPDH* (n=3). Mean ± SD; **p< 0,05; **p< 0,01, ***p< 0,001* by two-tailed t-test.

6.1.16 FN expression is affected by ER stress inducer Thapsigargin

Tunicamycin is a glucosamine-containing antibiotic which specifically blocks the N-linked glycosylation and thereby inhibits protein folding and inducing ER stress. FN is one of the glycosylated proteins. Therefore, to investigate whether the effect of Tunicamycin on FN expression is not exclusively due to inhibition of glycosylation, cells were also treated with Thapsigargin. The distinct responses of the *Kras* and *Kras; FNΔpanc* cells to ER stress inducers, this time to Thapsigargin, were unequivocally shown (Figure 16A). Proteins lysates were obtained from 14h Thapsigargin (1 uM) treated *Kras* and *Kras; FNΔpanc* cell lines. Immunoblot analysis of FN and Bip

indicated that Thapsigargin induced ER stress at 24h treatment and downregulated the expression of FN in *Kras* cell lines (Figure 16B). Interestingly, Thapsigargin treatment increased the expression of LC3-II in *Kras*; *FNΔpanc* cell lines compared to *Kras* control (Figure 16C) which could indicate the autophagy induction or inhibition. Further starvation experiments are required to make a conclusion. Secreted FN levels also analyzed upon 24h Thapsigargin treatment in *Kras* cell lines which also indicated the reduction of secreted FN upon Thapsigargin induction (Figure 16D). Moreover, the quantitative RT-PCR analysis of *FN* validated that Thapsigargin also transcriptionally regulated the FN expression in *Kras* cell lines Figure 16E). *CHOP* increase was also shown as an indicator of ER stress induction (Figure 16F).

A

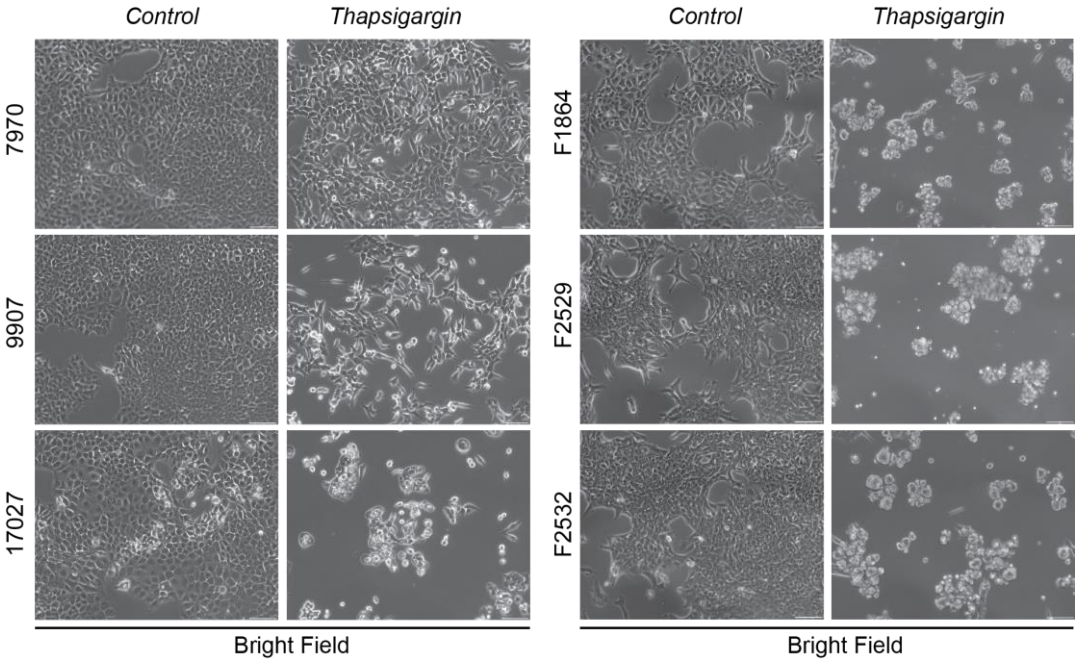

B

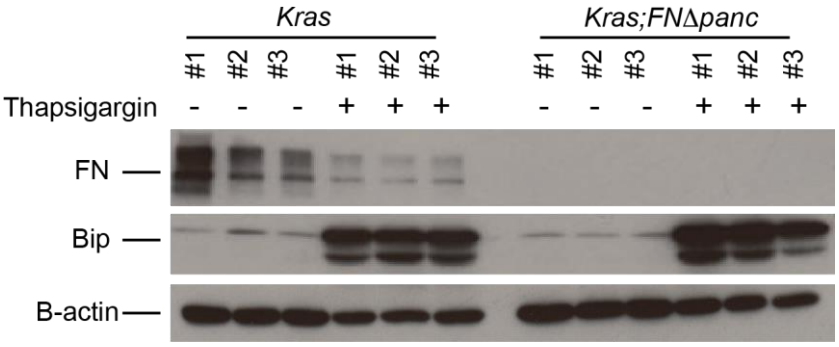

C

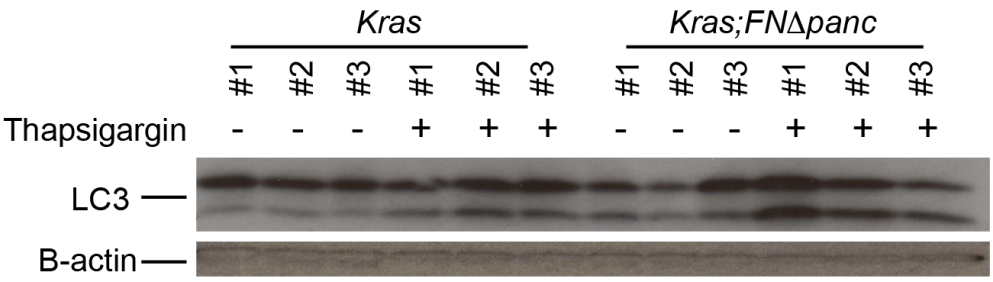

D

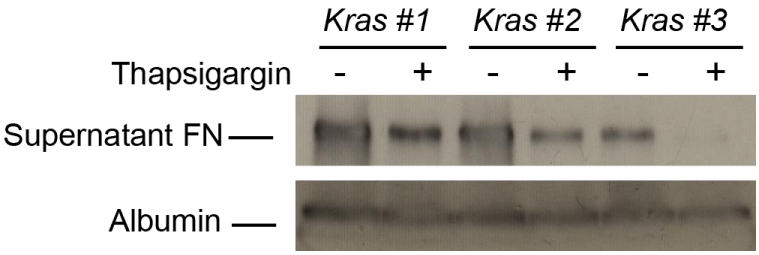

E

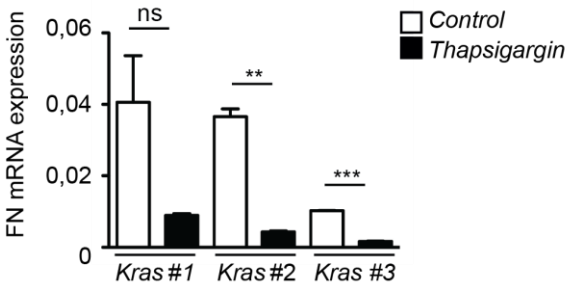

F

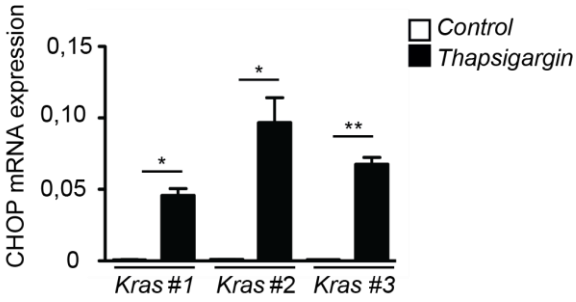

Figure 16: FN expression is affected by ER stress inducer Thapsigargin (A) Representative bright field images of untreated and treated *Kras* and *Kras; FNΔpanc* cell lines. (B) Immunoblot analysis of FN and Bip proteins in untreated and 24h Th (1 uM) treated *Kras* and *Kras; FNΔpanc* cell lines. (C) Immunoblot analysis of LC3 protein in untreated and 24h Thapsigargin (1 uM) treated *Kras* and *Kras; FNΔpanc* cell lines. (D) Immunoblot analysis of FN in supernatants of untreated and 24h Thapsigargin (1 uM) treated *Kras* and *Kras; FNΔpanc* cell lines. (E) Quantitative reverse transcriptase polymerase chain reaction of *FN* normalized to *GAPDH* (n=3). (F) Quantitative reverse transcriptase polymerase chain reaction of *CHOP* normalized to *GAPDH* (n=3). Mean ± SD; **p< 0,05; **p< 0,01, ***p< 0,001* by two-tailed t-test.

6.1.17 Basal levels of ER stress markers are not affected by FN deletion

As we demonstrated above, *FN* deletion sensitized the cells to ER stress inducers and stimulated cell death. In the line with that, we have analyzed the basal levels of various proteins which are important for UPR response. Nevertheless, basal levels of *Bip*, *Chop*, *Atf3* and *Atf4* were not affected by *FN* deletion (Figure 17).

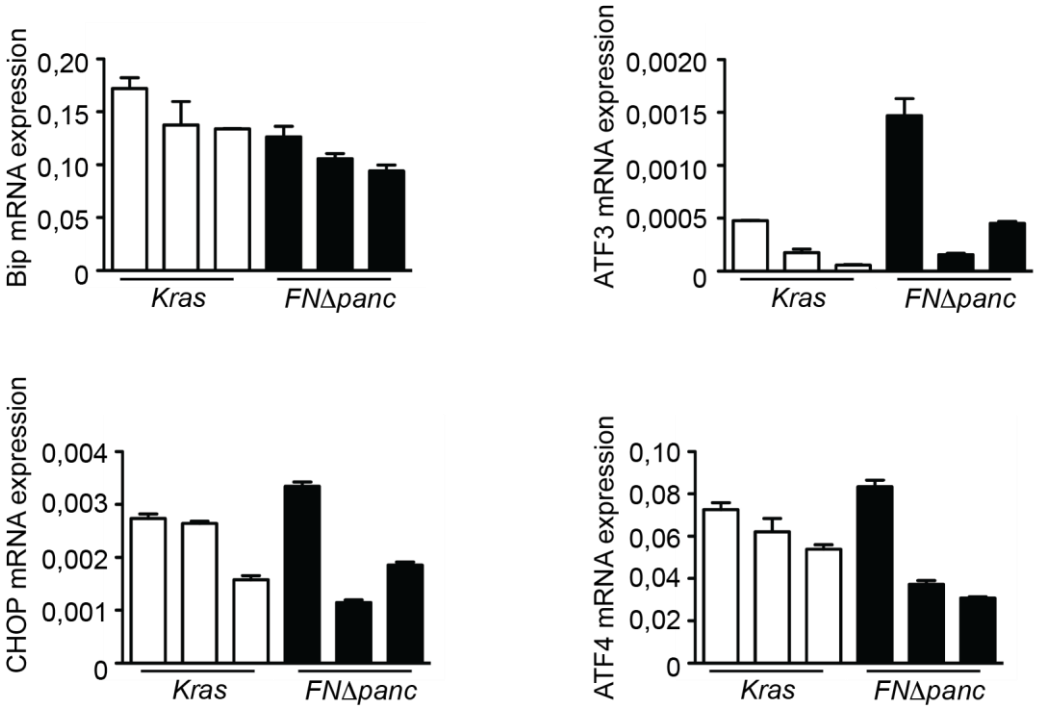

Figure 17: Basal levels of ER stress markers are not affected by FN loss. Quantitative reverse transcriptase polymerase chain reaction of *Bip, CHOP, ATF3* and *ATF4* normalized to *GAPDH* (n=3).

6.1.18 Smac mimetics induce apoptotic cell death slightly in both *Kras* and *Kras; FNΔpanc* cell lines

Since *Kras; FNΔpanc* cell lines undergo cell death upon ER stress inducers, we have characterized the cell death response of *Kras; FNΔpanc* cell lines in comparison with *Kras* controls upon treatment of different cell death inducers. *Kras* and *Kras; FNΔpanc* cells have been treated with Smac mimetics which are Birinapant (100nM) and LCL161 (1uM) for 24h, 48h, 72h, 96h and measured their cell viability by Cell Titer Glo Assay. Birinapant inhibits cIAP1/2 and XIAP while LCL161 inhibits cIAP1/2. Smac mimetics induces autocrine/ paracrine TNF mediated cells death which can be enhanced by the addition of TNF. Results were presented as a fold change of absolute cell number of

viable cells treated versus control-treated and it showed that *Kras* and *Kras; FNΔpanc* cells both were affected by Smac mimetic especially LCL161. In general, *Kras; FNΔpanc* cells were more susceptible to cell death induction but they did not give significant result due to one outlier cell line (Figure 18A, B). In addition, cells were also treated with apoptosis inhibitors zVAD (20 uM) and Emricasan (5 uM). *Kras* and *Kras; FNΔpanc* cells both were affected by apoptosis inhibition indicating substantial amount of apoptosis were happening in both cell lines (Figure 18C).

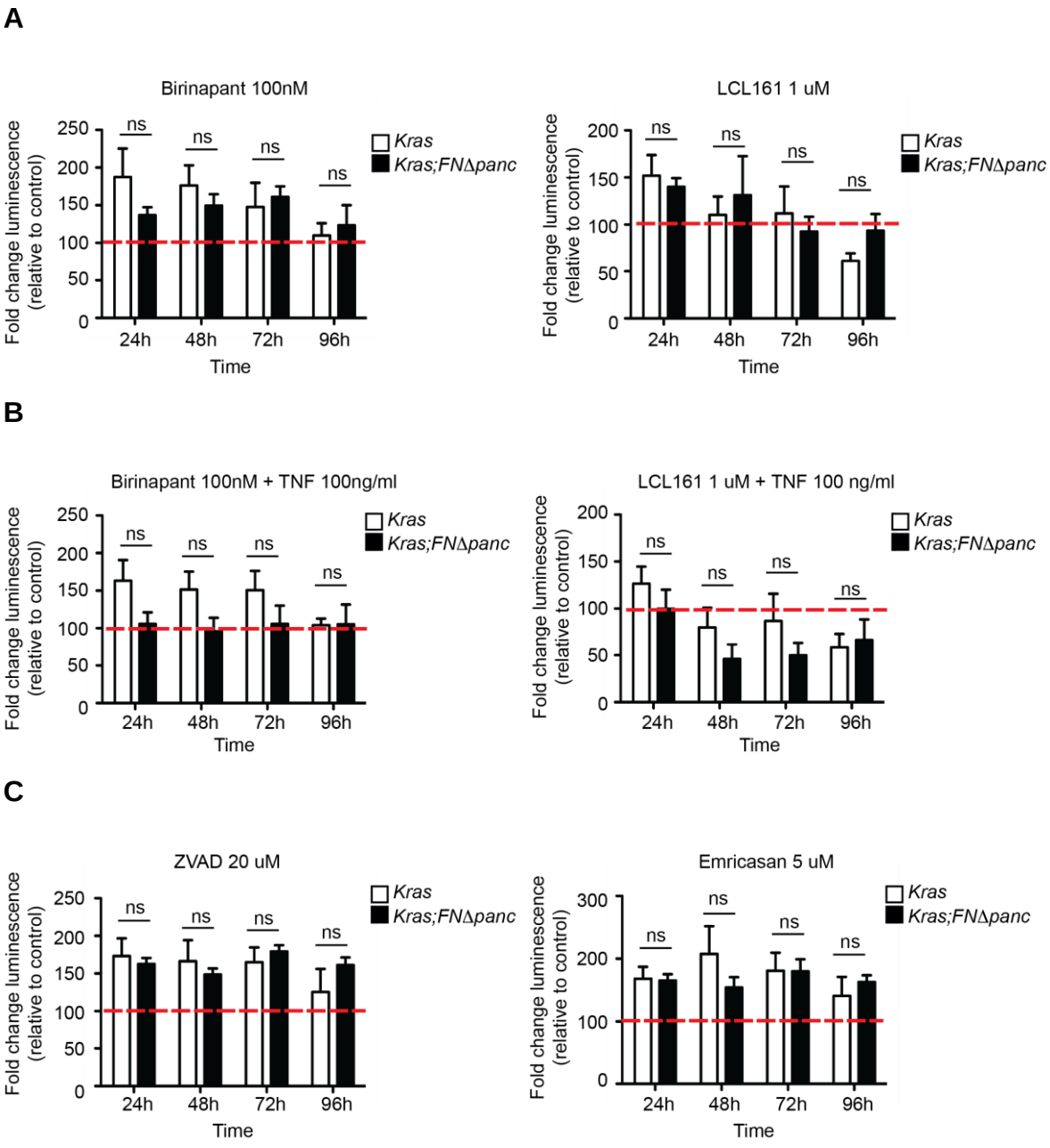

Figure 18: *Kras* and *Kras; FNΔpanc* are both affected by apoptosis induction and apoptosis inhibition. (A) Cellular viability of *Kras* and *Kras; FNΔpanc* cell lines were measured by Cell Titer Glo assay at indicated time points upon treatment with Smac mimetics Birinapant (100 nM) and LCL161 (1

uM). (B) Apoptosis induction is enhanced by the addition of TNF (100 ng/ml) to Smac mimetics. Viability was measured by Cell Titer Glo assay. (C) Cell were treated with apoptosis inhibitors zVAD (20 uM) and Emricasan (5 uM). Cell viability measured by Cell Titer Glo assay. Mean ± SD; **p< 0,05; **p< 0,01, ***p< 0,001* by two-tailed t-test

6.1.19 Loss of *FN* sensitizes cancer cells to necroptosis

To check the necroptosis response, cells were treated by necroptosis inhibitors Nec1s (30 uM) and GSK'872 (1 uM). Nec1s inhibits RIPK1 kinase activity, while GSK'872 inhibits RIPK3. Results showed that *Kras; FNΔpanc* cells profit from blocking of RIPK1/RIPK3 inflammatory signaling, indicating that necroptosis play role *Kras; FNΔpanc* cells' tumorigenesis (Figure 19A). Moreover, cells were treated with the combination of Birinapant (100 nM), TNF (100 ng/ml) and zVAD (20uM) also Birinapant (100 nM), TNF (100 ng/ml) and Emricasan (5uM) to force necroptosis induction. Whereas *Kras* cell lines did not seem to be affected by necroptosis induction, *Kras; FNΔpanc* cells were more susceptible to induction of necroptosis (Figure 19B).

A

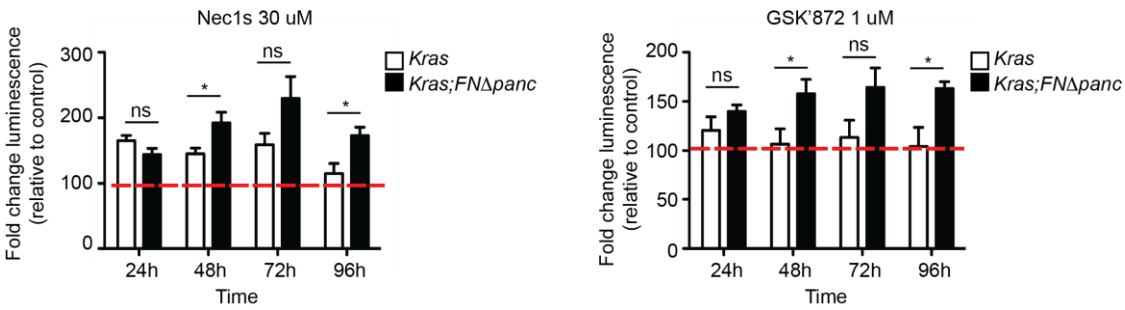

B

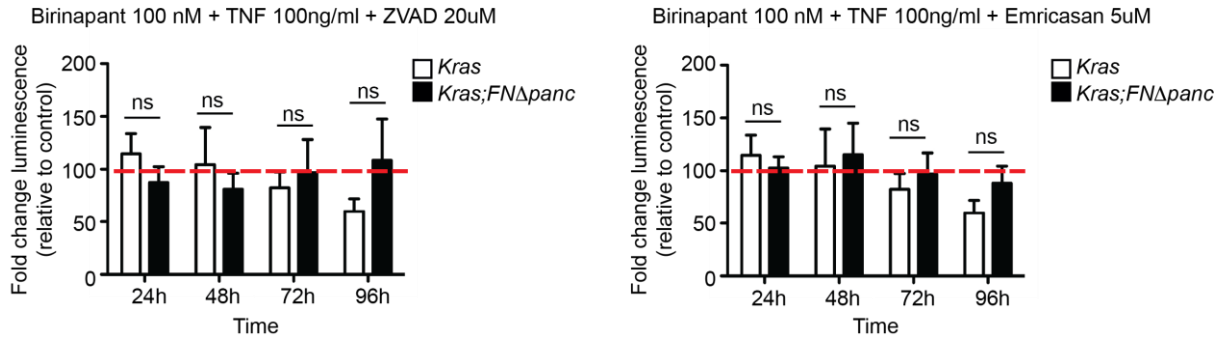

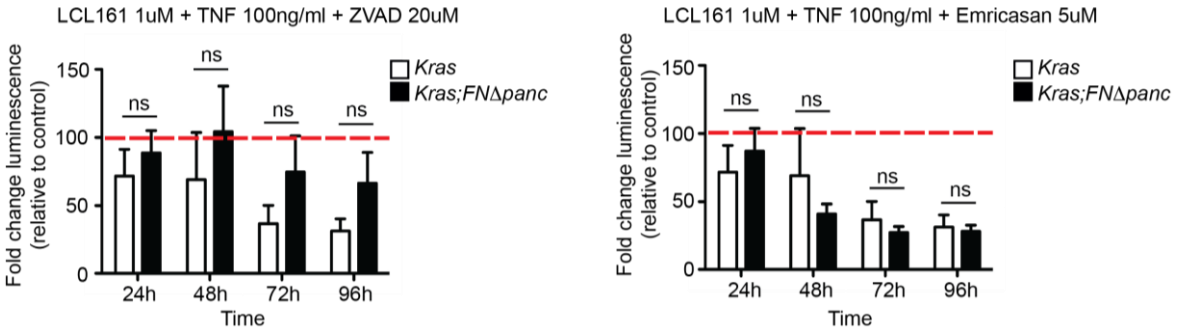

Figure 19: *Kras; FNΔpanc* cells profit from necroptosis inhibition and susceptible to necroptosis induction. (A) Cellular viability of *Kras* and *Kras; FNΔpanc* cell lines were measured by Cell Titer Glo assay at indicated time points upon treatment with Necroptosis inhibitors Nec1s (30 uM) and GSK'872 (1 uM). (B) Necroptosis was induced by the combination treatment of Birinapant (100nM), TNF (100 ng/ml) and zVAD (20 uM) or Emricasan (5 uM) and LCL161 (1 uM), TNF (100 ng/ml) and zVAD (20 uM) or Emricasan (5 uM). Cell viability measured by Cell Titer Glo assay. Mean ± SD; **p< 0,05; **p< 0,01, ***p< 0,001* by two-tailed t-test

6.1.20 Blocking apoptosis and necroptosis is beneficial most for *Kras; FNΔpanc* cell lines

Kras and *Kras; FNΔpanc* cells were treated with a combination of Smac mimetics (Birinapant or LCL161), TNF, apoptosis inhibitors (zVAD or Emricasan), and necroptosis inhibitor (Nec1s). Results showed that *Kras; FNΔpanc* cells profited most from blocking apoptosis and necroptosis, whereas for *Kras* cells blocking apoptosis versus blocking apoptosis and necroptosis gave largely similar results (Figure 20).

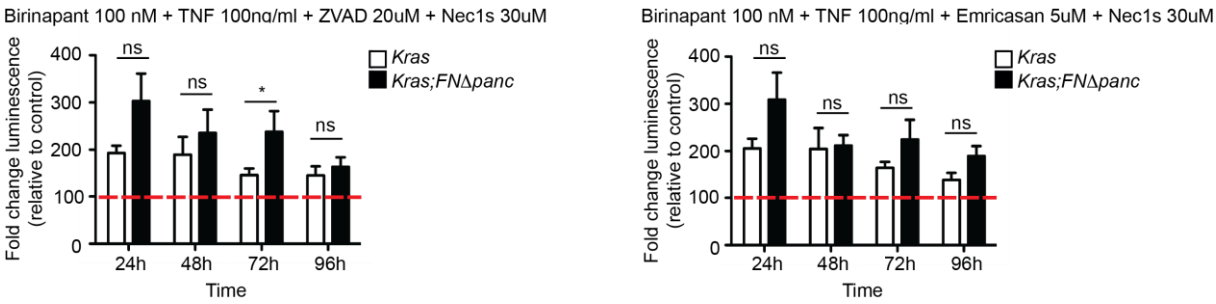

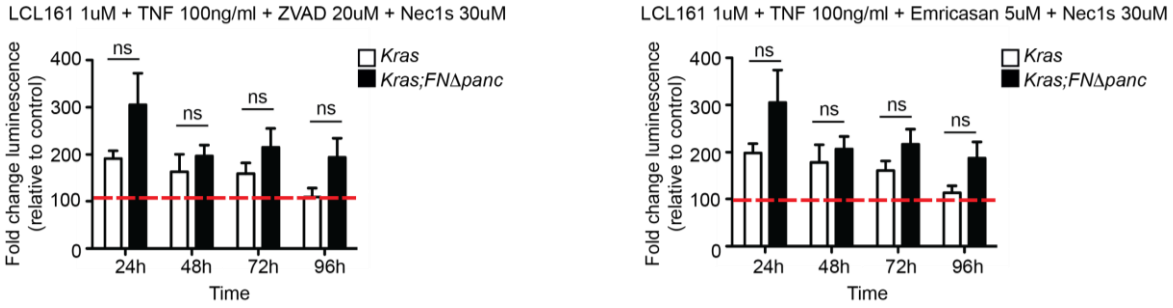

Figure 20: *Kras; FNΔpanc* cells profit from both apoptosis and necroptosis inhibition (A) Cellular viability of *Kras* and *Kras; FNΔpanc* cell lines were measured by Cell Titer Glo assay at indicated time points upon treatment with a combination of Smac mimetics (Birinapant or LCL161), TNF, apoptosis inhibitors (zVAD or Emricasan), and necroptosis inhibitor (Nec1s). Mean ± SD; *$p< 0,05$ by two-tailed t-test

6.1.21 Death receptor stimulation alone does not enough to induce cell death

Kras and *Kras; FNΔpanc* cells were treated with death receptor stimulators including FasL and TNF. Results were presented as a fold change of absolute cell number of viable cells treated versus control-treated and it demonstrated that FasL and TNF by themselves were not enough to induce cells death in *Kras* cells Also, *Kras; FNΔpanc* cells were slightly effected by TNF or FasL induction (Figure 21A). Besides, cells were also treated with ActD which is inhibitor of RNA synthesis and facilitates cell death. *Kras; FNΔpanc* cells were more susceptible to cell death induction upon ActD also in combination with ActD and TNF (Figure 21B).

A

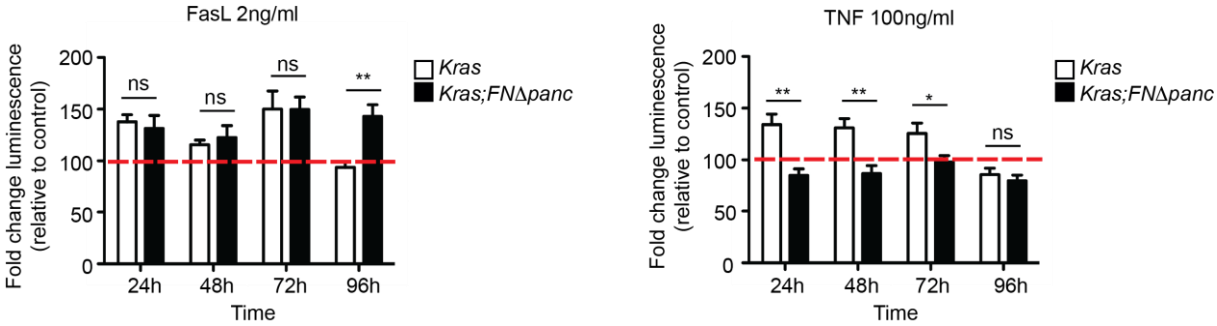

B

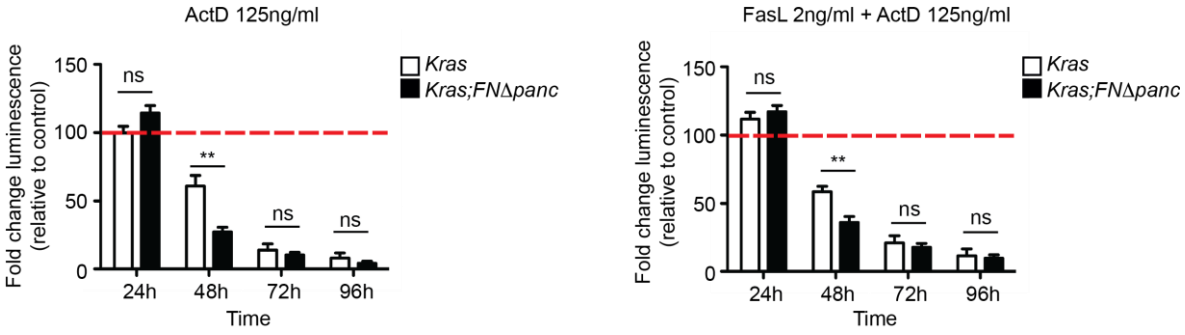

Figure 21: Cell death receptor stimulation alone is not sufficient to cell death. (A) Cellular viability of *Kras* and *Kras; FNΔpanc* cell lines were measured by Cell Titer Glo assay at indicated time points upon treatment with death receptor stimulators FasL (2ng/ml) and TNF(100ng/ml). (B) Cell were treated with ActD and combination of ActD (125 ng/ml) and TNF (100ng/ml). Mean ± SD; **p< 0,05; **p< 0,01, ***p< 0,001* by two-tailed t-test

6.1.22 RNA sequencing of *Kras* and *Kras; FNΔpanc* cell lines with and without treatment of Tunicamycin

To reveal the potential function of pancreas specific *FN* in pancreatic tumorigenesis, the differentially expressing genes in *Kras; FNΔpanc* cell lines cell lines were analyzed compared to cell lines harboring only *Kras* mutation by RNA sequencing (RNAseq). 4 distinct cell lines from each genotype (*Kras; FNΔpanc* and *Kras)* were used. The heat map represented the differentially expressing genes in cell lines from both genotypes irrespectively of treatment condition (Figure 22A). Highly expressed transcripts in *Kras; FNΔpanc* cell lines were enriched for Hypoxia pathway (Figure 22B, C) whereas transcripts with lower expression in *Kras; FNΔpanc* cell lines were enriched for Butanoate metabolism (Figure 22D). On the other hand, differentially expressing genes were also analyzed upon Tunicamycin treatment to reveal the underlying mechanism of Tunicamycin sensitivity of *Kras; FNΔpanc* cell lines. 24h Tunicamycin (5 ug/ml) treated 3 distinct cell lines from each genotype (*Kras; FNΔpanc* and *Kras)* were used. The heat maps representing the differentially expressing genes in cell lines from both genotypes based on treatment irrespective of genotype also the interaction between treatment condition and genotype have been shown (Figure 23A). Transcripts with higher expression in Tunicamycin treated *Kras; FNΔpanc* cell lines were enriched for Xenobiotic metabolism, Interferon alpha and gamma pathways and Inflammatory

pathway (Figure 23B). Additionally, transcripts with lower expression in *Kras; FNΔpanc* cell lines upon Tunicamycin treatment were enriched for MTORC1 signaling, UPR signaling, G2M checkpoints, Myc Target and E2F targets (Figure 23C).

A

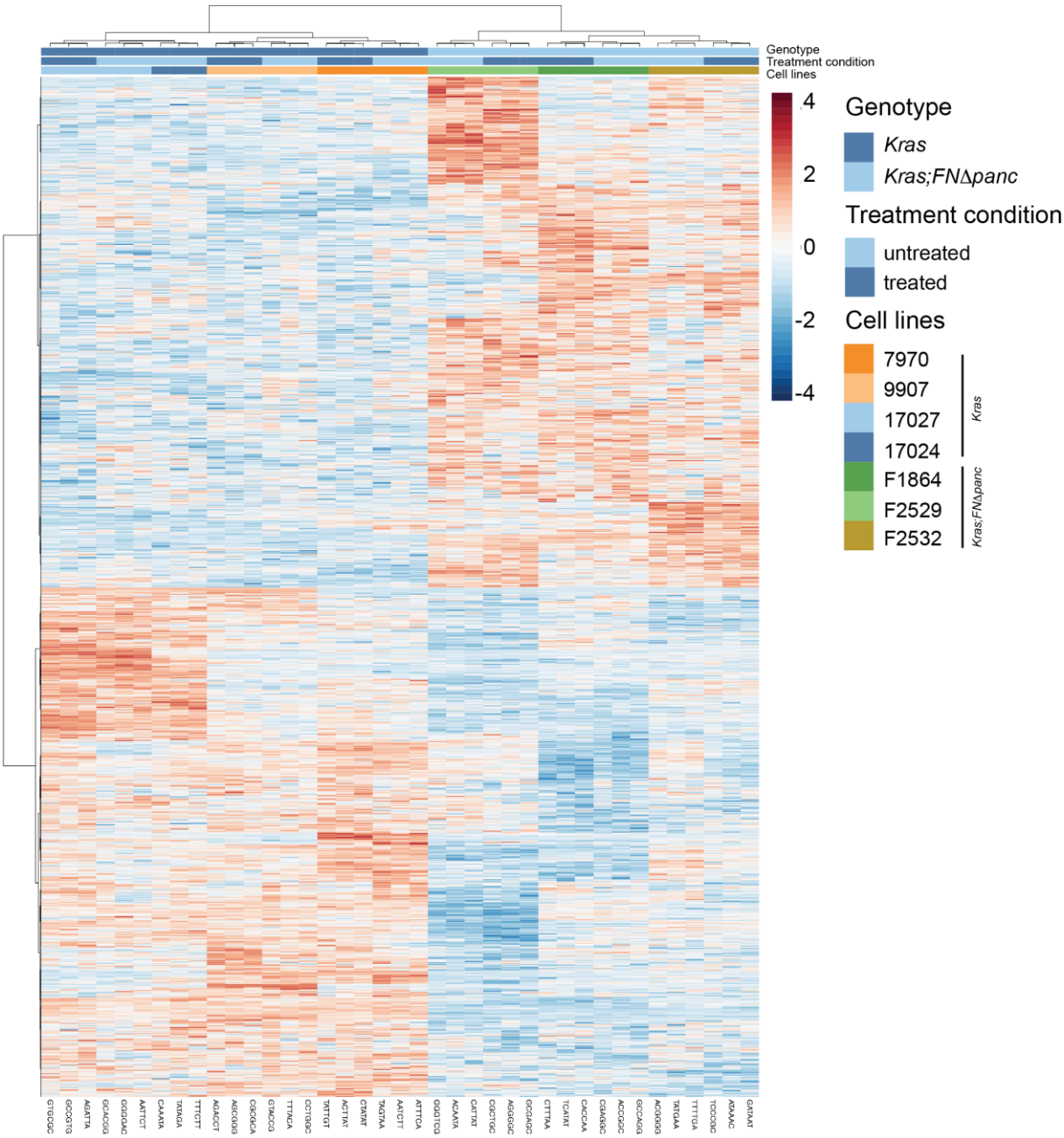

B

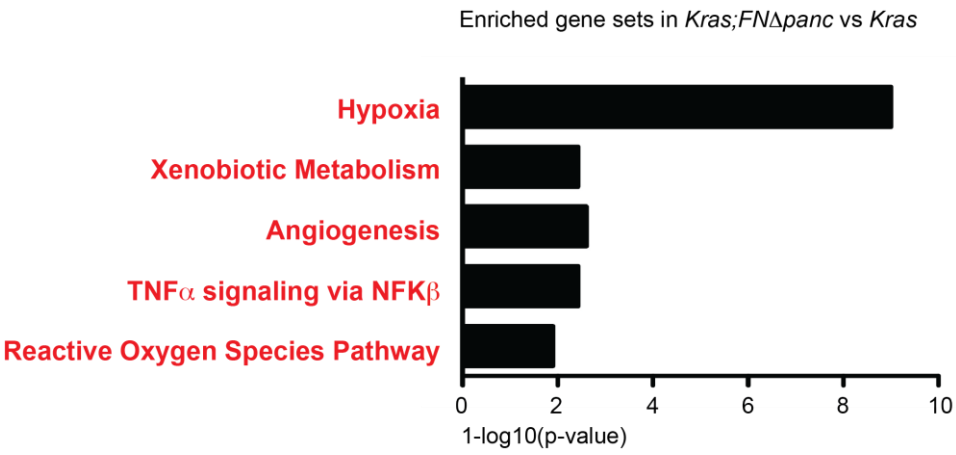
Enriched gene sets in *Kras;FNΔpanc* vs *Kras*
Hypoxia
Xenobiotic Metabolism
Angiogenesis
TNFα signaling via NFKβ
Reactive Oxygen Species Pathway
0
2
4
6
8
10
1-log10(p-value)

C

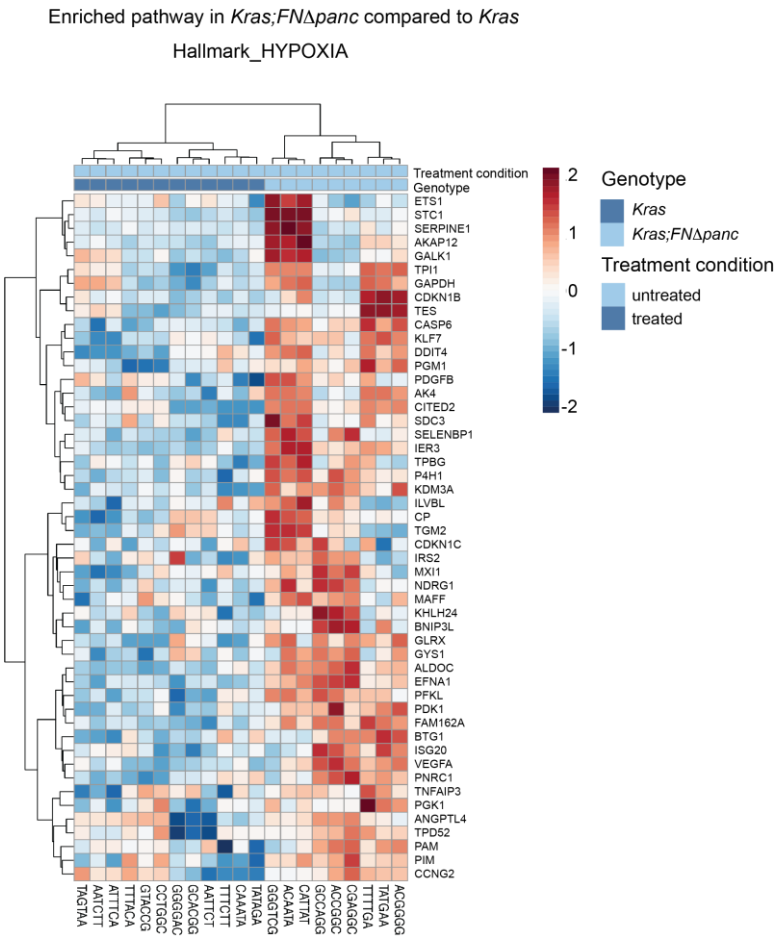
Enriched pathway in *Kras;FNΔpanc* compared to *Kras*
Hallmark_HYPOXIA
Treatment condition
Genotype
ETS1
STC1
SERPINE1
AKAP12
GALK1
TPI1
GAPDH
CDKN1B
TES
CASP6
KLF7
DDIT4
PGM1
PDGFB
AK4
CITED2
SDC3
SELENBP1
IER3
TPBG
P4H1
KDM3A
ILVBL
CP
TGM2
CDKN1C
IRS2
MXI1
NDRG1
MAFF
KHLH24
BNIP3L
GLRX
GYS1
ALDOC
EFNA1
PFKL
PDK1
FAM162A
BTG1
ISG20
VEGFA
PNRC1
TNFAIP3
PGK1
ANGPTL4
TPD52
PAM
PIM
CCNG2
TAGTAA
AATCTT
ATTTCA
TTTACA
GTACCG
CCTGGC
GGGGAC
GCACGG
AATTCT
TTTCTT
CAAATA
TATAGA
GGGTCG
ACAATA
CATTAT
GCCAGG
ACCGGC
CGAGGC
TTTTGA
TATGAA
ACGGGG
2
1
0
-1
-2
Genotype
Kras
Kras;FNΔpanc
Treatment condition
untreated
treated

D

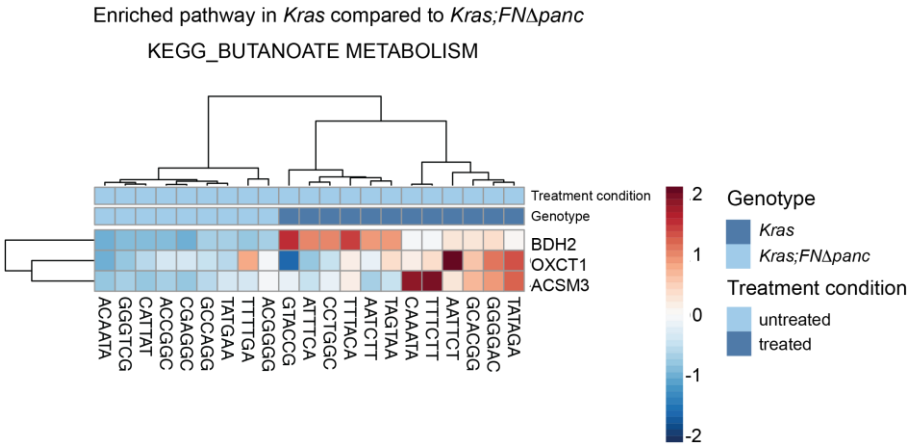

Figure 22:Heatmap representation of RNAseq analysis. (A) Heat map representing color-coded expression levels of differentially expressed genes (2-way Anova, up or down regulated) in *Kras; FNΔpanc* and Kras cell lines based on genotype treatment irrespective of the treatment (B) Classification of significantly enriched gene sets into categories in *Kras; FNΔpanc* compared to *Kras.* (C) Heat map representation of Hypoxia which is significantly enriched pathway in *Kras; FNΔpanc* compared to *Kras*. (D) Heat map representation of Butanoate metabolism which is significantly enriched in *Kras* compared to *Kras; FNΔpanc.*

A

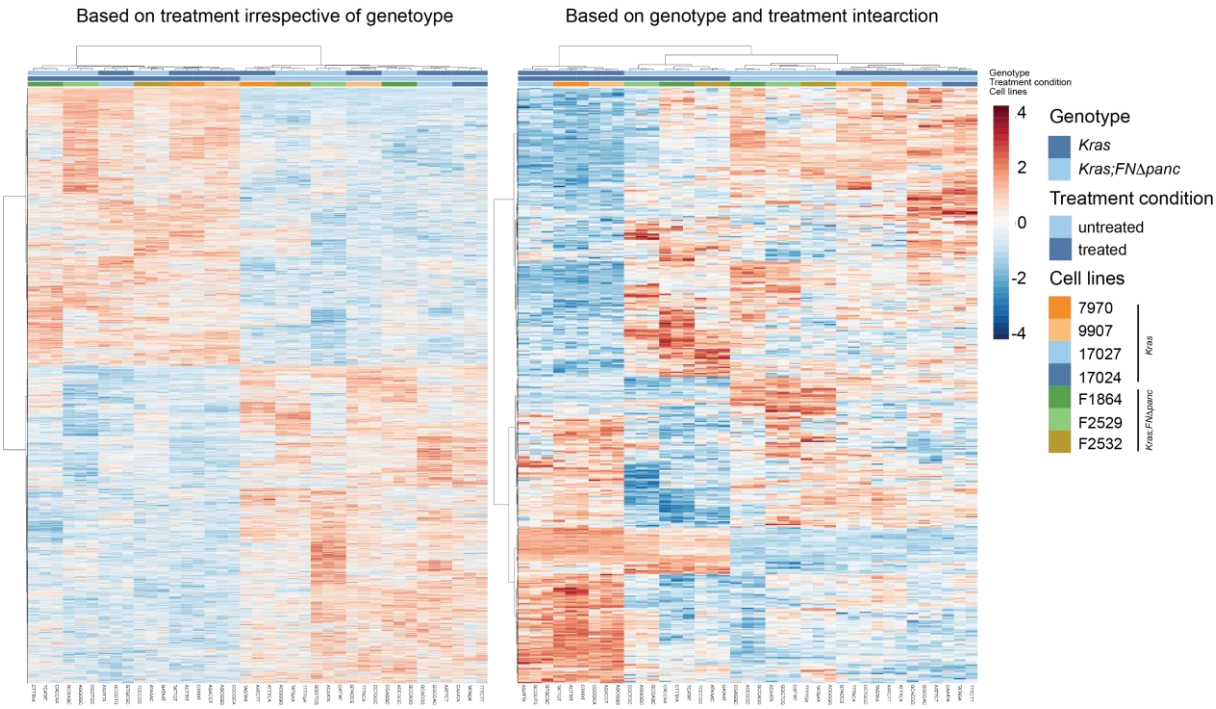

B

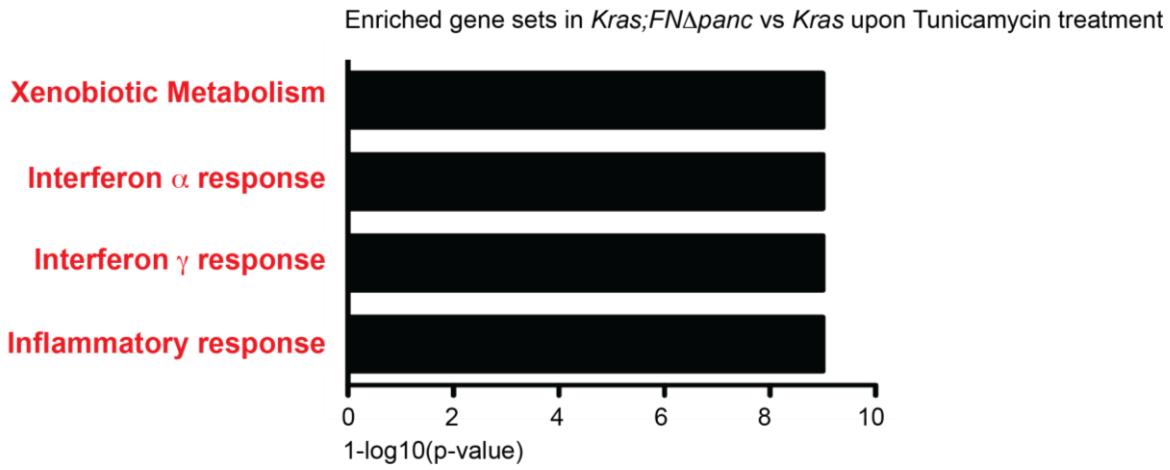

C

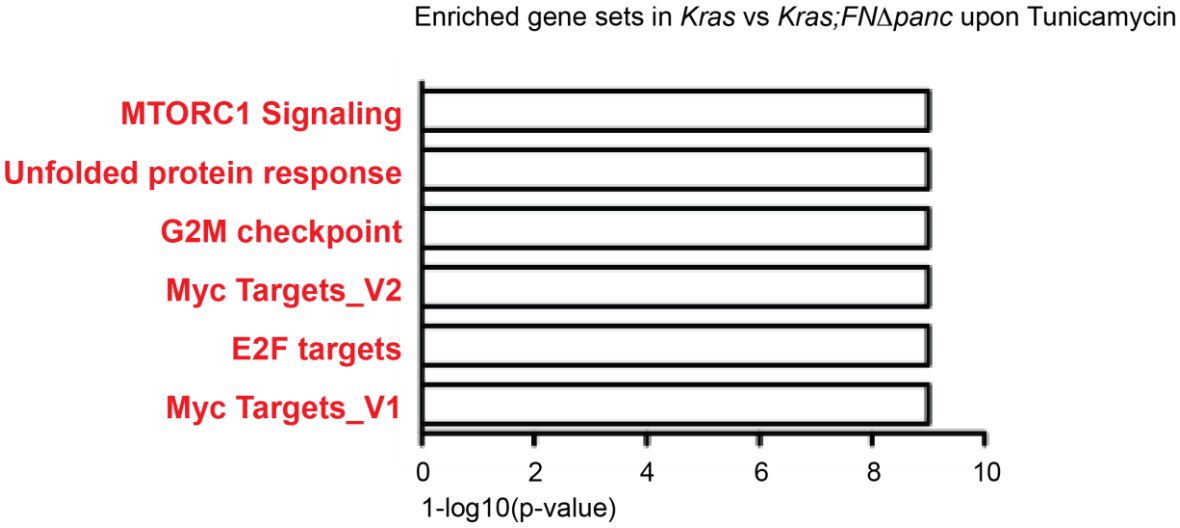

Figure 23: Heatmap representation of RNAseq analysis upon Tunicamycin Treatment. (A) Heat map representing color-coded expression levels of differentially expressed genes (2-way Anova, up or down regulated) in *Kras; FNΔpanc* and *Kras* cell lines based on Tunicamycin treatment irrespective of the genotype and respective of the genotype. (B) Classification of significantly enriched gene sets into categories in *Kras; FNΔpanc* compared to *Kras* upon Tunicamycin treatment. (C) Classification of significantly enriched gene sets into categories in *Kras* compared to *Kras; FNΔpanc* upon Tunicamycin treatment.

7 DISCUSSION

The role of FN in cancer is controversial in the literature. Before 1990s, FN is thought to be a tumor suppressor gene and some studies showed that most of the tumor cells do not express FN or reduced the expression whereas FN is detected in the surrounding stromal tissues (Hynes *et al.*, 1979) (Hayman *et al.*, 1982). Later, the role of FN in tumor progression and metastasis unequivocally has been reported. It is still ambiguous why there are two clearly different concept at these periods of times about the role of FN in carcinogenesis. Herewith, the effect of FN has been investigated specifically in pancreatic cells during carcinogenesis for the first-time *in vivo*. Interestingly, our study showed that pancreas specific loss of FN diminished the acinar compartment. Furthermore, whereas *FN* deletion did not influence Ras activity of the acinar cells, ADM formations significantly were accelerated in 9-week-old time points pancreata indicating *FN* deletion enhanced tumor initiation. However, number of PanIN structures was equal in both genotype at 9-week-old time point. Besides, *FN* deletion did not elevate ADM and PanIN structures at 18-week-old pancreata compared to *Kras* control. Stunningly, whereas desmoplastic microenvironment existed in early time points (9-weeks-old and 18-weeks-old), pancreatic *FN* deletion reduced the stromal reaction in the time of sickness. Pancreatic atrophy, lipomatosis and elevated the micro carcinoma formations were the other pathological findings in *FN* deleted pancreas during pancreatic carcinogenesis. These findings indicated that pancreas specific *FN* definitively has a role in the normal exocrine tissue integrity and PDAC tumorigenesis. Results suggested that acinar cells undergone cell death in the absence of *FN* and the ones that could form precancerous structures generated dormant micro carcinoma. The mechanisms are under investigation. Besides that, *FN* deletion augmented the immune infiltration and in the line with that the inflammation induced carcinogenesis by cerulein treatment resulted in the micro carcinoma formation and acinar cell loss. *In vitro* analysis demonstrated that *FN* deleted cell lines were more sensitive to ER stress inducers and necroptosis induction which could explain the pancreatic atrophy. The role of pancreas specific *FN* deletion has been examined also in AP model. *FN* deletion aggravated the effect of AP and more necrosis was observed following AP induction.

7.1 Loss of *FN* exacerbates the outcome of AP

Pancreatitis studies showed that premature trypsin activation in pancreas results in acinar cell injury and necrosis. During this process, inflammatory response is triggered by pro-inflammatory cytokines and induces the activation of PSCs which produce α-SMA and ECM molecules such as collagen type I and FN. Thus, FN is one of the component which is upregulated during acute pancreatitis by stromal cells (Lankisch, Apte and Banks, 2015) (Nathan *et al.*, 2010). In the line with this, our preceding analysis of FN expression in pancreatic tissue during acute pancreatitis at different time points was supporting the existing literature. The importance of FN expressed by acinar cells have further investigated *in vivo* for the first time in mouse model with homozygous deletion of *FN*. Homozygous deletion of *FN* augmented the pancreatic injury upon cerulein induction which was validated by the levels of amylase and lipase in the serum at 8h time point indicating protective role of FN during AP. Besides, *FN* deletion also accelerated lung inflammation and tissue necrosis during AP. These observations are associated with the findings about the sensitivity of *FN* deleted cancer cells to necroptosis induction and *FN* deleted cells could have tendency to undergo necroptosis, which will be discussed later.

7.2 Loss of *FN* induces micro carcinoma formation, stromal decrease and pancreatic atrophy

The contribution of FN to PDAC carcinogenesis has been shown in past studies. However, researchers have mainly focused on FN-integrin interaction which consequently upregulates proliferation, survival and chemoresistance usually in the cells seeded on FN-coated plates (Topalovski and Brekken, 2016). Besides, Immunohistochemical analysis validated that FN is primarily expressed in PDAC stroma, but it is also expressed in PC cells as we have also demonstrated. In this study, we have analyzed the role of pancreas specific FN in pancreatic carcinogenesis for the first time by using *Kras*-mutated mouse model with homozygous deletion of *FN* in exocrine pancreas *in vivo.* We found that *FN* deletion resulted in pancreatic atrophy which has initiated at early time points with an increase of stromal reaction and without any change in tumorigenesis, whereas pancreatic atrophy was accompanied with lipogenesis and decreased stromal reaction in time of sickness. Pancreatic atrophy

can be described as accelerated massive cell death by apoptosis and necroptosis but detecting cell death and cell death types were difficult on the tissue sections. Therefore, we have analyzed the susceptibility of cell lines isolated from *Kras; FNΔpanc* and *Kras* mice to different forms of cell deaths *in vivo*, showing that *Kras; FNΔpanc* cell lines were more susceptible to necroptosis. Together, *FN* deletion can accelerate the necroptosis in during *Kras*-mutation induced tumorigenesis which could be the reason for pancreatic atrophy.

In addition, stunningly, loss of *FN* induced micro carcinoma formation with non-fibrotic microenvironment. Even though FN has paradoxical role in cancer progression in the literature, some studies reported that FN silencing in pre-malignant cells enhanced the cancer progression including cell growth, migration, invasion and angiogenesis (Jia *et al.*, 2012) (Glasner *et al.*, 2018). FN was also reported as a senescence marker and is upregulated with premature cellular senescence which was provoked by various stresses including ER stress (Coppé *et al.*, 2010). Consequently, downregulation of endogenous FN expression is required to re-growth of senescent cells. Thus, *FN* depletion induced tumor formation can be explained by the subsequent suppression of senescence phenotype and this needs further investigation.

In a recent study, Ligorio et al reported that cancer cells acquire proliferative (PRO) and invasive (EMT) phenotypes when they are exposed to different tumor-stoma ratios. Ki67 and FN were used as an indicator for these PRO and EMT phenotypes, respectively. Researchers have also classified the human PDAC samples as 8 distinct tumor glands depending on the cellular composition having EMT, PRO, double positive or double negative phenotype. Interestingly, cells with DP and EMT phenotypes were associated with poor patient outcomes whereas cells with PRO phenotype was associated with improved survival (Ligorio *et al.*, 2019). In the line with this, our mouse model is essential to understand the tumors which are FN negative and to discover specific therapeutic options depending on the FN expression within the tumor structures.

High expression of FN is associated with poor patient outcome in some cancers including colorectal cancer and breast cancer (Yi *et al.*, 2016) (Bae *et al.*, 2013). Regarding PDAC, controversial finding has been reported. One study showed that high FN expression was associated with p-ERK presence and poor survival (Javle *et al.*,

2007). Besides, a recent study reported that low E-cadherin high FN expression ratio was found in high risk groups and was correlated with short event-free survival (Canlı *et al.*, 2020). On the other hand, another study showed that pancreatic tumors with high stromal FN expression are larger compared to tumor with low FN expression but there is no any overall survival difference between these two groups (Hu *et al.*, 2019). Nevertheless, our analysis of *FN* loss in specifically exocrine pancreas revealed significant decrease in survival rate in mouse model. This could be explained by pancreatic insufficiency due to pancreatic atrophy which is observed in *Kras; FN∆panc* pancreas. In addition, this could emphasize the different roles of FN in different cell compartments. Supportively, recent study investigating the contribution of ECM component produced by tumor cells and stromal cells to patient survival demonstrated that whereas tumor derived ECMs were associated with poor patient outcome, stroma derived ECMs could correlate with both poor and good survival (Tian *et al.*, 2019). Therefore, ECM proteins expressed by different tissue compartments should be considered for the survival analysis.

7.3 *FN* deletion does not affect the susceptibility of cells to conventional chemotherapy even increase resistance

There are studies showing the contribution of FN to chemotherapy resistance. In various tumor types including breast cancer, glioblastoma, small cell lung cancer, integrin-FN interaction results in the activation of signaling pathways culminating resistance of cells to chemotherapy. Disrupting the interaction between integrin and FN restores the sensitivity of tumor cells to therapeutic agents (Wang and Hielscher, 2017). Similarly in PDAC, PSC secreted FN promotes Gemcitabine resistance in PC cells (Amrutkar *et al.*, 2019). In contrast, in our study *FN* deleted tumor cell lines which are isolated from *Kras; FN∆panc* mice were demonstrated to have reduced cell cytotoxicity to Gemcitabine, Irinotecan and Paclitaxel and to have had same response to 5-FU and Oxaliplatin compared to *Kras* control cell lines.

In parallel with that RNA sequencing results showed that “Hypoxia Pathway” was significantly enriched in *Kras; FN∆panc* cell lines compared to *Kras* cells. It is known that hypoxia negatively affects therapy response by suppressing tumor growth and inducing cell cycle arrest since chemotherapies usually target rapidly proliferating cells.

Thus, the resistance of *Kras; FNΔpanc* cell lines to standard chemotherapies can be explained by the enhancement of hypoxia pathway in these cell lines. In addition, the enriched pathway in *Kras* cell lines compared to *Kras; FNΔpanc* cell lines was Butanoate metabolism. Studies reported that Hypoxia and Butanoate metabolism are antagonizing each other. Butanoate metabolism affected the epithelial oxygen consumption and suppressed the Hypoxia-inducible factor-1 activity (Rohwer and Cramer, 2011) (Colgan and Campbell, 2017) in epithelial cells which were supporting results.

7.4 FN expression sensitize the cell to necroptosis and ER stress inducers

Since we have observed pancreatic atrophy in the pancreas harboring *FN* deletion, we have investigated the cell death response of cells isolated from *Kras; FNΔpanc* and *Kras* mice upon treatment of different cell death inducers. Cell have treated with Smac mimetics (Birinapant and LCL161) and TNF which induce apoptosis and necroptosis. Birinapant inhibits cIAP1/2 and XIAP, while LCL161 inhibits cIAP1/2. All cell lines seem to be more sensitive to LCL161. The lines might be characterized by different expression levels of IAPs. Generally, *Kras; FNΔpanc* cell lines are more susceptible to cell death induction than the CK lines. However, there is one cell line per genotype that is more sensitive than the others. Therefore, a significant difference could not be found. Caspase inhibitors were beneficial for all cell lines indicating substantial amount of apoptosis was occurring in all cell lines. On the other hand, RIPK1 and RIPK3 inhibition were specifically beneficial for *Kras; FNΔpanc* cell lines, indicating necroptosis (potentially also pyroptosis) has profound impact on *Kras; FNΔpanc* tumorigenesis. FN is a large glycoprotein which is synthesized, processed and secreted from ER. In most of the tumor cells, FN is abundantly expressed. Therefore, unfolding process of FN can occur frequently, which in turn may cause ER stress. One study showed that ER stress was elicited by FN overexpression in macrophages (Du *et al.*, 2015). Thus, *Kras; FNΔpanc* and *Kras* cell lines were treated with ER stress inducers Tunicamycin and Thapsigargin and results demonstrated that *Kras; FNΔpanc* cell lines were sensitive to ER stress without altering the main ER markers such as Bip, CHOP, spliced Xbp1.

RNA sequencing results demonstrated that upon Tunicamycin treatment, Xenobiotic mechanism, Interferon alpha and gamma response and inflammatory response were significantly enriched in *Kras; FNΔpanc* cell lines compared to *Kras* cell lines. Interferons are multifunctional cytokines that exhibit anti-viral activity as well as anti-cancer function. The main anti-cancer roles of Interferon consist of tumor growth inhibition, cell death and senescence induction, suppression of cell migration, prevention of angiogenesis and regulation of immune response (Zhang, 2017). In the line with this result, Tunicamycin induced cell growth suppression and cell death shown in *Kras; FNΔpanc* cell lines could be explained by enhanced Interferon alpha and gamma response. Besides that, upon Tunicamycin treatment, DNA replication, UPR response E2F targets, S-phase, G2-M checkpoints and MYC targets were significantly enriched in *Kras* cell lines compared to *Kras; FNΔpanc* cell lines which indicated that *Kras* cell lines have ability to cope with the ER stress while *Kras; FNΔpanc* cells do not have. Detailed mechanism of *Kras; FNΔpanc* cell's sensitivity to ER stress inducer are under investigation.

7.5 FN expression is reduced by Tunicamycin and Thapsigargin treatment

Tunicamycin is a drug which inhibits the N-linked glycosylation by impeding the oligosaccharide addition, leading to protein blocking protein folding and consequently the ER stress. The impact of Tunicamycin on FN is controversial in the literature. While Olden et al showed that tunicamycin doesn't affect the expression of FN even though blocks the glycosylation of FN (Olden, Pratt and Yamada, 1979), Hemming et al reported reduced expression of FN (Hemming, 1985). Also in recent years, studies demonstrated that FN expression is decreased upon Tunicamycin treatment in non-small cell lung cancer cells (Qi *et al.*, 2018) and in colon cancer cells (You, Li and Guan, 2018). Thapsigargin results in the reduction of Ca^{+} storage in the ER by blocking the ER Ca^{+} dependent ATPase. Thereby, activity of Ca^{+} dependent chaperones impeded and consequently induced protein unfolding and UPR activation (Denmeade and Isaacs, 2005). Studies showed that Thapsigargin also decrease the expression of FN by decreasing the stored Ca^{+} in the ER in fibroblasts (Papp *et al.*, 2007) and in mesangial cells (Wu *et al.*, 2015). Supporting that, we have reported that Tunicamycin and Thapsigargin treatment diminished the FN expression in transcription and

translational levels. However, the molecular mechanism regulating FN expression upon Tunicamycin and Thapsigargin treatment is not clear. Tunicamycin and Thapsigargin induced eIF2a phosphorylation may inhibit the FN expression by blocking the protein synthesis.

7.6 p53 deletion is enough the switch the phonotype of FN deficient Kras mutated pancreas

p53 mutation occurs in %75 of human PDACs and *Kras; p53⊿panc* mice (KPC) mouse model is more clinically relevant and commonly used to recapitulate PDAC phenotype in mouse. In contrast to *Kras* model, *FN* deletion did not prevent fibrotic tumor formation in KPC model. This suggested that *p53* has key role in the *FN* deletion induced pancreatic acinar cell death. Furthermore, heterozygous deletion of *p53* in *Kras* mutant mice is used to investigate metastatic progression. *FN* deletion significantly decreased the survival rate of heterozygous *p53* deleted and *Kras* mutated mice *Kras; p53/+⊿panc* mice. However, to understand the effect of *FN* deletion on metastasis, we need more mice to be analyzed.

8 SUMMARY

The primary focus of the present study was to investigate the role of pancreas specific FN in pancreatic cancer development and progression. The contributions of cancer specific FN and stromal FN to tumor progression remain obscure and controversial. In PDAC, deletion of FN has been suggested to act against tumor development, but the roles of pancreas-specific FN have not been investigated yet in PC *in vivo*.

To determine the significance of pancreas-specific FN in pancreatic cancer development and progression, mice harboring pancreas specific homozygous deletion of FN and heterozygous deletion of Kras were established and characterized. Beside mouse model, isolated murine cancer cell lines from tumors that were generated in indicated mouse models were used to analyze the role of FN *in vitro*.

Pancreas specific FN deletion in Kras mutation harboring mice leads to acinar cell loss caused pancreatic atrophy, lipomatosis and micro carcinoma formation compared to Kras mice even though FN deletion did not affect the Kras activity of the acinar cells. Due to the micro carcinoma formations, tumor incidence rate is significantly higher in FN deleted mice, but metastasis incidence is less compared to the controls. Besides, FN deletion significantly diminish the survival rate compared to Kras control which can be explained by pancreatic insufficiency cause by pancreatic atrophy. In addition, in *Kras; FN∆panc* mice, immune infiltration was significantly upregulated compared to *Kras* controls. Whereas in early time points, reactive tissue stroma was observed, in the time of sickness stromal reaction was clearly decreased in *Kras; FN∆panc* pancreas. In vitro experiments indicated that FN deletion sensitized the cells to ER stress inducers. Also, whereas Kras cell lines do not seem to be influenced by necroptosis induction, *Kras; FN∆panc* cells are more susceptible to induction of necroptosis. The RNAseq analysis of *Kras; FN∆panc* and *Kras* cell lines showed that Hypoxia pathway is enriched in *Kras; FN∆panc* cell lines compared to *Kras.* Additionally, upon Tunicamycin treatment, Xenobiotic metabolism, Interferon alpha and gamma pathways and Inflammatory pathways were enriched in *Kras; FN∆panc* cell lines compared to *Kras*.

Altogether, even though the role of FN in tumor development is quite paradoxical in the literature, pancreas specific FN deleted pancreas cancer mouse model has

provided us essential information about the compartmental specific role of FN on pancreatic tumor development and progression.

9 REFERENCES

Aguirre-Ghiso, J. A. (2007) ‘Models, mechanisms and clinical evidence for cancer dormancy’, *Nature Reviews Cancer*, 7(11), pp. 834–846. doi: 10.1038/nrc2256.

Amrutkar, M. *et al.* (2019) ‘Secretion of fibronectin by human pancreatic stellate cells promotes chemoresistance to gemcitabine in pancreatic cancer cells’, *BMC Cancer*. BMC Cancer, 19(1), pp. 1–16. doi: 10.1186/s12885-019-5803-1.

Bae, Y. K. *et al.* (2013) ‘Fibronectin expression in carcinoma cells correlates with tumor aggressiveness and poor clinical outcome in patients with invasive breast cancer’, *Human Pathology*. Elsevier Inc., 44(10), pp. 2028–2037. doi: 10.1016/j.humpath.2013.03.006.

Bailey, P. *et al.* (2016) ‘Genomic analyses identify molecular subtypes of pancreatic cancer’, *Nature*. Nature Publishing Group, 531(7592), pp. 47–52. doi: 10.1038/nature16965.

Balanis, N. *et al.* (2013) ‘Epithelial to mesenchymal transition promotes breast cancer progression via a fibronectin-dependent STAT3 signaling pathway’, *Journal of Biological Chemistry*, 288(25), pp. 17954–17967. doi: 10.1074/jbc.M113.475277.

Barney, L. E. *et al.* (2020) ‘Tumor cell-organized fibronectin maintenance of a dormant breast cancer population’, *Science Advances*, 6(11). doi: 10.1126/sciadv.aaz4157.

Biankin, A. V. and Maitra, A. (2015) ‘Subtyping Pancreatic Cancer’, *Cancer Cell*. Elsevier Inc., 28(4), pp. 411–413. doi: 10.1016/j.ccell.2015.09.020.

Bynigeri, R. R. *et al.* (2017) ‘Pancreatic stellate cell: Pandora’s box for pancreatic disease biology’, *World Journal of Gastroenterology*, 23(3), pp. 382–405. doi: 10.3748/wjg.v23.i3.382.

Canlı, S. D. *et al.* (2020) ‘A novel 20-gene prognostic score in pancreatic adenocarcinoma’, *PLoS ONE*, 15(4), pp. 1–19. doi: 10.1371/journal.pone.0231835.

Carrara, M. *et al.* (2015) ‘ Crystal structures reveal transient PERK luminal domain tetramerization in endoplasmic reticulum stress signaling ’, *The EMBO Journal*,

34(11), pp. 1589–1600. doi: 10.15252/embj.201489183.

Chan, D. A. and Giaccia, A. J. (2007) ‘Hypoxia, gene expression, and metastasis’, *Cancer and Metastasis Reviews*. Cancer Metastasis Rev, pp. 333–339. doi: 10.1007/s10555-007-9063-1.

Chiquet-Ehrismann, R. *et al.* (1988) ‘Tenascin interferes with fibronectin action’, *Cell*, 53(3), pp. 383–390. doi: 10.1016/0092-8674(88)90158-4.

Chu, G. C. *et al.* (2007) ‘Stromal biology of pancreatic cancer’, *Journal of Cellular Biochemistry*, 101(4), pp. 887–907. doi: 10.1002/jcb.21209.

Colgan, S. P. and Campbell, E. L. (2017) ‘Oxygen metabolism and innate immune responses in the gut’, *Journal of applied physiology (Bethesda, Md. : 1985)*, 123(5), pp. 1321–1327. doi: 10.1152/japplphysiol.00113.2017.

Comerford, K. M. *et al.* (2002) ‘Hypoxia-inducible factor-1-dependent regulation of the multidrug resistance (MDR1) gene’, *Cancer Research*, 62(12), pp. 3387–3394.

Coppé, J.-P. *et al.* (2010) ‘The Senescence-Associated Secretory Phenotype: The Dark Side of Tumor Suppression’, *Annual Review of Pathology: Mechanisms of Disease*, 5(1), pp. 99–118. doi: 10.1146/annurev-pathol-121808-102144.

Costa-Silva, B. *et al.* (2015) ‘Pancreatic cancer exosomes initiate pre-metastatic niche formation in the liver’, *Nature Cell Biology*, 17(6), pp. 816–826. doi: 10.1038/ncb3169.

Czabotar, P. E. *et al.* (2014) ‘Control of apoptosis by the BCL-2 protein family: Implications for physiology and therapy’, *Nature Reviews Molecular Cell Biology*. Nature Publishing Group, 15(1), pp. 49–63. doi: 10.1038/nrm3722.

D’Angelo, A. *et al.* (2019) ‘Tumour infiltrating lymphocytes and immune-related genes as predictors of outcome in pancreatic adenocarcinoma’, *PLoS ONE*, 14(8), pp. 1–19. doi: 10.1371/journal.pone.0219566.

Dauer, P. *et al.* (2018) ‘GRP78-mediated antioxidant response and ABC transporter activity confers chemoresistance to pancreatic cancer cells’, *Molecular Oncology*, 12(9), pp. 1498–1512. doi: 10.1002/1878-0261.12322.

Denmeade, S. R. and Isaacs, J. T. (2005) ‘The SERCA pump as a therapeutic target: Making a “smart bomb” for prostate cancer’, *Cancer Biology and Therapy*, 4(1), pp. 21–29. doi: 10.4161/cbt.4.1.1505.

Du, H. *et al.* (2015) ‘Fibronectin Overexpression Modulates Formation of Macrophage Foam Cells by Activating SREBP2 Involved in Endoplasmic Reticulum Stress’, *Cellular Physiology and Biochemistry*, 36(5), pp. 1821–1834. doi: 10.1159/000430153.

Edderkaoui, M. *et al.* (2005) ‘Extracellular matrix stimulates reactive oxygen species production and increases pancreatic cancer cell survival through 5-lipoxygenase and NADPH oxidase’, *American Journal of Physiology - Gastrointestinal and Liver Physiology*, 289(6 52-6). doi: 10.1152/ajpgi.00197.2005.

Eke, I. *et al.* (2013) ‘Cetuximab attenuates its cytotoxic and radiosensitizing potential by inducing fibronectin biosynthesis’, *Cancer Research*, 73(19), pp. 5869–5879. doi: 10.1158/0008-5472.CAN-13-0344.

Erkan, M. *et al.* (2008) ‘The Activated Stroma Index Is a Novel and Independent Prognostic Marker in Pancreatic Ductal Adenocarcinoma’, *Clinical Gastroenterology and Hepatology*, 6(10), pp. 1155–1161. doi: 10.1016/j.cgh.2008.05.006.

Fulda, S. and Debatin, K. M. (2006) ‘Extrinsic versus intrinsic apoptosis pathways in anticancer chemotherapy’, *Oncogene*, 25(34), pp. 4798–4811. doi: 10.1038/sj.onc.1209608.

Glasner, A. *et al.* (2018) ‘NKp46 Receptor-Mediated Interferon-γ Production by Natural Killer Cells Increases Fibronectin 1 to Alter Tumor Architecture and Control Metastasis’, *Immunity*. Elsevier Inc., 48(1), pp. 107-119.e4. doi: 10.1016/j.immuni.2017.12.007.

Grendell, J. H. (2014) ‘Structure and function of the exocrine pancreas’, *Gastrointestinal Anatomy and Physiology: The Essentials*, pp. 78–91. doi: 10.1002/9781118833001.ch6.

Hammad, A. Y., Ditillo, M. and Castanon, L. (2018) ‘Pancreatitis’, *Surgical Clinics of North America*, 98(5), pp. 895–913. doi: 10.1016/j.suc.2018.06.001.

Han, S. W., Khuri, F. R. and Roman, J. (2006) ‘Fibronectin stimulates non-small cell lung carcinoma cell growth through activation of Akt/mammalian target of rapamycin/S6 kinase and inactivation of LKB1/AMP-activated protein kinase signal pathways’, *Cancer Research*, 66(1), pp. 315–323. doi: 10.1158/0008-5472.CAN-05-2367.

Han, S. W. and Roman, J. (2006) ‘Fibronectin induces cell proliferation and inhibits apoptosis in human bronchial epithelial cells: Pro-oncogenic effects mediated by PI3-kinase and NF-κB’, *Oncogene*, 25(31), pp. 4341–4349. doi: 10.1038/sj.onc.1209460.

Han, Z. and Lu, Z.-R. (2017a) ‘Targeting fibronectin for cancer imaging and therapy’, *J. Mater. Chem. B*, 5(4), pp. 639–654. doi: 10.1039/C6TB02008A.

Han, Z. and Lu, Z.-R. (2017b) ‘Targeting fibronectin for cancer imaging and therapy’, *J. Mater. Chem. B*. Royal Society of Chemistry, 5(4), pp. 639–654. doi: 10.1039/C6TB02008A.

Harburger, D. S. and Calderwood, D. A. (2009) ‘Erratum: Integrin signalling at a glance (Journal of Cell Science vol. 122 (159-163))’, *Journal of Cell Science*, 122(9), p. 1472. doi: 10.1242/jcs.052910.

Hayman, E. G. *et al.* (1982) ‘Codistribution of heparan sulfate proteoglycan, laminin, and fibronectin in the extracellular matrix of normal rat kidney cells and their coordinate absence in transformed cells’, *Journal of Cell Biology*, 94(1), pp. 28–35. doi: 10.1083/jcb.94.1.28.

Hemming, F. W. (1985) *Glycosyl Phosphopolyprenols*, *New Comprehensive Biochemistry*. Elsevier B.V. doi: 10.1016/S0167-7306(08)60023-X.

Hetz, C. and Papa, F. R. (2018) ‘The Unfolded Protein Response and Cell Fate Control’, *Molecular Cell*. Elsevier Inc., 69(2), pp. 169–181. doi: 10.1016/j.molcel.2017.06.017.

Hingorani, S. R. *et al.* (2018) ‘HALO 202: Randomized phase II Study of PEGPH20 Plus Nab-Paclitaxel/Gemcitabine Versus Nab-Paclitaxel/Gemcitabine in Patients With Untreated, Metastatic Pancreatic Ductal Adenocarcinoma’, *Journal of Clinical Oncology*, 36(4), pp. 359–366. doi: 10.1200/JCO.2017.74.9564.

Hu, D. *et al.* (2019) 'Stromal fibronectin expression in patients with resected pancreatic ductal adenocarcinoma', *World Journal of Surgical Oncology*. World Journal of Surgical Oncology, 17(1), pp. 1–8. doi: 10.1186/s12957-019-1574-z.

Hynes, R. O. (1973) 'Alteration of cell surface proteins by viral transformation and by proteolysis', *Proceedings of the National Academy of Sciences of the United States of America*. Proc Natl Acad Sci U S A, 70(11), pp. 3170–3174. doi: 10.1073/pnas.70.11.3170.

Hynes, R. O. *et al.* (1979) 'Cell surface fibronectin and oncogenic transformation.', *Journal of supramolecular structure*, 11(1), pp. 95–104. doi: 10.1002/jss.400110110.

Ide, T. *et al.* (2006) 'Tumor-stromal cell interaction under hypoxia increases the invasiveness of pancreatic cancer cells through the hepatocyte growth factor/c-Met pathway', *International Journal of Cancer*, 119(12), pp. 2750–2759. doi: 10.1002/ijc.22178.

Ignotz, R. A. and Massague, J. (1986) 'Transforming growth factor-β stimulates the expression of fibronectin and collagen and their incorporation into the extracellular matrix', *Journal of Biological Chemistry*, 261(9), pp. 4337–4345.

Infinity Reports Update from Phase 2 Study of Saridegib Plus Gemcitabine in Patients with Metastatic Pancreatic Cancer | *Business Wire* (no date). Available at: https://www.businesswire.com/news/home/20120127005146/en/Infinity-Reports-Update-Phase-2-Study-Saridegib (Accessed: 20 March 2020).

Jackson, E. L. *et al.* (2001) 'Analysis of lung tumor initiation and progression using conditional expression of oncogenic K-ras', *Genes and Development*. doi: 10.1101/gad.943001.

Jagadeeshan, S. *et al.* (2014) 'Transcriptional regulation of fibronectin by p21-activated kinase-1 modulates pancreatic tumorigenesis.', *Oncogene*. Nature Publishing Group, 34(4), pp. 1–10. doi: 10.1038/onc.2013.576.

Javle, M. M. *et al.* (2007) 'Epithelial-Mesenchymal Transition (EMT) and activated extracellular signal-regulated kinase (p-Erk) in surgically resected pancreatic cancer', *Annals of Surgical Oncology*, 14(12), pp. 3527–3533. doi: 10.1245/s10434-007-9540-

3.

Jeffrey, K. D. *et al.* (2008) 'Carboxypeptidase E mediates palmitate-induced β-cell ER stress and apoptosis', *Proceedings of the National Academy of Sciences of the United States of America*, 105(24), pp. 8452–8457. doi: 10.1073/pnas.0711232105.

Jia, D. *et al.* (2012) 'Fibronectin matrix-mediated cohesion suppresses invasion of prostate cancer cells', *BMC Cancer*. BioMed Central Ltd, 12(1), p. 94. doi: 10.1186/1471-2407-12-94.

Kaspar, M., Zardi, L. and Neri, D. (2006) 'Fibronectin as target for tumor therapy', *International Journal of Cancer*, 118(6), pp. 1331–1339. doi: 10.1002/ijc.21677.

Kennedy, R. H. *et al.* (1987) 'Pancreatic extracellular matrix alterations in chronic pancreatitis', *Pancreas*, 2(1), pp. 61–72. doi: 10.1097/00006676-198701000-00010.

Kim, I., Xu, W. and Reed, J. C. (2008) 'Cell death and endoplasmic reticulum stress: Disease relevance and therapeutic opportunities', *Nature Reviews Drug Discovery*, 7(12), pp. 1013–1030. doi: 10.1038/nrd2755.

Kim, S. *et al.* (2000) 'Regulation of angiogenesis in vivo by ligation of integrin (alpha5 beta1 wi ...', *Health (San Francisco)*, 5(4), pp. 1345–1362.

Kleeff, J. *et al.* (2016) 'Pancreatic cancer', *Nature Reviews Disease Primers*. Macmillan Publishers Limited, 2(April), pp. 1–23. doi: 10.1038/nrdp.2016.22.

Kleeff, J. *et al.* (2017) 'Chronic pancreatitis', *Nature Reviews Disease Primers*. Macmillan Publishers Limited, 3, pp. 1–18. doi: 10.1038/nrdp.2017.60.

Klieser, E. *et al.* (2015) 'Endoplasmic reticulum stress in pancreatic neuroendocrine tumors is linked to clinicopathological parameters and possible epigenetic regulations', *Anticancer Research*, 35(11), pp. 6127–6136.

Koong, A. C., Chauhan, V. and Romero-Ramirez, L. (2006) 'Targeting XBP-1 as a novel anti-cancer strategy', *Cancer Biology and Therapy*, 5(7), pp. 756–759. doi: 10.4161/cbt.5.7.2973.

Korah, R., Boots, M. and Wieder, R. (2004) 'Integrin α5β1 promotes survival of growth-arrested breast cancer cells: An in vitro paradigm for breast cancer dormancy

in bone marrow', *Cancer Research*. Cancer Res, 64(13), pp. 4514–4522. doi: 10.1158/0008-5472.CAN-03-3853.

Kubisch, C. H. and Logsdon, C. D. (2008) 'Endoplasmic reticulum stress and the pancreatic acinar cell', *Expert Review of Gastroenterology and Hepatology*, 2(2), pp. 249–260. doi: 10.1586/17474124.2.2.249.

Kumra, H. and Reinhardt, D. P. (2016) 'Fibronectin-targeted drug delivery in cancer', *Advanced Drug Delivery Reviews*. Elsevier B.V., 97, pp. 101–110. doi: 10.1016/j.addr.2015.11.014.

Lafaro, K. J. and Melstrom, L. G. (2019) 'The Paradoxical Web of Pancreatic Cancer Tumor Microenvironment', *American Journal of Pathology*. American Society for Investigative Pathology, 189(1), pp. 44–57. doi: 10.1016/j.ajpath.2018.09.009.

Lankisch, P. G., Apte, M. and Banks, P. A. (2015) 'Acute pancreatitis', *The Lancet*. Elsevier Ltd, 386(9988), pp. 85–96. doi: 10.1016/S0140-6736(14)60649-8.

Lenselink, E. A. (2015) 'Role of fibronectin in normal wound healing', *International Wound Journal*, 12(3), pp. 313–316. doi: 10.1111/iwj.12109.

Lew, D., Afghani, E. and Pandol, S. (2017) 'Chronic Pancreatitis: Current Status and Challenges for Prevention and Treatment'. doi: 10.1007/s10620-017-4602-2.

Ligorio, M. *et al.* (2019) 'Stromal Microenvironment Shapes the Intratumoral Architecture of Pancreatic Cancer', *Cell*. Elsevier Inc., 178(1), pp. 160-175.e27. doi: 10.1016/j.cell.2019.05.012.

Lomas, A. C. *et al.* (2007) 'Fibulin-5 binds human smooth-muscle cells through α5β1 and α4β1 integrins, but does not support receptor activation', *Biochemical Journal*, 405(3), pp. 417–428. doi: 10.1042/BJ20070400.

Mahadevan, D. and Von Hoff, D. D. (2007) 'Tumor-stroma interactions in pancreatic ductal adenocarcinoma'. doi: 10.1158/1535-7163.MCT-06-0686.

Makohon-Moore, A. and Iacobuzio-Donahue, C. A. (2016) 'Pancreatic cancer biology and genetics from an evolutionary perspective', *Nature Reviews Cancer*. Nature Publishing Group, 16(9), pp. 553–565. doi: 10.1038/nrc.2016.66.

Marino, S. *et al.* (2000) 'Induction of medulloblastomas in p53-null mutant mice by somatic inactivation of Rb in the external granular layer cells of the cerebellum', *Genes and Development*, 14(8), pp. 994–1004. doi: 10.1101/gad.14.8.994.

Martinez-Useros, J. *et al.* (2015) 'Identification of Poor-outcome Biliopancreatic Carcinoma Patients With Two-marker Signature Based on ATF6α and p-p38 "STARD Compliant"', *Medicine*, 94(45), p. e1972. doi: 10.1097/MD.0000000000001972.

Meng, X. N. *et al.* (2009) 'Characterisation of fibronectin-mediated FAK signalling pathways in lung cancer cell migration and invasion', *British Journal of Cancer*, 101(2), pp. 327–334. doi: 10.1038/sj.bjc.6605154.

Miyamoto, H. *et al.* (2004) 'Tumor-Stroma Interaction of Human Pancreatic Cancer: Acquired Resistance to Anticancer Drugs and Proliferation Regulation Is Dependent on Extracellular Matrix Proteins', *Pancreas*, 28(1), pp. 38–44. doi: 10.1097/00006676-200401000-00006.

Nakhai, H. *et al.* (2007) 'Ptf1a is essential for the differentiation of GABAergic and glycinergic amacrine cells and horizontal cells in the mouse retina', *Development*. doi: 10.1242/dev.02781.

Nathan, J. D. *et al.* (2010) 'Protection Against Chronic Pancreatitis and Pancreatic Fibrosis in Mice Overexpressing Pancreatic Secretory Trypsin Inhibitor', *Pancreas*, 39(1), pp. e24–e30. doi: 10.1097/MPA.0b013e3181bc45e9.

Neesse, A. *et al.* (2011) 'Stromal biology and therapy in pancreatic cancer', *Gut*, 60(6), pp. 861–868. doi: 10.1136/gut.2010.226092.

Niu, Z. *et al.* (2015) 'Elevated GRP78 expression is associated with poor prognosis in patients with pancreatic cancer', *Scientific Reports*. Nature Publishing Group, 5, pp. 1–12. doi: 10.1038/srep16067.

Olden, K., Pratt, R. M. and Yamada, K. M. (1979) 'Role of carbohydrate in biological function of the adhesive glycoprotein fibronectin', *Proceedings of the National Academy of Sciences of the United States of America*, 76(7), pp. 3343–3347. doi: 10.1073/pnas.76.7.3343.

Olive, K. P. *et al.* (2009) 'Inhibition of Hedgehog signaling enhances delivery of

chemotherapy in a mouse model of pancreatic cancer', *Science*, 324(5933), pp. 1457–1461. doi: 10.1126/science.1171362.

Olmeda, D. *et al.* (2007) 'Snail silencing effectively suppresses tumour growth and invasiveness', *Oncogene*, 26(13), pp. 1862–1874. doi: 10.1038/sj.onc.1209997.

Özdemir, B. C. *et al.* (2014) 'Depletion of carcinoma-associated fibroblasts and fibrosis induces immunosuppression and accelerates pancreas cancer with reduced survival', *Cancer Cell*, 25(6), pp. 719–734. doi: 10.1016/j.ccr.2014.04.005.

Palam, L. R. *et al.* (2015) 'Integrated stress response is critical for gemcitabine resistance in pancreatic ductal adenocarcinoma', *Cell Death and Disease*. Nature Publishing Group, 6(10), pp. e1913-13. doi: 10.1038/cddis.2015.264.

Pandiri, A. R. (2014) 'Overview of Exocrine Pancreatic Pathobiology'. doi: 10.1177/0192623313509907.

Papp, S. *et al.* (2007) 'Calreticulin affects fibronectin-based cell-substratum adhesion via the regulation of c-Src activity', *Journal of Biological Chemistry*, 282(22), pp. 16585–16598. doi: 10.1074/jbc.M701011200.

Paron, I. *et al.* (2011) 'Tenascin-c enhances pancreatic cancer cell growth and motility and affects cell adhesion through activation of the integrin pathway', *PLoS ONE*, 6(6). doi: 10.1371/journal.pone.0021684.

Pommier, A. *et al.* (2018) 'Unresolved endoplasmic reticulum stress engenders immune-resistant, latent pancreatic cancer metastases', *Science*, 360(6394). doi: 10.1126/science.aao4908.

Pontiggia, O. *et al.* (2012) 'The tumor microenvironment modulates tamoxifen resistance in breast cancer: A role for soluble stromal factors and fibronectin through β1 integrin', *Breast Cancer Research and Treatment*. Breast Cancer Res Treat, 133(2), pp. 459–471. doi: 10.1007/s10549-011-1766-x.

Provenzano, P. P. *et al.* (2012) 'Enzymatic Targeting of the Stroma Ablates Physical Barriers to Treatment of Pancreatic Ductal Adenocarcinoma', *Cancer Cell*. Elsevier Inc., 21(3), pp. 418–429. doi: 10.1016/j.ccr.2012.01.007.

Qi, W. *et al.* (2018) ‘Tunicamycin induces apoptosis in non-small cell lung cancer cells through C / EBP homologous protein activation-mediated endoplasmic reticulum stress’, 11(5), pp. 5310–5322.

Ramanathan, R. K. *et al.* (2018) ‘A phase IB/II randomized study of mFOLFIRINOX (mFFOX) + pegylated recombinant human hyaluronidase (PEGPH20) versus mFFOX alone in patients with good performance status metastatic pancreatic adenocarcinoma (mPC): SWOG S1313 (NCT #01959139).’, *Journal of Clinical Oncology*. American Society of Clinical Oncology (ASCO), 36(4_suppl), pp. 208–208. doi: 10.1200/jco.2018.36.4_suppl.208.

Reed, J. C. (1999) ‘Dysregulation of apoptosis in cancer’, *Journal of Clinical Oncology*, 17(9), pp. 2941–2953. doi: 10.1200/jco.1999.17.9.2941.

Reuter, S. *et al.* (2010) ‘Oxidative stress, inflammation, and cancer: How are they linked?’, *Free Radical Biology and Medicine*, 49(11), pp. 1603–1616. doi: 10.1016/j.freeradbiomed.2010.09.006.

Rhim, A. D. *et al.* (2014) ‘Stromal elements act to restrain, rather than support, pancreatic ductal adenocarcinoma’, *Cancer Cell*. Elsevier Inc., 25(6), pp. 735–747. doi: 10.1016/j.ccr.2014.04.021.

Ritzenthaler, J. D., Han, S. and Roman, J. (2008) ‘Stimulation of lung carcinoma cell growth by fibronectin-integrin signalling.’, *Molecular bioSystems*, 4(12), pp. 1160–1169. doi: 10.1039/b800533h.

Rohwer, N. and Cramer, T. (2011) ‘Hypoxia-mediated drug resistance: Novel insights on the functional interaction of HIFs and cell death pathways’, *Drug Resistance Updates*. Elsevier Ltd, 14(3), pp. 191–201. doi: 10.1016/j.drup.2011.03.001.

Ruoslahti, E. *et al.* (1973) ‘Fibroblast surface antigen: A new serum protein’, *BBA - Protein Structure*. Biochim Biophys Acta, 322(2), pp. 352–358. doi: 10.1016/0005-2795(73)90310-3.

Rybak, J. N. *et al.* (2007) ‘The extra-domain A of fibronectin is a vascular marker of solid tumors and metastases’, *Cancer Research*. Cancer Res, 67(22), pp. 10948–10957. doi: 10.1158/0008-5472.CAN-07-1436.

Sakai, T. *et al.* (2001) ‘Plasma fibronectin supports neuronal survival and reduces brain injury following transient focal cerebral ischemia but is not essential for skin-wound healing and hemostasis’, *Nature Medicine*, 7(3), pp. 324–330. doi: 10.1038/85471.

Schwarz, R. E. *et al.* (2010) ‘Antitumor effects of EMAP II against pancreatic cancer through inhibition of fibronectin-dependent proliferation’, *Cancer Biology and Therapy*, 9(8), pp. 632–639. doi: 10.4161/cbt.9.8.11265.

Schwarzbauer, J. E. and DeSimone, D. W. (2011) ‘Fibronectins, their fibrillogenesis, and in vivo functions’, *Cold Spring Harbor Perspectives in Biology*, 3(7), pp. 1–19. doi: 10.1101/cshperspect.a005041.

Senthebane, D. A. *et al.* (2017) ‘The role of tumor microenvironment in chemoresistance: To survive, keep your enemies closer’, *International Journal of Molecular Sciences*, 18(7). doi: 10.3390/ijms18071586.

Serres, E. *et al.* (2014) ‘Fibronectin expression in glioblastomas promotes cell cohesion, collective invasion of basement membrane in vitro and orthotopic tumor growth in mice.’, *Oncogene*. Nature Publishing Group, 33(26), pp. 3451–62. doi: 10.1038/onc.2013.305.

Shi, Q. *et al.* (1999) ‘Constitutive and inducible interleukin 8 expression by hypoxia and acidosis renders human pancreatic cancer cells more tumorigenic and metastatic’, *Clinical Cancer Research*, 5(11), pp. 3711–3721.

Shimoyama, S. *et al.* (1995) ‘Altered expression of extracellular matrix molecules and their receptors in chronic pancreatitis and pancreatic adenocarcinoma in comparison with normal pancreas’, *International Journal of Pancreatology*, 18(3), pp. 227–234. doi: 10.1007/BF02784946.

Shuda, M. *et al.* (2003) ‘Activation of the ATF6, XBP1 and grp78 genes in human hepatocellular carcinoma: a possible involvement of the ER stress pathway in hepatocarcinogenesis’, *Journal of Hepatology*, 38(5), pp. 605–614. doi: 10.1016/S0168-8278(03)00029-1.

Stenman, S. and Vaheri, A. (1981) ‘Fibronectin in human solid tumors’, *International*

Journal of Cancer, 27(4), pp. 427–435. doi: 10.1002/ijc.2910270403.

T, S. Dh. Sh. (1994) 'Integrin-mediated signal transduction linked to Ras pathway by Grb2 binding to focal adhesion kinase', *Nature*, 30(4), pp. 367–369.

Teodoro, T. *et al.* (2012) 'Pancreatic β-cells depend on basal expression of active ATF6α-p50 for cell survival even under nonstress conditions', *American Journal of Physiology-Cell Physiology*, 302(7), pp. C992–C1003. doi: 10.1152/ajpcell.00160.2011.

Tian, C. *et al.* (2019) 'Proteomic analyses of ECM during pancreatic ductal adenocarcinoma progression reveal different contributions by tumor and stromal cells', *Proceedings of the National Academy of Sciences of the United States of America*, 116(39), pp. 19609–19618. doi: 10.1073/pnas.1908626116.

To, W. S. *et al.* (2011) 'Plasma and cellular fibronectin: distinct and independent functions during tissue repair', *Fibrogenesis & Tissue Repair*, 4(1), p. 21. doi: 10.1186/1755-1536-4-21.

Topalovski, M. *et al.* (2016) 'Hypoxia and transforming growth factor β cooperate to induce fibulin-5 expression in pancreatic cancer', *Journal of Biological Chemistry*, 291(42), pp. 22244–22252. doi: 10.1074/jbc.M116.730945.

Topalovski, M. and Brekken, R. a. (2016) 'Matrix control of pancreatic cancer: New insights into fibronectin signaling', *Cancer Letters*. Elsevier Ireland Ltd, 381(1), pp. 252–258. doi: 10.1016/j.canlet.2015.12.027.

Uzunparmak, B. and Sahin, I. H. (2019) 'Pancreatic cancer microenvironment: a current dilemma', *Clinical and Translational Medicine*. Springer Berlin Heidelberg, 8(1), pp. 1–8. doi: 10.1186/s40169-019-0221-1.

Wang, J. P. and Hielscher, A. (2017) 'Fibronectin: How its aberrant expression in tumors may improve therapeutic targeting', *Journal of Cancer*, 8(4), pp. 674–682. doi: 10.7150/jca.16901.

Wang, M. and Kaufman, R. J. (2016) 'Protein misfolding in the endoplasmic reticulum as a conduit to human disease', *Nature*, 529(7586), pp. 326–335. doi: 10.1038/nature17041.

Whatcott, C. J. *et al.* (2015) 'Desmoplasia in primary tumors and metastatic lesions of pancreatic cancer', *Clinical Cancer Research*, 21(15), pp. 3561–3568. doi: 10.1158/1078-0432.CCR-14-1051.

Wu, H., Ng, B. S. H. and Thibault, G. (2014) 'Endoplasmic reticulum stress response in yeast and humans', *Bioscience Reports*, 34(4), pp. 321–330. doi: 10.1042/BSR20140058.

Wu, P. *et al.* (2015) 'Store-operated Ca2+ channels in mesangial cells inhibit matrix protein expression', *Journal of the American Society of Nephrology*, 26(11), pp. 2691–2702. doi: 10.1681/ASN.2014090853.

Xiang, L. *et al.* (2012) 'The extra domain a of fibronectin increases VEGF-C expression in colorectal carcinoma involving the PI3K/AKT signaling pathway', *PLoS ONE*. PLoS One, 7(4). doi: 10.1371/journal.pone.0035378.

Yamada, K. M. (1978) 'OF TRANSFORMATION-SENSITIVE FIBROBLAST L o c a l i z a t i o n , R e d i s t r i b u t i o n , a n d R o l e in Cell S h a p e The major cell surface glycoprotein of chick embryo fibroblasts , cellular fibronec- tin (formerly known as CSP or LETS protein', *Journal of Cell Biology*, 78, pp. 520–541.

Yi, W. *et al.* (2016) 'High expression of fibronectin is associated with poor prognosis, cell proliferation and malignancy via the NF-B/p53-apoptosis signaling pathway in colorectal cancer', *Oncology Reports*, 36(6), pp. 3145–3153. doi: 10.3892/or.2016.5177.

You, S., Li, W. and Guan, Y. (2018) 'Tunicamycin inhibits colon carcinoma growth and aggressiveness via modulation of the ERK-JNK-mediated AKT/mTOR signaling pathway', *Molecular Medicine Reports*, 17(3), pp. 4203–4212. doi: 10.3892/mmr.2018.8444.

Yu, M. *et al.* (2012) 'RNA sequencing of pancreatic circulating tumour cells implicates WNT signalling in metastasis', *Nature*. Nature Publishing Group, 487(7408), pp. 510–513. doi: 10.1038/nature11217.

Yuan, J. *et al.* (2015) 'Acquisition of epithelial-mesenchymal transition phenotype in the tamoxifen-resistant breast cancer cell: A new role for G protein-coupled estrogen

receptor in mediating tamoxifen resistance through cancer-associated fibroblast-derived fibronectin and β1-', *Breast Cancer Research*. BioMed Central Ltd., 17(1). doi: 10.1186/s13058-015-0579-y.

Yuan, X. P. *et al.* (2015) 'GRP78 promotes the invasion of pancreatic cancer cells by FAK and JNK', *Molecular and Cellular Biochemistry*, 398(1–2), pp. 55–62. doi: 10.1007/s11010-014-2204-2.

Zeng, S. *et al.* (2019) 'Chemoresistance in pancreatic cancer', *International Journal of Molecular Sciences*, 20(18), pp. 1–19. doi: 10.3390/ijms20184504.

Zhang, K. (2017) 'Overview of Interferon: Characteristics, signaling and anti-cancer effect', *Archives of Biotechnology and Biomedicine*, 1(1), pp. 001–016. doi: 10.29328/journal.hjb.1001001.

- Publications include:

1. Görgülü Kivanc; Diakopoulos Kalliope N; **Kaya-Aksoy Ezgi**; Ciecielski Katrin J; Ai, Jiaoyu; Lesina Marina; Algül Hana. The role of Autophagy in Pancreatic Cancer; From Bench to Dark Bedside. *Cells.* 24 April 2020 1063:doi:10.3390 /ceşşs9031063

2. Görgülü Kivanc, Diakopoulos, Kalliope N; Ai, Jiaoyu; Schoeps, Benjamin, Kabacaoglu Derya; Karpathaki, Angeliki-Faidra; Ciecielski, Katrin J; **Kaya-Aksoy, Ezgi**; Ruess, Dietrich A; Berninger, Alexandra; Kowalska Marlena; Stevanovic, Marija; Wörmann Sonja M; Wartmann, Thomas; Zhao, Yue; Halangk, Walter; Voronina, Svetlana; Tepikin, Alexey; Schitter, Anna Melissa; Steiger, Katja; Artati, Anna; Adamski, Jerzy; Aichler, Michaela; Walch,Axel; Jastroch, Martin; Hartleben, Götz; Mantzoros, Christos S; Weichert, Wilko, Schmid, Roland M; Herzig, Stephan; Kriger, Achim; Sainz, Bruno; Lesina, Marina; Algül, Hana. Levels of the Autophagy Related 5 Protein Affect Progression and Metastasis of Pancreatic Tumors in Mice. *Gastroenterology*. 2018 Oct 5. pii: S0016-5085(18)35087-X. doi: 10.1053/j.gastro.2018.09.053.

3. Ruess DA, Heynen GJ, Ciecielski KJ, Ai J, Berninger A, Kabacaoglu D, Görgülü K, Dantes Z,Wörtmann SM, Diakopoulos KN, Karpathaki AP, Kowalska M, **Kaya-Aksoy E**, Long L, van der Laan EAZ, Lopez Alberka MP, Nazare M, Reichert M, Saur D, Erkan MM, Hopt UT, Sainz B Jr, Birchmeier W, Schmid RM, Lesina M, Algül, H Mutant KRAS-driven cancers depend on PTPN11/SHP2 phosphatase. *Nat Med*. 2018;24(7):954-960. doi:10.1038/s41591-018-0024-8

4. **Kaya-Aksoy E**, Cingoz A, Senbabaoglu F, Seker F, Sur-Erdem I, Kayabolen A, Lokumcu T, Sahin GN, Karahuseyinoglu S, Bagci-Onder T. The pro-apoptotic Bcl-2 family member Harakiri (HRK) induces cell death in glioblastoma multiforme. *Cell Death Discovery*. 2019 Feb 8;5:64. doi: 10.1038/s41420-019-0144-z.

5. Kurt IC, Sur I, **Kaya E**, Cingoz A, Kazancioglu S, Kahya Z, Toparlak OD, Senbabaoglu F, Kaya Z, Ozyerli E, Karahüseyinoglu S, Lack NA, Gümüs ZH, Onder TT, Bagci-Onder T. KDM2B, an H3K36-specific demethylase, regulates

apoptotic response of GBM cells to TRAIL. *Cell Death Disease*. 2017 Jun 29;8(6):e2897. doi: 10.1038/cddis.2017.288.

6. Senbabaoglu F, Cingoz A, **Kaya E**, Kazancioglu S, Lack NA, Acilan C, Bagci-Onder T. Identification of Mitoxantrone as a TRAIL-sensitizing agent for Glioblastoma Multiforme. *Cancer Biol Ther*. 2016 May 3;17(5):546-57. doi: 10.1080/15384047.2016.1167292. Epub 2016 Mar

10 ABBREVIATIONS

ADEX	Aberrantly differentiated endocrine exocrine
ADM	Acinar to ductal metaplasia
AMPK	AMP-activated protein kinase
AP	Acute pancreatitis
ASI	Activating stromal index
ATF	Activating transcription factor
Bip	Binding immunoglobulin protein
BrdU	Bromodeoxyuridine
CAF	Cancer associated fibroblasts
CHOP	CCAAT-enhancer binding protein homologous protein
CP	Chronic pancreatitis
DISC	Death inducing signaling complex
EGF	Epidermal growth factor
ECM	Extracellular matrix
EDTA	Ethylenediaminetetraacetic acid
EIF2α	Eukaryotic translation initiation factor 2α
EMT	Epithelial to Mesenchymal transition
ER	Endoplasmic reticulum
FADD	Fas associated protein with death domain
FAK	Focal adhesion kinase
FGF	Fibroblast growth factor
FN	Fibronectin
5-FU	Fluorouracil
HA	Hyaluronic acid/Hyaluronan
HE	Hematoxylin and eosin
HGF	Hepatocyte growth factor
HIF1α	Hypoxia inducible factor α
IGF-1	Insulin like growth factor-1
IL	Interleukin
IRE1α	Inositol requiring enzyme 1α
LC3	Microtubule-associated protein 1A/1B-light chain 3
MAPK	Mitogen-activated protein kinase
MMP	Matrix metalloproteinase
mTORC1	Mammalian target of rapamycin complex 1
NEAA	Non-essential amino acid
PanIN	Pancreatic intraepithelial neoplasia
PBS	Phosphate-buffered saline
PC	Pancreatic cancer
PDAC	Pancreatic ductal adenocarcinoma
PERK	Protein kinase RNA-like endoplasmic reticulum kinase

PSC	Pancreatic stellate cell
pFN	Plasma FN
qRT-PCR	Quantitative real time polymerase chain reaction
αSMA	Alpha smooth muscle actin
TGFα	Transforming growing factor α
TGFβ	Transforming growing factor β
TME	Tumor microenvironment
TNF-α	Tumor necrosis factor - alpha
TIMP	Tissue inhibitors of metalloproteinase
ULK	Unc-51 like autophagy activating kinase
UPR	Unfolded protein response
Xbp1	X-box binding protein 1
XIAP	X-linked inhibitor of apoptosis protein

11 ACKNOWLEDGEMENTS

First and foremost, I would like to express my sincere gratitude and thanks to my thesis advisor Prof. Dr. med. Hana Algül who supported me during my research with his enthusiasm, scientific advices and immense knowledge. I truly enjoyed working in this project and It was a great privilege to work under his supervision. I would also like to express my deepest appreciations to PD. Dr. Marina Lesina who provided me invaluable guidance during my research with her caring, patience and encouragement. I would also like to thank my committee members, Prof. Dr. Philipp Jost and PD. Dr. Guido von Figura for their advice, insightful comments and enlightening ideas. Furthermore, I appreciate Dr. Ulrike Höckendorf for her support and collaboration during my last months of the research.

I am deeply grateful to Dr. Kıvanç Görgülü, my dear benchmate who supported and motivated me all the time during my research period with his insightful discussions and suggestions. I am grateful to him for his genuine friendship and days with lots of fun. Special thanks to Katrin for being wonderful supporter and friend during these years. My special thank also go to Nan for his amazing foods and positive energy accompanying me in these years. Additionally, I would like to offer my special thanks to all group members including Nina, Alex, Franze, Larissa, Derya and Yuhui also former group members including Jiaoyu, Marlena and Dietrich for their support, genuine friendship and making my work life enjoyable. Particularly, the helps of Nina, Katrin and Kıvanç were remarkable during writing my thesis writing.

I am fully indepted to my former advisor Assoc. Prof. Dr. Tugba Bagci-Onder who supported me in every respect and has been great role-model as a scientist and mentor.

Finally, I owe my special thanks to my lovely friends and family. Firstly, my heartfelt appreciation goes to my best friends Tülin Tatar and Alperen Taciroglu for their endless support and encouragement even though we live very far away from each other. Additionally, I owe my special thanks to my friends including, Volkan, Nesrin, Mehmet, Büşra, Berkan, Aysu, İbrahim, Anıl and Tuğba for providing me invaluable support,

making my life more fun and make me feel like at home all the time in Munich.

Last but not the least, I am highly grateful and indebted to my parents Nihal and Hüseyin Kaya, and my sister Bilgesu for their support, caring and love that they have given me throughout of my life. I could not have done this thesis without them.

I would like to show my heartfelt appreciation to Sercan Aksoy, my dearest husband and my best friend for his constant love and for always believing in me during my PhD time. Thank you for being so understanding and sharing this journey with me and making my life more meaningful and fun.